UNIVERSITY OF SAAD DAHLAB BLIDA1

Faculty of Technology

Department of Civil Engineering

DOCTORAT THESIS

Civil Engineering

DEVELOPMENT OF A NN-BASED CONTROLLER APPLIED TO A SHAKING TABLE

By

Selma Hanane LARBI - CHABANE

Thesis committee composed by:

D. Amar Bouzid	Professor (full), University of Blida1, Blida	President
M. Abdessemed	Assistant Professor, University of Blida1, Blida	Examiner
M. Hadid	Professor (full), National School of Public Works, Kouba, Algiers	Examiner
H. Airouche	Assistant Professor, CGS, Hussein Dey, Algiers	Examiner
N. Bourahla	Professor (full), National Polytechnic School of Algiers, El Harrach, Algiers	Supervisor
H. Benchoubane	Assistant Professor, University of Blida1, Blida	Co-supervisor

Blida, July 2021.

ABSTRACT

Nowadays, the shaking tables represent a staple in earthquake engineering laboratories. Considered as the most powerful experimental technique to assess the seismic performance of full- and reduced-scale structures under dynamic excitations similar to real earthquakes, the shaking tables is aimed to real-time replicate the desired time histories at the base of the specimen as accurately as possible. Because of the inherent nonlinearities of the shaking table system, the coupling effects between the DOFs, the sensitivity of the shaking table to the behaviour of the specimen and its dynamic characteristics, the tracking performance of a shaking table in following a defined signal remains an important technical challenge. Usually, the reproduced accelerations are distorted by phase delay, amplitude attenuation and harmonic distortions. Hence, the accuracy in acceleration waveform replication must be significantly enhanced such that the effective reliability assessment of the tested structures is achieved. Various control methods for shaking table tests have been proposed to improve the tracking performance of the shaking table. Recently, the success of Artificial Intelligence (AI) has created new possibilities in the field of shaking table control, to achieve a high accuracy performance over traditional controllers. The use of neural networks (NNs) has been extensively extended in control applications due to their capabilities to build up control laws suitable for dynamic, complex and nonlinear systems, without requiring any mathematical model of the controlled system. Therefore, this thesis proposes an innovative control strategy by using a NN control algorithm to improve the acceleration tracking performance of a shaking table originally controlled by a conventional controller. Several numerical simulations have been carried out to test the feasibility and efficiency of the proposed control methodology. Through the sufficient numerical results, an experimental implementation of the designed NN control function in the QUANSER STIII is realised. The shaking table is a bi-axial shaking table driven by three linear motors and controlled by a Simulink-based proportional-derivative feedforward (PDFF) controller that shows several inabilities in reproducing prescribed acceleration signals. The designed three-layer feedforward NN is used as a basic control function which compensates for the distortions measured in the acceleration feedback signals and acts on the command signal to minimize the tracking errors. The database for offline training, testing, and validating the NN is the acceleration real-time signals recorded on the shaking table

during the tests using real earthquake records. Subsequently, the NN function block is implemented online in the outer control loop of the shaking table and performs in conjunction with the original PDFF controller.

The potential of the NN controller to enhance the fidelity in acceleration signals reproduction of the shaking table is verified for different load conditions by performing numerous bare and loaded table tests. Several comparative analysis in terms of intended and achieved responses in time and frequency domains as well as attained and desired PGA are undertaken. For both loaded and unloaded shaking table tests, the experimental results confirmed that the designed NN control algorithm helped the PDFF controller to track desired accelerations by reducing the distortion in peak amplitudes and by decreasing the time delays. In the frequency domains, results demonstrated the high capacity of the NN to cope with nonlinearities and resonance frequencies of the shaking table system as well as coupling effect due to the interaction between the shaking table system and the specimen, which is an important source of traditional control defiance. Moreover, the improvement in the acceleration tracking performance of the shaking table achieved by using the same NN model after a unique training process, for different excitation signals and different load conditions attests of the robustness of the proposed control methodology.

Key words*: shaking table, earthquake simulator, neural networks, control system, PD-Feedforward controller, acceleration tracking, distortion.*

ملخص

تعد الطاولات الهزازة ركيزة في مخابر الهندسة المقاومة للزلازل فهي تعتبر أنجع تقنية تجريبية لتقييم مدى كفاءة العينات الموضوعة قيد الدراسة - سواء كانت نماذج مصغرة أو بأبعاد حقيقية – ضد تأثيرات ديناميكية محاكية للزلازل.

الطاولات الهزازة مصممة لبعث الاشارات المرغوبة بصفة متزامنة و متطابقة قدر الامكان. تطرح كفاءة الطاولات لنقل هذه الاشارات اشكال تقني كبير بفعل لاخطية و ترابط درجات الحرية للنظام و كذا بفعل تأثير الخصائص الديناميكية للعينات.

غالبا ما تسجل فوارق زمنية بين التسارع المرجو و الحاصل وكذلك انخفاض في السعات و تحريفات تناسقية. مما يوجب ضبط هذه الفوارق للتمكن من التقييم الفعلي للعينات المدروسة بطريقة موثوقة.

طرحت عدة طرق للضبط بغية تحسين فعالية الطاولات الهزازة ويتيح الذكاء الاصطناعي امكانيات من شأنها تحسين كفاءتها في الضبط مقارنة مع وسائل الضبط السابقة.

انتشر استعمال الشبكات العصبونية الاصطناعية في الضبط بشكل واسع بفضل قدرتها على صياغة قوانين ضبط فعالة لأنظمة ديناميكية معقدة دون الرجوع الى نماذج رياضية دقيقة للأنظمة.

هذه الأطروحة تناقش استراتيجية ضبط مبتكرة تتم من خلالها تجربة شبكة عصبونية اصطناعية على طاولة هزازة ذات نظام ضبط كلاسيكي بغرض تحسين فعاليتها.

تم القيام بالعديد من عمليات المحاكات الرقمية لاختبار امكانيات و نجاعة هذه الطريقة. و بعد الحصول على نتائج رقمية مشجعة تم تجريب الشبكة العصبونية الاصطناعية على طاولة QUANSER STIII. هذه الأخيرة هي طاولة هزازة مزدوجة المحاور تعمل بثلاث محركات خطية ومضبوطة بنظام Proportional-derivative feedforward (PDFF) مفعل على Simulink.

يحمل هذا الضابط عدة نقائص من حيث تطابق التسارعات الصادرة مع التسارعات المرجوة. شبكة العصبونات الاصطناعية من نوع feedforward تحتوي على ثلاث طبقات عصبونية وتستعمل كأداة ضبط أساسية, تتصرف في إشارات التحكم بغرض احتواء فروقات التسارعات المسجلة.

تم تشكيل قاعدة البيانات المستعملة في التلقين والمصادقة و اختبار الشبكة بطريقة منفصلة (Offline) عن طريق جمع بيانات التسارعات المسجلة أثناء التجارب على الطاولة الهزازة. بعدها تحمل الشبكة العصبونية بطريقة متصلة (Online) في حلقة الضبط الخارجي للطاولة بغية القيام بعملها تزامنا مع الضابط المرفق بالطاولة (PDFF). تم التحقق من قدرة الشبكة العصبونية لتحسين اشارات التسارع بتجريبها في وضعيات مختلفة و ذلك بإجراء تجارب بطاولة فارغة أو محملة بعينة دراسة.

تمت مقارنة التسارعات الناتجة بتلك المرجوة و ذلك في المجالين الزمني و الترددي. كذلك تمت مقارنة PGA. نتائج التجارب أكدت دور الضابط المقترح في مساعدة الضابط (PDFF) على محاكات التسارعات المرجوة بصورة أدق وهذا بالتمكن من ضبط الفوارق المسجلة سابقا في الحالتين سواء كانت الطاولة فارغة أو محملة بعينة دراسة. النتائج المسجلة في المجال الترددي أكدت قدرة الشبكة العصبونية

على تجاوز مشكلة لاخطية النظام والتقليل من ترددات الصدى الملاحظة في تجاوبه, كذلك بالنسبة لمشكلة ترابط درجات الحرية الناتجة عن تفاعل النظام الطاولة-العينة. هذا الأخير عادة ما يشكل أهم سبب عدم نجاعة الضوابط الكلاسيكية. تحسين كفاءة الطاولة الهزازة في محاكات تسارعات مختلفة في حالات مختلفة و ذلك باستعمال نفس الشبكة العصبونية الملقنة مرة واحدة يدل على مدى فعالية و قوة الضابط المقترح.

كلمات مفتاحية : طاولة هزازة, محاكات الزلازل, شبكة عصبونية اصطناعية, نظام ضبط, محاكات التسارع, ضابط PD-Feedforward

RESUME

De nos jours, les tables vibrantes représentent un outil capital pour les laboratoires de Génie parasismique. Considérée comme étant la technique expérimentale la plus efficace pour évaluer les performances sismiques des spécimens à échelle réduite ou réelle sous des excitations dynamiques similaires aux séismes réels, la table vibrante est destinée à reproduire en temps réel les signaux désirés à la base des spécimens, le plus fidèlement possible. La performance de la table vibrante à suivre un signal prédéfini reste un problème technique majeur à cause des non-linéarités internes du système, aux effets de couplage entre les degrés de liberté (DDL) de la table et à l'influence du comportement et des caractéristiques dynamiques du spécimen. Généralement, les accélérations reproduites sur la plateforme montrent des temps de retard, une atténuation des amplitudes ainsi que des distorsions harmoniques. Par conséquent, la fidélité dans la reproduction des signaux d'accélération doit être considérablement améliorée de telle sorte que la fiabilité de l'évaluation des structures testées soit atteinte. Nombreuses méthodes de contrôle de tables vibrantes ont été proposées afin d'améliorer la performance de celles-ci. Récemment, le succès que connait l'Intelligence Artificielle (IA) a créé de nouvelles possibilités dans le contrôle des tables vibrantes, visant à atteindre de meilleures performances que celles obtenues par des contrôleurs standards. L'utilisation des Réseaux de Neurones Artificiels (RNA) dans le contrôle a largement augmenté de par leur efficacité à produire des lois de contrôle efficaces pour des systèmes dynamiques, complexes et non-linéaires, sans besoin d'un modèle mathématique précis du système à contrôler.
Cette thèse propose donc une stratégie de contrôle innovante où un RNA est appliqué à une table vibrante ayant un contrôleur classique, afin d'améliorer ses performances. Plusieurs simulations numériques ont été réalisées pour tester la faisabilité et l'efficacité de la méthode de contrôle proposée. A travers l'obtention de résultats satisfaisants, le RNA est expérimentalement implémenté dans la table vibrante QUANSER STIII. Cette dernière est une table bi-axiale, actionnée par trois moteurs linéaires et contrôlée par un proportionnel-dérivative feedforward (PDFF) implémenté dans Simulink qui montre nombreuses défaillances quant à la reproduction des accélérations désirées. Le RNA de type feedforward, constitué par trois couches de neurones est utilisé comme une fonction de contrôle basique, compense les distorsions mesurées dans les réponses en accélérations et agit sur le signal de

commande afin de minimiser les erreurs. La base de données utilisée, en offline, pour l'apprentissage, la validation et le test du RNA est constituée des signaux d'accélérations récoltés lors des essais sur table vibrante. Par la suite, le RNA est implémenté online dans la boucle de contrôle extérieure de la table afin d'effectuer la compensation des distorsions en conjonction avec le PDFF.

Le potentiel du RNA à augmenter la qualité des signaux d'accélérations reproduits sur table vibrante est vérifié pour différentes conditions de chargement en exécutant des tests sur table non chargée et chargée. Nombreuses analyses comparatives entre les réponses en accélération obtenues et désirées ainsi que le PGA atteint et désiré sont effectuées dans les domaines temporel et fréquentiel. Les résultats expérimentaux ont confirmé que le schéma de contrôle proposé a aidé le contrôleur PDFF à suivre plus précisément les accélérations désirées, et ce en réduisant les distorsions des pics d'amplitudes et des temps de retard, dans le cas de table non chargée et chargée. Les résultats dans le domaine fréquentiel ont également démontré la capacité du RNA à pallier aux non-linéarités du système, à atténuer les fréquences de résonance observées dans les réponses du système ainsi qu'à faire face à l'effet de couplage dû à l'interaction table-spécimen, qui généralement présente la source principale de défaillance des contrôleurs classiques. De plus, l'amélioration de la performance de la table vibrante à suivre les signaux d'accélérations désirées est accomplie grâce à un même modèle de RNA ayant subi un seul apprentissage, pour différents signaux d'excitation et différents cas de chargement de la table, ce qui atteste la robustesse du contrôle proposé.

Mots clés : *table vibrante, simulateur de séisme, réseaux de neurones artificiels, système de contrôle, PD-Feedforward controller, suivi d'accélération, distorsions.*

ACKNOWLEDGMENTS

First and foremost, prayers and thanks to Allah, The Almighty (swt) for blessing me through this achievement, for giving me the health to complete it and the strength to not give up.

I would like to express my highest appreciation and deepest gratitude to my supervisor, Pr. Nouredine Bourahla for giving me the chance to surpass my limits and learn new skills without fearing failure. He has taught me to step out my comfort zone, to take risks and to live new experiences. He has taught me more than lessons of structure or seismic analysis, but lessons of life. I would not be able to find the words to express my admiration for the person who he is. Without him, I would have given up so many times. From the deepest of my heart, thank you.

I sincerely thank my co-supervisor, Pr. Hacine Benchoubane, who honored us to be part of this research work. He helped me finding solutions to problems that I could never solved without his awareness, experience and guidance, as I seriously needed some basic knowledge in electronic. He also joined us to the University of Djelfa and made the shaking table tests more enjoyable.

My sincere acknowledgments to Dr. Mohammed Badaoui of the University of Djelfa, without whom the experimental part of this research would never happened. He believed in us and freely permitted to us to carry out the shaking table tests without any reluctance.

To Khireddine Choutri who brought the key help to this work and was always present, thank you very much.

I would like to thank the members of the thesis committee for making time to review my thesis and for giving me a constructive feedback that would make it better.

My special acknowledgements are to my parents, who continue to always believing in me and in my choices. When I was kid, I held their hand even if I did not know where we were going. Today, and especially in this PhD journey, the roles have been

inverted; they held my hand and blindly followed me during years, with the only intuition that I will reach my goal inchallah.

How to express my deepest gratitude to my husband without whom I would never been at this stage of my life. He believes in me like anyone else, he brings me higher and makes me want to go further. His help, patience and support are incomparable.

Many thanks to all the people who helped me directly or indirectly, the ones who encouraged me even with one word.

The tiny persons who bring me so much love and give so much sense to my life, this thesis is dedicated to you.

CONTENTS

LIST OF FIGURES

LIST OF TABLES

CHAPTER 1

INTRODUCTION

1. Background and motivation

Development of seismic analysis and design is fundamentally underpinned by experiments and testing. A tremendous research effort has been placed into the experimental field of earthquake engineering in order to better assess the seismic performance of structural and nonstructural components subjected to earthquake-generated excitations to predict their dynamic behaviours more accurately, with the main scope of minimizing the seismic risk, assuring the environment safety and protecting humans' lives.

In cases where theoretical analysis and analytical simulations reach their limits, such as for indigenous constructions, high rise buildings and complex structures, experimentation is the best means that provides reliable data and accurate knowledge. The experimental side, often defined as a technique of acquiring information through physical observations and measurements, has been and should remain to be a major aspect of earthquake engineering research. Even if the experimentation costs much higher compared to numerical techniques, it remains the only valuable alternative in the study of complex phenomena that cannot be mathematically modeled or accurately simulated and more broadly, the experimentation is carried out to validate or improve the proposed design for the new structures, evaluate and upgrade the existing structures, verify the analytical studies, establish realistic loading criteria for complex environmental effects such as wind or earthquakes or study the response characteristics of structural structures with controlled variations of the input parameters [66].

Recent sophisticated experimental tools have been widely used. Three key types of testing techniques are available to study the dynamic performance of structures:

- Quasi-static tests: generally applied to study material properties and assess structural performances such as energy dissipation, collapse modes, through the application of cyclic displacements or forces to the test specimen at a quasi-static (low) rate via hydraulic actuators. Instead of following a predefined strain rate or specific displacement trajectory imposed by a particular earthquake, the structural element is subjected to predetermined numbers of displacements

controlled quasi static loading cycles to predetermined displacement ductility factors or drifts. The main advantage of the slow loading rate is that the quasi-static tests provide a valuable understanding of the structure's behavior in the post-yielding regime and give conservative estimations of the real strength of the structural element. Despite the fact that the quasi-static cyclic loading tests have the major benefit of requiring far less complicated loading and recording equipment, a main disadvantage can be highlighted which is the elimination of the acceleration-dependent inertial forces and the velocity-dependent damping forces that can be significant for some types of structures.

- Pseudo-dynamic tests: also called computer-actuator online test or hybrid tests, consist of the slow application of varying forces to the tested structures in order to determine realistic nonlinear responses, by combining an online computer simulation of the dynamic response of the structure with direct measurements from the structure during the test. Inertial and damping forces, required during the analysis process, for the solution of the equations of motion are modeled analytically. The main advantage of the PsDT is that the process automatically accounts for the hysteretic damping, due to inelastic deformation and damage to the structural materials, which is usually the major source of energy dissipation. Inertia forces are not experimentally produced and are modeled numerically. This eliminates conducting the test on a real time-scale, and allows very large models of structures to be tested with only a relatively modest hydraulic power requirement. The fact that the cyclic displacement history has to be defined before the test may not cover the range of displacements which the structure would undergo under dynamic action and represents the main disadvantage of the PsDT.
- Dynamic tests: they are the most realistic real-time tests. Dynamic tests are divided into two categories: The first one represents the system identification testing in the linear-elastic test range. It aims to obtain the model characteristics of the structure through testing at low amplitude. The second category that performs in the nonlinear-inelastic range, is the shaking table test, considered as the most advanced seismic testing technique by reproducing the dynamic effects that earthquakes impose on structures. The most common physical dynamic tests are the shaking table tests.

1.1. Shaking table testing

It is well known that shaking tables have largely impacted the earthquake engineering domain since 1890. An historical review of the development of shaking tables could be found in the literature, describing the earliest shaking tables that have been developed between 1890- 1950 [123]. Consisting of a moving platform on which the tested structure is mounted, the shaking table is meant to simulate an earthquake movement along one or more axis and accurately reproduce the dynamic forces involved. These innovative devices have been enhanced dramatically to lead to the 1-DOF shaking table (Japan 1962, Illinois 1969, Romania, early 1960) with assistance from the newly-created (1966) MTS System Corporation, and the use of early forms of the digital computer, driven in that time by a single actuator or by two electro-hydraulic actuators which were claimed to provide useful results despite of their simplicity. Shaking tables have continued to grow in size and capacities since that time, allowing the test of full-size structures under reproduced ground motions with maximum accelerations.

Nowadays, the value of the shaking table testing is greatly recognized [124]. In fact, shaking tables are considered as a fundamental device in earthquake and structural engineering for evaluating the dynamic performance of full- and reduced-scale structures under dynamic excitations similar to those induced by real earthquakes. Until now, there are only two shaking tables in the world which are large enough to test full-scale structures, the E-DEFENSE shaking table in Japan [96] and the NEES-UCSD shaking table in the USA [100]. Consequently, similitude and magnitude scaling methodologies are applied to produce a model ground motions testing the reduced-scale structures. In the two cases, shaking tables are aimed to reproduce the most realistic simulation of the predefined input motion at the tested specimen bases.

The type of input signals depends on the aim of the test. In general, the input signals which represent the reference accelerations are either recorded accelerations during earthquake, synthetic accelerations from attenuation and seismological study, or some sort of waveforms such as ambient vibrations, sinusoidal or random waves.

Various types of sensors and hardware are used to measure the response of the structure. Acceleration and displacement are often measured with strain-

gage acceleration sensors. Tri-axial geophones or voltage displacement transducers (LVDT's) can be placed on the structure to convert movement into voltage that can be recorded.

1.2. Typical components of a shaking table

Typically, a hydraulic shaking table is composed of three sub-systems: mechanical, hydraulic and electronic components [100]:

- The mechanical sub-system contains a movable platform representing the main body of the shaking table, on which is attached the tested structure, vertical and lateral bearings to guide the platform in motion, hold-down struts and actuators. These mechanical parts work as one rigid system operating in a defined frequency bandwidth, with a specific maximum acceleration amplitude and displacement.
- The hydraulic sub-system: considered as an arrangement of individual components interconnected, basically constituted by a power supply (pumps, accumulators, cooler, filter, reservoir, etc.), control elements (servo-valves, sensors, controller, etc.) and actuating elements (cylinder and/or motor). In a power supply stage of a standard valve-controlled hydraulic system, the pump converts mechanical power from the prime mover to hydraulic power at the actuator. The fluid storage and conditioning elements (filter, accumulator and cooler) ensure the efficient quality, quantity and cooling of the fluid. Then, the valves (controlled by a voltage current signal generated by the controller) are used to control the direction of the pump flow, the level of the power produced and the amount of fluid and pressure on the actuator. Finally, a linear actuator (cylinder) or rotary actuator (motor) converts the hydraulic power to usable mechanical power output [79].
- Finally, the electronic components are the controller, signal conditioning units, feedback sensors and accelerometers that provide the position and acceleration measurements from the platform, the actuators and the structure, and a data acquisition system to collect the measured data.

The interaction between these three subsystems is illustrated in Figure 1 [88].

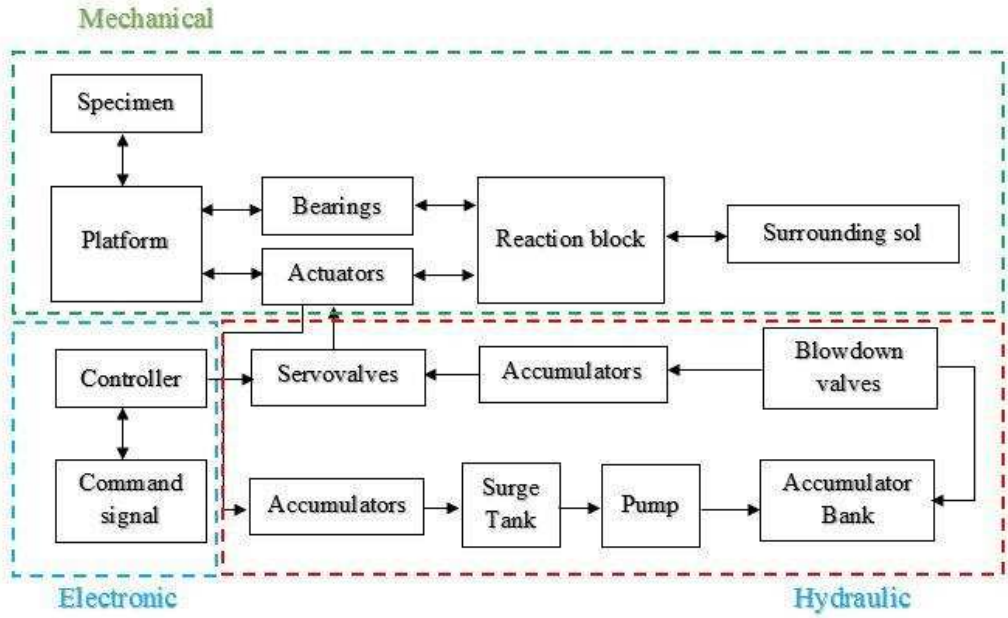

Figure 1: Interaction diagram between the shaking table subsystems [Credit: Moghaddam et al., 2014].

In order to simulate a desired signal on the shaking table platform, an electrical command signal is sent from the personal/connected computer to the controller. Then, the controller produces the appropriate control input to the servovalve which opens or closes the valve orifice allowing the circulation of the adequate hydraulic flow provided by the pump into the actuator. The fluid forces the actuator arm which is connected to the platform to move along the desired trajectory. Measurements are made from the different components to the personal computer for control purpose or data acquisition.

Nowadays, the shaking tables are known to be the most realistic and valuable experimental technique to evaluate the nonlinear behaviour of the tested structures under earthquake loads. However, the requirement of large forces and displacements in shaking tables, the nonlinear dynamic characteristics of the systems and the mutual influence between the different types of the shaking table components, have led to a main technical challenge in shaking table testing which is the high-fidelity in the reproduction of the desired acceleration on the platform. The most important causes that deteriorate the quality of signal reproduction in shaking tables are described briefly in the section below.

2. Problem statement

In shaking table tests, the seismic performance of structures and scaled buildings' models is assessed through base excitations until the structural condition reaches an ultimate level or collapse. In this conditions, the mounted specimen exhibits high nonlinear behaviours resulting in significant deterioration of the accuracy of the shaking table control system. Because the control precision determines the reality of earthquake replication and directly influences the performance research, the control system of the shaking table is known to be the key part of an effective shaking table test. Obtaining a highly accurate acceleration signal that matches closely the desired one is hard to achieve [183]. Due to the influence of the specimen behaviour, the cross-coupled characteristic, the system nonlinearities and external disturbances, the control system fails to achieve an accurate tracking performance for different reference signals under different loading conditions.

Few shaking tables operate in displacement mode in which the displacement feedback is used to control the platform trajectory. Since the seismic response of structures is driven by inertia forces, the aim of shaking tables is to reproduce on the platform prescribed acceleration signals, which are usually earthquake records. A proper displacement tracking does not necessarily lead to an efficient acceleration tracking, as a small variation in displacement in a short time may yield a significant error in the acceleration response [142, 158]. In general, the acceleration responses are usually distorted by phase delay, amplitude attenuation and harmonic distortions [180]. For some shaking table tests, the acceleration signal is reproduced with errors that can exceed 100% compared to the desired signal in terms of amplitudes [90]. Several studies avoid the use of direct acceleration measured signal as it is known to be inherently unstable and results in unacceptable table drifting phenomenon [91]. In fact, the real-time acceleration feedbacks are always accompanied by bigger noises and disturbances than displacements. To use acceleration signals, there are principally two approaches: direct use in feedback loop to improve the tracking error in combination with displacement and velocity measurements, and indirect use by an observer to compensate for time delay by filtering the noises in the measurements. Usually, the reference acceleration signal is converted to reference displacement signal by means of double integrating the acceleration signal and removing the corresponding drifting components. However, as the shaking table is meant to replicate reference

accelerations, the accuracy of the acceleration tracking remains practically difficult to achieve.

There are several interdependent sources that cause this undesirable waveform distortion in the measured accelerations. In general, the most important cause is the nonlinear behaviour of the entire system [104, 149]. It has been widely revealed that servo hydraulic systems contain inherent high nonlinearities [108]. The dynamic behaviour of the servo valves and the flow-pressure characteristics in the servo-valves, the relationship between the servo-valve control flow and the chambers pressures in the actuators, the oil leakage and several other hydraulic parameters uncertainties, lead to a significant deterioration of the signal replication. A large number of dynamic and nonlinear effects present in servo-hydraulic systems contribute significantly in affecting the control tracking performance of shaking tables. Nonlinear torque motor, nonlinear flow forces on flapper, spool dynamics, pressure dynamics, nonlinear flow forces on spool and so on, have been the object of nonlinear identification and modelling [162].

Another technical challenge that servo-hydraulic systems face, and shaking table in particular, is the nonlinear friction effect. A nonlinear relationship between the velocity and the friction force in the actuators [80], a high dry friction in the motors [51] as well as the hydraulic cylinder friction have been taken into account in recent researches. The nonlinear friction that has a time-varying characteristics highly deteriorates the dynamic performance of the entire system.

Moreover, as for every servo-hydraulic system, the external disturbances and internal uncertainties have a significant impact on the accuracy of the system output. Several estimation methods, such as UIO (Unknown Input Observer), DOC (Disturbance Observer) [46], POB (Perturbation Observer), ESO (Extend State Observer), have been used in order to estimate, and subsequently, cancel the external disturbances effects or attenuate them to an acceptable level. A history of disturbance cancellation is detailed in [166].

Despite the fact that several studies have aimed to improve the shaking tables' performance, the important impact that the mechanical coupling effect between the DOFs have on the control precision is often ignored [190]. Generally, 6DOFs shaking tables are controlled using more than six actuators, and hence has a greater stiffness than a serial connection of actuators [108]. Due to geometric effects, different electric

parameters and installation errors of eight actuators can cause a large dynamic internal coupling force in the shaking table system [107, 45].

The interaction between the shaking table and the mounted specimen is a major cause that deteriorates considerably the tracking control and even leads to the system instability. This interaction phenomena has been the focus of numerous research works that aimed to enhance shaking table performance. The strength of the interaction table-specimen mainly depends on the mass, stiffness and nonlinear characteristics of the specimen. Early studies have proved the sensitivity of the shaking table to the tested structure characteristics [24, 161]. A model of shaking table with and without specimen has been discussed [47]. The degree of flexibility of the payload as well as its mechanical properties and dynamic characteristics affect the accuracy of shaking table outputs. In fact, a strong dynamic interaction between the payload and the shaking table, especially important resonant vibrations between the payload and the oil column in the actuator frequently occur and affect the frequency response characteristics of the shaking table. The interaction effects are characterized by a peak-notch distortion in the amplitude-frequency response and a violent phase lag in a frequency band close to the natural frequency of the specimen [38]. For instance, it is stated that it is easier to achieve accurate seismic shaking table output for large-mass rigid specimen [47].

The effect of the payload behaviour over the accuracy of the signal reproduction is also observed through an overturning moment [118] caused in several cases when the center of gravity integrated with the table and the specimen does not match the action axis of the actuator. Moreover, the specimen often weighs far more than the table and when it exhibits plastic behaviour or collapse, a drastic variation in the table-specimen system parameters occurs.

The boundary conditions and the anchorage points between the platform and the payload as well as the local deformations between the platform and the payload during tests represent an additional sources of signal distortion that should be taken into account in order to enhance the quality of the replicated signals [70].

Most of shaking table tests are performed to study a nonlinear behaviour of tested specimen or investigate some collapse processes. However, the reaction force generated by a nonlinear specimen on the shaking table deteriorates considerably the shaking table motion accuracy [120]. Several developed works have been devoted to develop robust nonlinear controllers that take into account the nonlinear specimen

[178, 179] behaviour and compensate for the resonance in specimen responses resulting in significant errors between the desired and the measured shaking table signals [55, 184].

In a word, the inherent dynamic characteristics of the shaking table, the payload behaviour during the test and their nonlinear interaction deteriorate the accuracy of time histories reproduction by causing an important signal distortion that remains a large challenge for researchers and civil engineers. This undesired phenomena open the area to develop advanced control techniques in order to enhance the control system performance and the fidelity in signal replication. Numerous works study the applicability of different control algorithms to servo hydraulic shaking tables while recently, modern control techniques have attracted an important interest such as improved feedback control [128, 159], robust control [138], sliding mode control [21, 79], adaptive techniques [149, 136] and intelligent control [77, 10, 142, 186-188]. ,

3. Thesis scope

With the recent success of the Artificial Intelligence (AI) in control applications, and the advanced computation resources that allow the development of large computational models, the idea of implementing a novel methodology on shaking table control systems has credit to be investigated. This research study focuses on assessing the efficiency of a modern control methodology based on Neural Networks (NN) in improving the quality of the shaking table acceleration tracking performance.

NNs are powerful tools that are taking place through a large number of simple processing elements, build up complexity out of simple blocks. They adjust the connection weights between the nodes so that the output target is reproduced. Recently, the use of NN in control applications has extensively extended due to the tremendous online learning capabilities, robustness and adaptation to the process parameters variations. The main advantage of incorporating this type of intelligent algorithms is their efficiency to build up control laws suitable for dynamic, complex and nonlinear systems, without requiring any mathematical model of the controlled system. The difficulty of shaking table parameters identification has been an important motivation to conduct research on non-model based control methodology. It has been verified, through considerable research that has been made in using NNs in control applications, that NN can achieve significant improvement in motion control

performance. Consequently, a NN is used to increase the acceleration tracking accuracy of shaking table.

The starting point is the evaluation of the applicability of the proposed control methodology on a numerical framework of a simulated shaking table. That means that a first theoretical model of the used shaking table has been established using the model established by QUANSER, the laboratory equipment producer. The QUANSER shaking table is a high-powered bi-axial moving platform, actuated using three linear electric motors to achieve optimal position tracking performance. The given shaking table is controlled by a classic PD-feedforward (PDFF) controller to regulate the platform position. The theoretical model gives a simplified mathematical relationship between the platform position and the applied motor current. In a second stage, an estimated numerical model has been developed based on the experimental data collected through a significant program of real-time shaking table tests. A number of real earthquake records have been used as input signals on the QUANSER shaking table. These numerical models are used to carry out several simulations with realistic behaviour of the real shaking table in unloaded and loaded conditions. For instance, the numerical models can only be used to simplify the shaking table model and predict a similar response to the real measured acceleration outputs, taken into account the effect of the nonlinearities without including the explicit nonlinear parameters. Thus, a multi-layer feedforward NN is designed and trained offline using input-output data collected through numerical simulations. This numerical validation leads to an experimental evaluation of the performance of the proposed NN control algorithm through experimental real-time tests with the online implementation of the NN block. The performance of the proposed control scheme is assessed through several comparisons between the measured acceleration signal and the desired one, using the Root Mean Square Error (RMSE) as a main index assessment computed in time and frequency domains.

4. Outline of the thesis

An overview of the contents of the thesis are presented in this section.

- Chapter 1: Literature review

In this chapter, numerous control techniques that have been developed and applied to hydraulic servo systems in general and to shaking tables in particular are briefly described. The main purpose of this literature review is to provide a knowledge of the existing control techniques used in shaking table systems, from conventional classic controllers, advanced controllers, nonlinear controllers to hybrid and intelligent controllers, and situate the contribution of the proposed control methodology.

- Chapter 2: Shaking table modelling

Numerous models of shaking tables can be found in the literature. This chapter presents the most common modeling techniques of shaking tables based on the published research works. The shaking table used in this study, which is the QUANSER Shaking Table III is described. Also, the chapter presents the detailed theoretical model that will be developed on MATLAB/Simulink in the next chapter.

- Chapter 3: Numerical implementation of the NN-PDFF controller

The aim of this chapter is to provide a numerical framework of the implementation of the proposed control methodology in order to assess the potential of the NN control algorithm to enhance the acceleration tracking performance of shaking tables. Based on the results obtained through several simulations of two models of shaking tables under predefined earthquake records, the efficiency of the designed NN enables to implement it in real-time shaking table system.

- Chapter 4: Experimental implementation of the NN-PDFF controller

Numerous shaking table tests are carried out on the QUANSER STIII by applying different input signals. The analysis of the acceleration responses of the QUANSER STIII under several excitation signals, in time and frequency domains, indicate the nonlinear behaviour of the real system. The aim of this study is to implement the designed NN control algorithm in the MATLAB/Simulink-based control system of the

QUANSER STIII. The proposed controller runs in conjunction with the original PDFF controller. The experimental results of the closed-loop system controlled by the NN-PDFF controller, with considering two loading conditions are presented. By comparing the performance of the proposed control scheme with the performance of the original controller, the enhancement in the measured acceleration signals due to the neural control function is confirmed.

- Conclusion and future work

This last chapter provides a summary of the research findings, conclusions and recommendations for future work and research.

CHAPTER 1

LITERATURE REVIEW

1.1. Introduction

The shaking table can be simply defined as a means of dynamic testing with a platform to support specimens and capable of reproducing pre-defined dynamic signals. Although, there are electrical shakers, most of sizeable shaking tables are made of an assembly of electrohydraulic servo systems. Schematically, they are constituted of a hydraulic cylinder, a servo-valve, a moving platform and displacement and/or acceleration sensors providing direct measurements feedback. Nonlinearities that exist universally in electrohydraulic servo systems are a main problem which is not effectively solved yet. They are caused by inherent sources such as the dynamics of the electrohydraulic components, the hydraulic power mechanism, friction, dead zones and so on. Uncertainties, unknown and/or time-varying parameters, the coupling effects between the systems DOF, external disturbances, are among others sources that affect the accuracy of the shaking tables' control systems.

Modern control systems aim to track a reference trajectory point by point. In particular, the control purpose of shaking tables is to reproduce the expected acceleration signals, generally recorded ground motions from historical earthquakes, on the platform in real-time. However, high accuracy acceleration tracking performance is required, representing an extreme challenge in shaking table testing.

An important research interest has been dedicated to the development of efficient control techniques to drive efficiently electrohydraulic servo systems.

Typically, the control strategies in general can be classified into three categories:

- Classical control strategy (including PID control and improved PID control, TVC (Three-Variable-Controller), and so on);
- Modern control strategy (Nonlinear control, adaptive control, variable structure control, H2/H∞ robust control and so on);
- Intelligent control strategy (neural control, fuzzy control, neural fuzzy control, adaptive learning control and so on);

Numerous control technologies used for shaking table systems have been reviewed in [106] and [181]. In order to choose an appropriate control methodology for both

academic investigations and industrial applications, an overview of an experimental comparison between all these control approaches could be found in [127].
In this chapter, a brief literature review about some control approaches applied to servo hydraulic systems, and most specifically to shaking tables is described.

1.2. Control strategies: a review

1.2.1. Classical control strategies

1.2.1.1. PID controller

The most practical and common feedback controller used in industrial devices is no doubt the PID controller due to its simple structure, low cost and easy implementation. Traditionally, the shaking table motion has been controlled by a classic PID controller for many years. The input is the reference signal to be tracked and the output is the measured response as schematized in Figure 1.1. The basic expression of a PID controller in time domain is given in Equation 1.1.

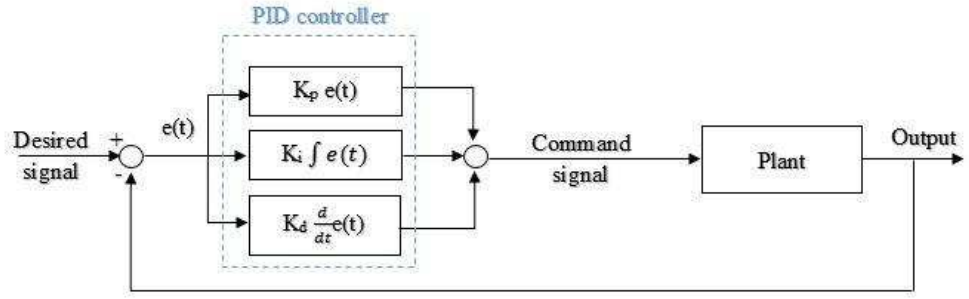

Figure 1.1: PID feedback control scheme.

$$u(t) = K_p e + K_d \frac{de}{dt} + K_i \int e\, dt \qquad (1.1)$$

The PID uses the proportional, derivative and integral gains, i.e. Kp, Kd and Ki, to minimize the error signal e that represents a direct difference between these two signals. In theory, the proportional gain provides accurate tracking, the derivative gain compensates the phase lag and the integral gain reduces the steady-state error [169].

Since the 80s, a wide-investigated PID tuning literature has been developed. Tuning the PID gains and defining appropriate values using basic tuning rules that have been developed and largely used, is a simple task that can achieve a satisfactory performance for simple linear, stationary and deterministic systems.

The common design and tuning of the PID assumes that the controlled system parameters are a priori known and remain unchanged during the test. This assumption makes its application in industrial systems, including shaking tables and electrohydraulic servo systems inappropriate [117]. In fact, as the constant gains values are defined prior to the test, the control scheme is considered out of real-time [94] and assures only local stability.

Therefore, the re-tuning of the PID gains is an obvious technique to adjust the controller to the process time-varying parameters. Performed through trial and error method, the re-tuning is a time consuming procedure and it requires a skillful operator [126]. The auto-tuning PID controllers have been explored lately, leading to the development of more advanced control algorithms, detailed in the sections below.

Moreover, a great number of studies have stated the inability of the PID controller to control nonlinear systems, time-delayed systems and time-varying systems [19, 30, 101, 82, 143] and to achieve the requirements of earthquake engineering in term of high control performance and large control bandwidth [79, 155].

It is well-known that even if the PID controller provides reasonable robustness in the low frequency range and shows a satisfying displacement tracking performance, the accuracy of the acceleration reproduction is not guaranteed over a certain frequency bandwidth of interest [18, 176]. Yet, as the target signal of shaking table is acceleration signal, high-frequency control performance is poorer when the PID controller based on displacement control is adopted, causing large waveform distortion [41].

A common strategy to achieve higher performance when using the PID controller in complex systems is the linearization of the controlled plants. Due to the linearization of the system, significant dynamic parameters are lost, such as the change of viscosity and the bulk modulus of the elasticity of hydraulic oil, fluid compressibility, servo valve flow-pressure, dead band,

variations in supply pressure and control volumes, stiffness, leakage and friction [48].

Consequently, more advanced control algorithms have been developed in order to deal with the high nonlinear properties of shaking tables.

1.2.1.2. Three-Variable-Control (TVC)

In order to improve the addressed shortcomings of the PID controller, a TVC controller, also known as a Three-State-Feedback controller, has been proposed. The TVC consists of a feedback and a feedforward controller, based on displacement, velocity and acceleration variables. Thus, six parameters have to be adjusted: the displacement to control low frequency, the velocity to control the mid-frequency and the acceleration to control the high frequency. A simplified diagram is depicted in Figure 1.2.

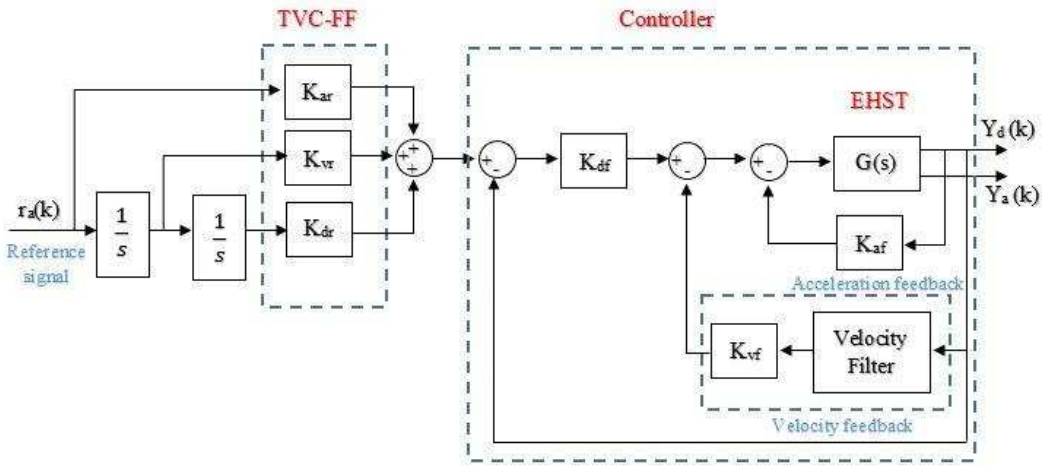

Figure 1.2: Block diagram of a basic TVC (credit: Shen et al., 2016).

As can be seen from the figure, the TVC feedback signal consisting of displacement, velocity and acceleration, and the displacement and acceleration signal are directly acquired by sensors, i.e. displacement is measured by an LVDT and acceleration is measured by an accelerometer mounted on the table, The velocity feedback signal is synthesized using a low-pass filter with the displacement and a high pass-filter with the acceleration. K_{vf}, K_{df} and K_{af} are the three feedback parameters, while K_{dr}, K_{vr} and K_{ar} are the three feedforward parameters, respectively. The signal

$r_d(k)$ is the reference position signal and $y_d(k)$ is the output position signal; $r_a(k)$ is the reference acceleration signal.

Compared to the PID, the conventional TVC controller has drawn a lot of attention and has been employed in several large shaking tables such as the E-DEFENSE (Japan) and the CGS shaking table (Algeria) [128, 130, 133, 159, 181]. The principle is to replace the unwanted dynamics with the desired dynamics [153]. It has shown great capabilities to extend the frequency bandwidth of the closed-loop acceleration response [127], improve the stability of the entire system and increase the system damping ratio [176].

Various comparisons between the performance achieved by a PID-controlled and a TVC-controlled system have been performed. In a simulation framework built in Simulink, a basic comparison between the tracking responses for the Irpinia Italy earthquake record of the plant for both PID and TVC controllers has been illustrated in Figure 2.3, showing a clear tracking enhancement with the TVC, in both time and frequency responses. Figure 1.3 is reported from [79].

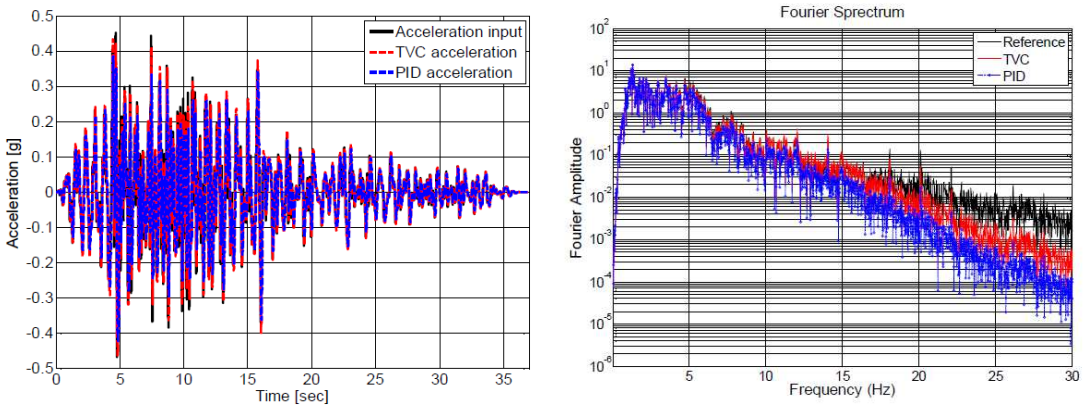

(a) (b)

Figure 1.3: (a) Time domain (b) frequency domain comparison between a TVC and PID controllers [J.Y., Lin, 2017].

However, the TVC remains imperfect because it is still a fixed-gains control method and shows numerous drawbacks in the acceleration tracking accuracy as it is significantly affected by the nonlinear characteristics of electrohydraulic servo systems.

1.2.2. Modern control techniques

1.2.2.1. Adaptive Control (AC)

An adaptive control attempts to avoid degradation of the dynamic performance of a control system when environmental variations occur. While the feedback control system aims to eliminate the effect of state perturbation, the adaptive control system aims to eliminate the effect of structural perturbation upon the performance of the control system. It consists of three functions: identification of the dynamic characteristics of the plant, a decision making based on the identification of the plant, modification or activation based on the decision made. A block diagram of an adaptive control system is depicted in Figure 1.4.

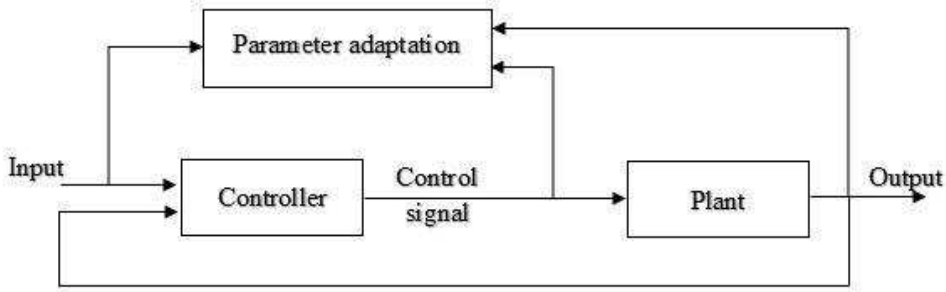

Figure 1.4: A block diagram of an adaptive control system.

Early published academic works have introduced the concept of adaptive controllers applied to hydraulic servo systems, proposing two types of adaptive control schemes: the self-regulation adaptive control and the model reference adaptive control [31].

The MRC is the most common adaptive control approach, designed to adapt to changing characteristics of the plant. It can considerably cope with nonlinear behavior by tuning its internal parameters (gains) during the test performance. Studies have shown number of advantages of the MRC in tracking control problems and have guaranteed the easiness of its implementation, its stability and the convergence of the plant, even if its parameters are unknown [65].

Even if the adaptive controllers have progressively emerged in industries since the last quarter of the 20th century, its first use in earthquake

engineering has been in 1992 when Stoten and Gomez (2001) applied Stoten's adaptive Minimal Control Synthesis (MCS) to a group of European shaking tables [148, 149]. This algorithm has been implemented in a small-scale and medium-scale shaking table to obtain a guideline of enhancing control systems by using a large-scale shaking table [136].

Among adaptive techniques, the advantages of using the MCS for shaking table has been cited in their valuable research work as listed in [149]: No knowledge of the shaking table dynamics is necessary, which represents a great advantage since the dynamics of the table is strongly dependent on the specimen and on its working regime as well, the stability and robustness of the adaptive algorithm have been formally proven and tested [147, 148], the capability to cope with internal parameter variations, external disturbances due to the specimen parametric changes and nonlinear dynamics, which shaking tables exhibit over their range of operation. In addition to this, many shaking-table experiments are carried out in order to research the nonlinear behaviour of materials and models, a regime that is difficult to explore using conventional analytical methods. Also, the MCS can be used on a 'self-tune and lock' basis, allowing it to work as a virtual fixed-gain controller during the test itself. The tuning, however, is conducted in a precise and automated manner prior to the test. This contrasts with the standard tuning process of a conventional controller, which relies almost exclusively on the expertise of the shaking-table operator.

Other types of adaptive control methodologies have been developed and applied to shaking tables. An adaptive controller based on an adaptive notch filter has been developed to compensate for disturbances caused by the reaction forces generated by a specimen during the shaking table tests [120].

According to adaptive control laws, a staple backstepping adaptive control technique is applied in real-time hybrid simulation (RTHS) to generate a command trajectory to a servo hydraulic system with unknown dynamics and frequency-dependent time lags caused by the interaction of numerical and experimental components [99].

Some popular adaptive control methodologies use the model reference adaptive control in which stable control of the system parameters is

achieved by comparing the output signal with the output signal of the object reference model. The difference between these signals is the starting point aimed to be minimized by the controller settings.

In early published works, the performance of an adaptive control applied to an electrohydraulic servo system, incorporating internal model principle for asymptotic tracking performance of systems with uncertainties, unmodelled dynamics and disturbances, has been examined under periodic loads [152]. An indirect adaptive model reference control algorithm has been applied to a position tracking and disturbance rejection for hydraulic actuators [192] and experimental results have confirmed the adaptive controller's ability to deal with the deadband and the nonlinear opening characteristics of the valves.

The effectiveness of an adaptive controller used in an electrohydraulic servo controller has been examined theoretically and experimentally, proving that the main advantage of the adaptive control scheme is its universal use in both laboratory and industrial applications [171].

An online adaptive controller has been combined with an offline inverse compensation model and applied to a six DOF electrohydraulic shaking table which has considerably improved the acceleration frequency bandwidth and tracking accuracy of the system [129]. This proposed control scheme has associated the benefits of the offline compensation and the online adaptive control and has achieved a fast rate of convergence and an accuracy in acceleration signal reproduction.

A model reference adaptive control (MRAC) has been implemented to position control of a loaded shaking table [36] accompanied with a Smith predictor to compensate the error produced by the system time delay.

The time response and the acceleration tracking performance of a hydraulic actuator has been improved with a composed PID controller and a Model Reference Adaptive Control [195] and results have shown a faster time response at the transient phase and better tracking performance.

As a critical control challenge, the change in the specimen dynamics during the test leads to a change in the frequency response characteristics of electrohydraulic servo systems. Another common adaptive approach includes the adaptive inverse control (AIC) algorithm, which has shown an

efficient performance to reproduce the reference shock pulse even if the specimen characteristics vary considerably during the test [62].

A high fidelity acceleration waveform replication has been achieved on an electrohydraulic servo system by combining an AIC with an offline feedforward compensator [128].

The tracking accuracy of an electrohydraulic shaking table has been reached by combining a feedforward inverse model to extend the system frequency bandwidth with an AIC to adaptively adjust the time-domain drive signal [131].

A combined control framework has been developed to improve the electrohydraulic shaking table performance. The proposed controller constituted by an AIC feedforward controller for the acceleration closed-loop ITF estimation, combined with an improved IMC as a modeling error estimator, has shown great capabilities in extending the frequency bandwidth of an electrohydraulic shaking table system, overcoming the stability problem, improving the acceleration real data replication and minimizing the system uncertainties [132].

The merits of an AIC and the advantages of MCS control algorithm have been experimentally proven to be powerful in enhancing the position closed-loop system frequency range and improving its tracking performance [134].

A direct method of adaptive control has been applied to single input single output (SISO) stable and unstable systems [37]. The Recursive Least Square (RLS) algorithm has been used to online adjust the PID gains in order to force the process to behave like the reference model. Results have confirmed the tracking capability and robustness against process variation of the used controller.

Even if the adaptive control approaches exhibit a high-quality waveform replication of the desired signals on shaking tables, a great robustness against specimen dynamics and an effective cancellation of the shaking table dynamics [27], inefficient adaptation may occur, especially when rapid parameter variations occur in the controlled system. In fact, a high-quality waveform replication of the desired signals can be obtained but this is often accompanied by a poor transient response when it is initiated.

1.2.2.2. Nonlinear control

Several research works have highlighted the numerous disadvantages of conventional linear controllers in industrial processes and their mediocre performance tracking in real-world controlled systems as they are highly nonlinear.

In order to improve the tracking performance of electrohydraulic servo systems and dealing with their dynamic characteristics, early works have proposed a switch control which is switching between position control loop and speed control loop based on the actual position error. Results have shown that the nonlinear switch control strategy has excellent robustness against inertia load changes [83, 163].

The development of nonlinear control algorithms has continued to expand until recently. Various control approaches have been designed and incorporated to improve the shaking table control stability, especially when the interaction between the table and specimen is important and when the specimen reaches high nonlinear states. Based on Lyapunov stability theorem, a nonlinear control strategy has achieved an excellent control tracking performance when applied to a shaking table with a nonlinear SDOF specimen [178]. The objective of the proposed nonlinear control was to take into account the nonlinear response, the model uncertainties and various disturbances that affect the test while being performed.

In order to compensate the reaction force and disturbances caused by a nonlinear specimen in real-time, a nonlinear control methodology has presented high efficiency in maintaining desired accelerations of the shaking table [29].

A real-time compensation technique of the reaction algorithm has been proposed to address the disadvantages of the interaction between the shaking table and a SDOF specimen by developing a theoretical model of the specimen [160].

A force feedback compensation technique has been proposed to reduce the interaction between dual shaking tables and specimen and improve the reproductive accuracy of the shaking tables [73].

Further studies have developed sophisticated control algorithm to deal with the nonlinear interaction between the specimen and the shaking table. A Nonlinear Single-Based Control (NSBC) has been applied to nonlinear MDOF systems and has showed great capabilities to deal with nonlinearities and time-varying system properties. This approach can be simply designed based on classical control theory and expressed using transfer functions, requiring a minimum amount of information about the nonlinearities in the system [34].

A nonlinear robust adaptive control has presented a high position tracking performance when applied to a symmetric double acting electrohydraulic servo-drive system, by taking into account the nonlinearities associated with hydraulic dynamics, parametric uncertainties as well as uncertain nonlinearities from uncompensated friction dry forces [138].

Originated from Lyapunov theory, a popular nonlinear control technique which is the sliding mode control (SMC), is a common approach used for conducting nonlinear stability analyses and control designs. Studies have showed that systems with sliding modes are an efficient tool to control complex high-order nonlinear dynamic plants operating under uncertainty conditions, a common problem for many processes of modern technology. In addition, the SMC features remarkable properties of accuracy, robustness and easy tuning and implementation [79].

The SMC has largely been investigated in early studies, trying to address the Variable Structural Control chattering problems [81] of hydraulic servo systems and compensating for the nonlinear friction effects [21, 23].

A time-varying SMC algorithm has been applied to an electrohydraulic servo system to deal with the uncertainties and disturbances [43], presenting a satisfying position tracking performance and global robustness.

A nonlinear adaptive SMC has been highly efficient to compensate the nonlinear uncertain parameters of an electrohydraulic servo system [44, 72].

A SMC has demonstrated a high effectiveness and stability to accurately control a piston position through a desired path with a broad range of the load mass variation [2].

To solve the tracking problems of electrohydraulic servo systems with nonlinearities and uncertainties, the implementation of robust controllers

such as the SMC to shaking tables has significantly increased. A robust SMC based on computed torque control design has been designed and applied to a two-axis motion control system and has significantly enhanced the motion tracking performance, the robustness of the system to parameter variations, external disturbances, cross-coupled interference and friction force [77].

A nonlinear robust control constituted by a SMC has been designed and implemented on a multi-purpose earthquake simulator, showing experimentally the stability of the control approach and its important efficiency in the reduction of position tracking errors [150].

A fuzzy-sliding-mode supervisory controller has been designed and implemented to control a shaking table, showing a successful performance at robust tracking of some harmonic and seismic excitations in the presence of parametric uncertainties [142].

A novel adaptive reaching law sliding mode controller (ARLSMC) for double shaking tables system with parameter uncertainty and disturbance, combining a SMC based on a novel adaptive reaching law to improve dynamic performance with an adaptive controller to estimate the uncertain parameters online has proved to have a fast dynamic response performance, a high control precision, a strong robustness, and a great capability in reducing the system chattering [189].

1.2.2.3. Advanced model-based compensation techniques

To further improve the performance of standard controllers, researchers have already put forward a series of advanced compensation control algorithms with the main scope of improving the tracking performance of shaking tables.

A reaction force compensation technique has been combined with a disturbance observer-based control have been proposed to take into account the nonlinear behavior of the specimen [55].

Another practical control methodology to compensate for the influence of the specimen on the shaking table and achieve the disturbance suppression

performance was to identify the frequency online using a feedback compensator based on an adaptive notch filter [119, 122].

A model-based control approaches have proven good performance for a wide range of operating conditions. The process of tuning a model-based-controller reduces to adjusting a simple bandwidth knob in order to achieve the desired performance for the specific application. The main advantage of this controller is the superior performance that is achieved, which is very important advantage for the customers in today's manufacturing environment.

As an efficient shaking table delay compensation technique, a feedforward compensation method has been developed in order to compensate for high frequency actuator dynamics and time delays in RTHS [104], using an inverse model of the closed-loop shaking table.

The experimental implementation of the model-based multi-metric feedback control strategy has improved the tracking of the desired acceleration signal for a shaking table loaded with both linear and nonlinear specimen, by improving the peak acceleration matching and reducing the high frequency oscillations.

A model-based actuator delay compensation technique has been used to predict the future response of the entire structure and send the command signal (displacement signal) to the shaking table at each sampling time. This compensation technique has shown great capabilities to address the actuator dynamics and time delay if this latter is constant and an experimental comparison between the uncompensated and compensated shaking table responses has been investigated [144].

The development of another type of real-time compensation technique which is the Infinite-Impulse-Response (IIR) has shown powerful capabilities for compensating shaking table time delays as well as the effects of complex control-structure-interaction [146].

A friction compensation method based on the LuGre model has been designed for a hydraulic shaking table system using the control theory of backstepping integral and the Lyapunov stability theory to ensure global asymptotic stability of the closed-loop system [157]. The effectiveness of the controller has been verified through experimental tests proven its capabilities

to compensate for unknown interference and the friction properties of the system, to achieve a higher acceleration tracking accuracy and to improve the correlation between the reproduced signals and the desired ones.

Some advanced control techniques constituted by a cascade control and a notch filter has been widely used [75]. This control methodology has proven its capability to achieve a higher level of control especially in presence of backlash or resonance. The controlled variable, typically the position, constitutes the robust control loop while the outer controller represents the classic controller and a notch filter to compensate the system resonances. The frequency bandwidth and the stability of the control have been increased while the sensitivity to the dynamic behaviour of the specimen has been reduced.

1.2.3. Intelligent control

1.2.3.1. Neural Networks (NN)-based control

1.2.3.1.1. PID-based NN

The PID still remains the most common and popular controller used in industrial applications. Its great success is due to its simple structure and easy implementation. A number of tuning methods exists in order to tune the PID parameters in the best way. The necessity of retuning the PID is almost unavoidable as the system parameters change during the process. The inconvenient of re-tuning the PID through a trial and error procedure which is time consuming and requires skillful operators, has led to the development of adaptive controllers and more specifically PID-based NN. The ability of the NNs to approximate any nonlinear functions have become extensively used in the control of nonlinear processes. In fact, Neural Networks (NN) have become one of the most popular field of study nowadays. From the perspective of control engineering, NNs should be viewed as nonlinearities tuners. The typical structure of a PIDNN controller is illustrated in Figure 1.5.

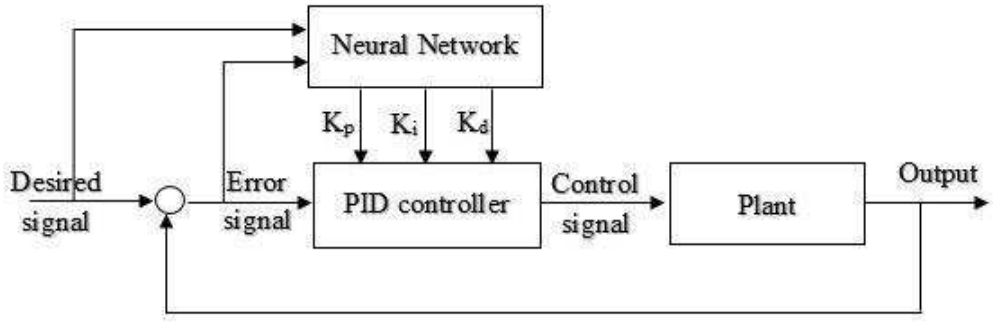

Figure 1.5: PIDNN structure.

The usual idea while combining Neural Networks (NN) within a PID controller was first proposed by Huaillin et al., (2000) in order to tune the PID gains. The structure of the PIDNN itself is still a PID structure. The hidden layer of the NN works simply as a PID controller through their activation functions. This easy-designed control methodology, has been widely used for multivariable nonlinear multi-input-multi-output (MIMO) processes. The NN weights are automatically updated according to the errors of the closed-loop system, and the controller helps to implement nonlinear and adaptive real-time online control for the controlled system. A comparative study between a direct PIDNN and two other conventional adaptive PID has been performed [126]. The direct PIDNN that performs an adaptive control through online learning process has shown a higher performance and robustness over the classic cancellation and pole placement controllers in the case of model mismatch and also process with non-minimum pole behavior.

A PID based-NN has been successfully applied to speed control a brushless DC while the PID tuning procedure has been performed using NNs [164].

An adaptive PID-based NN (APID-NN) controller has been used to establish a unified framework to get fast better tracking performance of a nonlinear control system, by combining an adaptive PID with a NN indirect adaptive control (NN-AIC) [141]. In a later study, the effectiveness of a combined adaptive PID controller with an explicit neural structure has been confirmed for a nonlinear MIMO system, where the NN weights are updated online in order to select the suitable values

of the PID gains [140]. Results have demonstrated that the controller has achieved an improved and stable tracking performance.

Higher speed response, stronger robustness and dynamic decoupling effect have been addressed using an adaptive PID decoupling control based on Radial Basis Function (RBF) NN in a quadrotor aircraft, when the online PID tuning process has been performed using the self-learning ability of RBFNN and the corresponding decoupling control algorithm is performed by a conventional PID controller [49].

A new control technique for nonlinear system has been investigated using a closed-loop control system consisting of two NNs [5]. The first NN is a feedforward NN that is employed as a predictive hybrid model of the plant. The second NN is a PID-based NN which has been pre-trained offline as an inverse black box model of the plant.

The simple structure of the adaptive PIDNN controller has provided a gain in computation time and has proven its effectiveness not only for set point tracking and stability but also for the process robustness through an optimal online tuning of the PID parameters [193].

An adaptive PIDNN controller used with a Particle Swarm optimization (PSO) in a complex nonlinear MIMO system with a strong coupling effect, has been able to obtain high precision with shorter time [60].

A PIDNN controller has been designed for an air supply channel of a coal-gas furnace [20]. The control scheme constituted by a feedforward pre-trained NN used for auto-tuning and a PID in parallel, has shown high trajectory tracking performance.

1.2.3.1.2. Model Reference Adaptive Control (MRAC)

As seen in several works, neural networks are widely used for modeling and controlling complex physical systems because of their high ability to handle complex input-output mapping without the need of detailed analytical models of the controlled plant.

A popular NN-based controller is a Model Reference Adaptive Controller (MRAC), generally used to control nonlinear systems. An early study has proposed a learning multilayer feedforward NN used as direct adaptive

controller for different nonlinear plants [8]. Another combination of NN and a robust MRAC has been effective in controlling a nonlinear electro-pneumatic servo system [156]. The NN has been used to compensate for constructing a linearized model of the nonlinear plant while the MRAC has performed the model-matching for the uncertain linearized model to a given linear reference model.

A Model Reference Adaptive PID controller, based on Radial Basis Function Neural Networks (RBFNN), has been developed to improve the performance of a hydraulic parallel robot. The RBFNN has been used to identify the hydraulic servo-system and update the PID gains online in order to make the control more adaptive and results have shown the robustness enhancement of the system [103].

A direct Model Reference neural adaptive controller has shown high performance in controlling a highly time-varying nonlinear plants with noise effect [35]. Using a multilayer perceptron network topology, the control strategy has defined the adaptation control law based on the convergence of the tracking error between the actual plant output and the target output which is the response of the reference model.

A MRAC has also been used for a nonlinear hydraulic servo system, achieving a significant elimination of the steady-state error, a fast response and a less overshoot [112].

A composite controller of a nonlinear NN with a continuous Robust Integral Signal Error (RISE) feedback controller has achieved a semi-global asymptotic stability when applied to hydraulic systems with heavy disturbances, including parametric uncertainties and unknown disturbances [186]. The feedforward NN has been used based on MRAC structure, to have a compensation for unknown state-dependent disturbances and to further improve the accuracy of the feedforward compensation.

An effective NNMRAC, consisting of a conventional PID and a NN inverse dynamic compensator has been applied to servo systems, affirming its ability to compensate for the nonlinear dynamics of the plant and for nonlinear disturbances [98].

A high tracking precision of nonlinear servo system has been achieved by using a MRAC and a NN controller in a flight simulator [52]. The online NN implemented in the velocity-loop was aimed to reduce unknown models dynamics, parameter variations and disturbances and to adjust the system to track the nominal velocity-loop reference model. The robust MRAC has been used to guarantee the global steady.

The performance of a new neuro-adaptive controller has been investigated through a designed deep NN based-MRAC applied to a 6-DOF quadrotor [57]. The proposed neuro-adaptive controller has presented a high performance in achieving reference model tracking, robustness and stability.

As it is shown, the fast learning and robustness of NNs have made them suitable for several neural control applications. A Model Reference adaptive Position Control has been designed and applied for an electrohydraulic servo valve system [187] using a feedforward NN showing a very successful and robust control performance over the traditional PID controller.

1.2.3.2. Fuzzy Logic-based control

It is found that using hybrid control techniques based on the combination of traditional controllers and intelligent algorithms such as the Fuzzy Logic, has been an efficient tool to achieve high control performance of nonlinear systems. Fuzzy control algorithm is based on the linguistic variables - the human thought process; the input signal is fuzzified at first, then goes through the fuzzy reasoning process under operational experience and expert knowledge, and finally the control signal is defuzzified and sent out [12]. In the literature, several researches stated that Fuzzy Logic Control (FLC) has already been successful in many control areas. It produces better performance over conventional controllers such as the PID for the most parts in regards to the time response and settling time [26].

A critical evaluation of the FLC and the PID controller both applied in electrohydraulic servo actuator, has ended with the conclusion that the FLC

achieves a faster response, has no oscillations and then is more suitable for many important and high precision applications [1].

A robust fuzzy-neural-network (FNN) sliding-mode control based on computed-torque control design has been applied to a two-axis motion control system in XY table, proving the robustness of the dynamic behaviors of the proposed controller with regard to uncertainties [76].

An integrated hybrid fuzzy controller design has been developed for a dual-cylinder electrohydraulic lifting system, in order to achieve a synchronized positioning objective with unbalanced loadings, uncertainties and disturbances [17].

In position control applications, the FLC has been extensively successful. A Fuzzy Logic Controller has been developed for position control of a servo motor [85, 110] given a better dynamic performance and providing more robustness for industrial position control drive applications.

An accurate tracking performance has been achieved for an electrohydraulic actuator system using a FLC optimized by Particle Swarm Optimization PSO algorithm [170]. The study has shown that the proposed control technique has been able to overcome the nonlinearities and uncertainties in the system and achieve accurate tracking reference trajectories.

Another study has described the effectiveness of the application of a FL position control to an electrohydraulic servo system, where the mathematical model of the system included an internal leakage [59].

A PI-like Fuzzy Logic position intelligent Control has been developed to control the position of a nonlinear electrohydraulic servo-actuator in a military aircraft in order to get a desired position during a specific time with the requirement of a minimum steady state error, settling time and oscillations in the position response [61].

A fuzzy gain-scheduling position controller has been efficient in reducing the error of position reference tracking in a flexible load servo hydraulic system and increasing the system damping [188].

The possibility to apply a self-learning Fuzzy algorithm for position control of a hydraulic servo drive has been discussed [28]. A self-tuning Fuzzy PID controller has been developed to enhance the performance of an electrohydraulic actuator, when the FL has been used to tune each parameter

of the PID controller, based on the mathematical model of the system [194]. The main disadvantage of this proposed control methodology is that it has not taken into account the load of the hydraulic system, the friction in the hydraulic cylinder and the leakage in the hydraulic actuator system.

A complex control strategy of main controller combined with FLC based on wavelet transform has been applied to a multi-variable electrohydraulic servo system. A NN containing the PID control tuning rules has played a leading role in the whole system while the FLC has been used as a compensation technique to ensure rapid response of the system [137]. The proposed combined controller has achieved its main goal which was to eliminate the mutual interference between the different closed-loops of the system and the influence of load variation and external disturbances.

The promising results achieved by Fuzzy Logic Controllers, their simple operational methodology and their adoption of fuzzy language to describe the dynamic characteristics of the system, have made them more attractive for shaking table implementation. The performance of a FL to structural vibration control of earthquake-excited and wind-excited 1 DOF and 2DOFs models has been investigated on a small shaking table [40]. Results have proven that the Fuzzy active Control has been practical and robust but in order to make the proposed control more practical, the tuning parameters and shapes of membership functions in the fuzzy inference rules was needed.

A FLC has been designed and implemented on a shaking table based on the data feedback value of the drive to achieve desired motor speed with different loads intensity [10].

Successful performance has been achieved by designing and implementing a Fuzzy-Sliding-Mode supervisory controller on an electric seismic shaking table [142]. The aim of the proposed controller was to develop a robust tracking of predefined earthquake records in presence of model uncertainties and unmodeled dynamics.

As it can be seen through the overall works dedicated to the Fuzzy Logic control methodology, the later is highly promising for structural control. However, it requires a substantial computational power due to the complexity of the controlled process. Dealing with fuzzification, rule base, inference mechanism

and defuzzification operations, larger set of rules lead to a more accurate control at the expense of longer computational time [54].

1.2.3.3. Genetic Algorithm-based control

Genetic Algorithm has been recently used as a modern alternative optimization tool to conventional methods. The suitability of using GA towards various types of control system engineering has been discussed [39]. Different from normal optimization technique and search procedures, GAs has shown significant capabilities for global optimization, powerful searching capabilities and good control robustness, as it can be reviewed in [114].

The idea of using GA for feedback control gains optimization has continued to extend from the late 90s. Finding optimal gain values has always been an extremely time-consuming trial-and-error task. An optimization feedback gains based on GA has been proposed for a double-loop controller for the speed control of an over-centered variable-displacement hydraulic motor [53].

GA-based optimization method has been used to design a feedback controller for shaking table system [42]. The methodology has been evaluated using two fitness indexes to ensure the required performance that are the feedback controller stability and disturbance suppression performance, as well as the servo characteristic.

Though many algorithms found in the literature to tune the PID parameters, a number of successful applications of GAs have been reported. Early studies have proposed the use of GAs in PID tuning process [97, 109, 165]. For example, an experimental evaluation of a tuning method, using GA to provide optimal PID parameters online for a seesaw system modeled by NNs [173].

In number of published works, a typical use of GA with PID has been investigated through simulated models. Parameters optimization has been carried out for a small helicopter based on the stability and adaptability of the system [168]. An adaptive GA has been successful to find the optimal PID gains considering the stable convergence while keeping the population diversity and enhancing the local search abilities [74].

A real-coded GA (RGA) technique has been applied for system identification and control tuning for a model reference adaptive control (MRAC) for a hybrid

tank system [7]. A self-tuning PID controller based on GA has been developed and implemented using adaptive mutation and crossover probabilities to avoid premature convergence [78]. Tuning parameters of a fuzzy-PID controller has been performed using GA for high order plants with time delays [102].

The speed and position control of a DC servo motor using a GA tuned PID controller, providing an improved performance in terms of time specification such as settling time and rise time [86].

A comparison between a PID gains tuning based on GA and a classic tuned PID using Ziegler and Nichols method has been carried out to evaluate the tracking force control performance of an electrohydraulic system [175].

GA has also been used in vibration control. In an early study, a GA-based control method has been used on an active mass driver system to attenuate the responses of a structure under seismic excitation. The results have shown a better performance and robustness of this controller over other control methodologies [64].

In order to increase the reliability, controllability and utilizing the high speed of response achievable from electrohydraulic systems, a GA optimization technique has been extensively used in number of studies, in order to tune optimally the three gains of a PID [4, 33, 174]. The obtained results have shown that the developed controller has been able to overcome system nonlinearities, achieve a minimum settling time with no overshoot and nearly zero steady state error.

A model combining the advantages of an adaptive GA and a modified Newton method has been developed for system identification and vibration suppression of a building structure with an active mass damper. The GA with adaptive reproduction, crossover and mutation operators has been useful to search for initial weight and bias of the NN, while the modified Newton method has been used to increase the NN training performance [16]. The proposed controller has shown an interesting performance and robustness against variations in system parameters.

A main shortcoming for a standard GA algorithm may be a pre-maturity and stagnation while looking for a global optimal solution [56].

1.3. Conclusion

A shaking table is an experimental tool meant to replicate dynamic loads in order to evaluate the seismic performance of structures through base excitations. The complexity of the system, the inherent nonlinearities, the internal coupling effect between DOFs, the nonlinear interaction between the specimen and the table, the nonlinear behavior of the tested specimen and so on, lead to significant difficulties in signal replication. The distortion between the command signal and the measured signal is considerably affecting the accuracy and reliability of the real shaking table tests. In fact, the utility of the shaking table tests to study the dynamic behavior of structures depends on the capacity of the table, on which the structure is mounted, to faithfully reproduce motions whose effects are important to analyze. Therefore, the requirement of designing and implementing robust control systems rendering an accurate tracking control to drive the table along a selected signal is an important research area.

A vast array of compensation techniques for acceleration signal replication, such as Feedforward-Inverse-Model-Control (FIMC) have been successfully employed to cancel out the dynamic characteristics of the shaking table. Based on the estimated transfer function model and the designed inverse model of the acceleration closed-loop system, the main disadvantage of these compensation techniques is the fact that the transfer function model as well as the inverse model of the shaking table must be accurate. Then, the shaking table needs repetitive excitations that will damage the specimen before testing it at the desired amplitude excitation.

Numerous investigations have turn to adaptive control methodologies, such as the Adaptive Inverse Control (AIC) and the Minimal Control Synthesis (MCS). A high quality waveform replication accuracy can be achieved after converging to their optimal solution, even with internal parameter variations, external disturbances due to the specimen parametric changes and nonlinear dynamics. However, they can exhibit poor transient response when they are initiated, especially when the frequency bandwidth of the desired acceleration exceeds the frequency bandwidth of the acceleration closed-loop system of the shaking table.

More advanced control strategies, such as nonlinear controllers, have been designed and implemented to further improve the acceleration tracking performance of the

shaking table, dealing with system nonlinearities, uncertainties, internal friction forces and external unmodeled disturbances.

Recently, the investigation in intelligent controllers has drew a lot of attention. Developing hybrid controllers, as a combination between conventional controllers and intelligent control algorithms for gains tuning and parameters optimization objectives, as well as an outer-loop controller to shape the command signals, has unanimously established a conclusion that these controllers achieve a better tracking performance for nonlinear systems. Numerous studies have shown their promising results in terms of robustness, stability and control performance when applied to complex servo systems. This thesis is a continuing effort in implementing intelligent algorithms to enhance the performance of shaking tables in reproducing accurate seismic acceleration time histories.

CHAPTER 2

SHAKING TABLE SYSTEM MODELING

2.1. Introduction

In order to understand the shaking table challenges and limitations, but also to properly design a tuned controller able to replicate the desired trajectories with a minimum of errors, modeling of shaking tables is required. Methods for the dynamic modelling of servo-hydraulic systems have been developed over a number of decades. Based on the existing research works, there is a wide variation in the complexity and sophistication of the models of shaking tables. At one side, there are numbers of linear analytical models developed using several assumptions and dynamics cancelations of some shaking table's components. Generally, these linearized models are used in the design of most conventional controllers because of their simplicity to be developed, simulated and implemented. At the other side, more advanced modelling techniques could be found in the literature taking into account the most relevant dynamics and nonlinearities. The main objective of system modeling is that the derived model is able to simulate the behaviour of the shaking table as accurately as possible. This chapter presents the most popular models of standard servo-hydraulic shaking tables. The first part concerns analytic models of a shaking table that assume a linear relationship between the excitation signal and the system response. Therefore, advanced shaking tables models that tend to include the nonlinear dynamics of the shaking table are exposed. Nonlinear modeling of servovalves, actuators and tested specimen are briefly presented. The last part of the chapter that concerns the presentation of the shaking table used in this case study, the QUANSER STIII, provides a description of the system as well as a theoretical model of the shaking table.

2.2. Description of a servo-hydraulic shaking table

Servo-hydraulic shaking tables are complex systems commonly composed of servovalves, actuators (with cylinder and pistons), a control system, a platform and sensors mounted on a reaction mass which is isolated or directly embedded on the ground. The cylinder as an actuator is driven by a servo valve through a power

amplifier based on the control signal. The actuator is conventionally controlled by a feedback compensator using the measured displacement of the piston. Figure 2.1 shows the main components of a typical six axis shaking table.

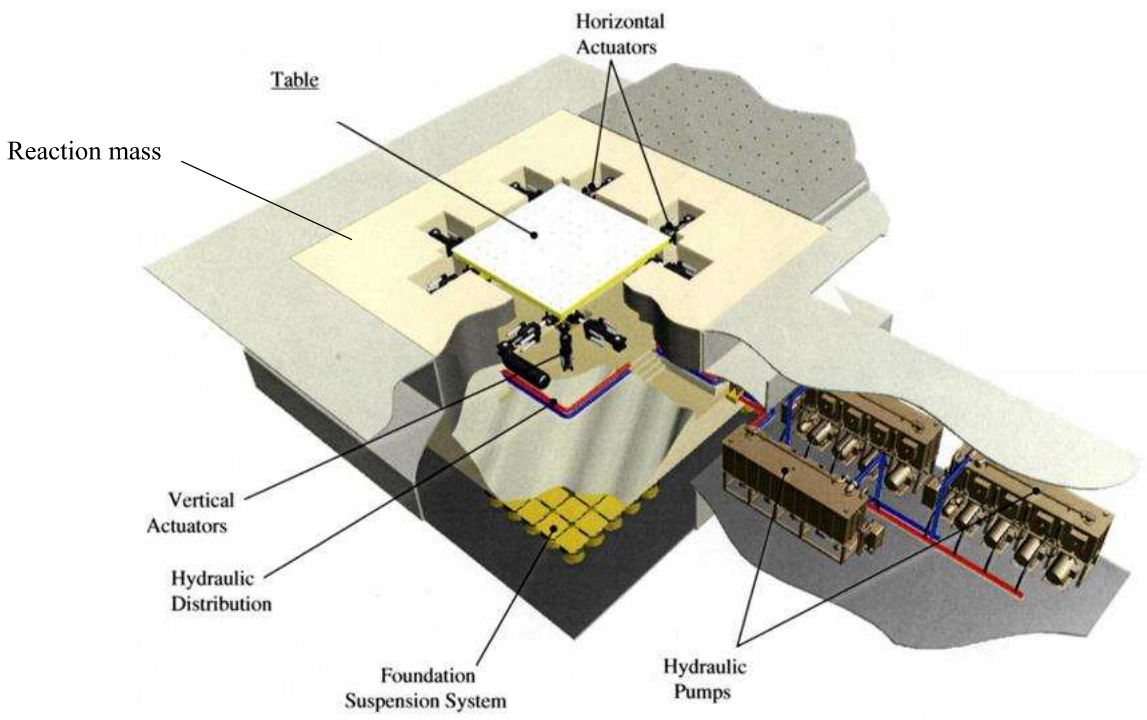

Figure 2.1: Main components of a typical servo-hydraulic shaking table [Airouche et al., 2014].

A classic illustrative configuration of a uniaxial shaking table with a simplified working principle of an actuator are represented in Figure 2.2.

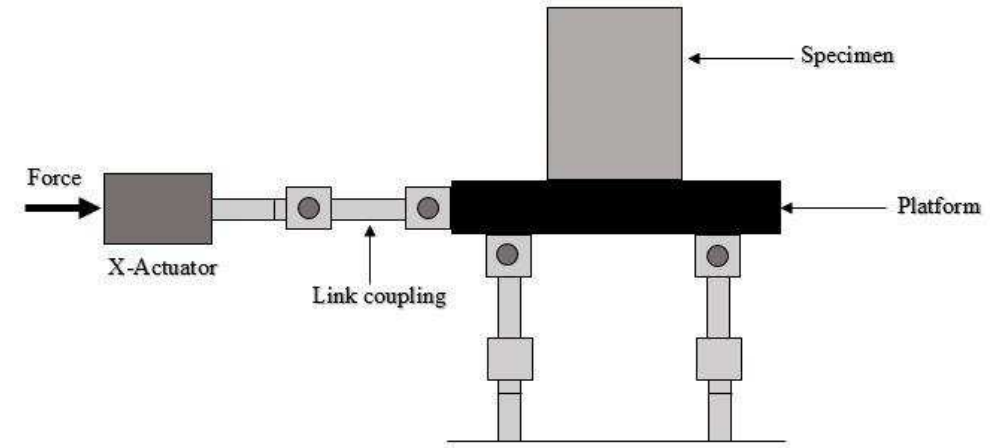

(a)

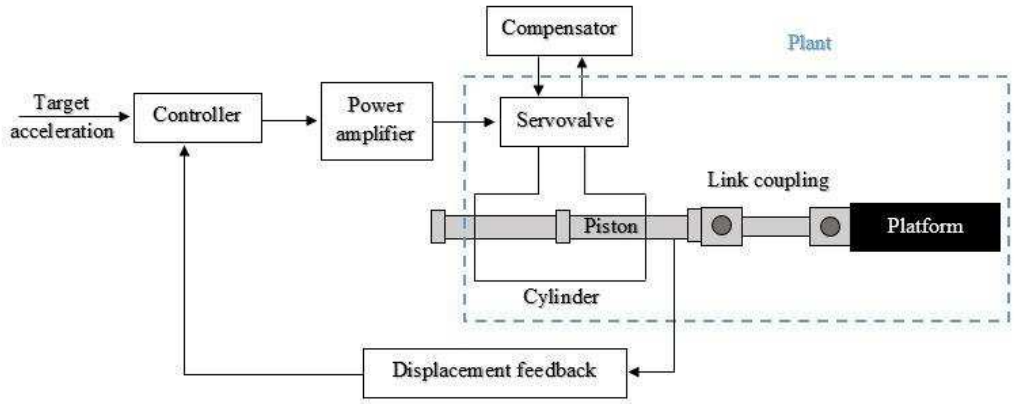

(b)

Figure 2.2: (a) Shaking table system configuration (b) simplified working principle of the actuator [Seki & Iwasaki 2017].

The operating process of a shaking table test can be summarized as follows: the controller compares the feedback signal from sensors with the input demand to determine the error and produces a command signal to drive the flow control valve. Thus, the control valve adjusts the fluid flow to move the actuator arm until the desired position is obtained. The condition is that the error signal between the obtained position and the measured one is falling to zero.

The purpose of the shaking table is to replicate a defined time-history data, which are generally acceleration earthquake records, on the platform within a range of reasonable accuracy, in order to examine the structural behaviour of the tested structure through base excitations.

In classical control theory, the controlled dynamic systems can be modelled using differential equations through Laplace transform of the system input and output. One important key to design an efficient control algorithm to achieve a high fidelity replication of the desired signal is to faithfully simulate the controlled system.

2.3. Linear models of servo-hydraulic shaking tables

Most of the shaking table modelling techniques use the linearized dynamics for both the hydraulic actuator and the test structure [105, 109, 118, 158]. Assuming that the shake table system is linear, the analytical model represents mathematically the input-output relationship between the excitation u(t) and the output y(t). For a displacement-controlled shaking table, a typical target motion $y_m(t)$ for the shake table is derived from an earthquake acceleration record while the excitation input u(t) is the desired table displacement $x_d(t)$. The output y(t) is the achieved displacement measured from sensors (LVDT). Most of the shaking table models found in the literature are developed for uni-axial shaking tables, or concern just one axis of a multi-axis shaking table systems. However cross-coupling components would replace the single mathematical model [105].

In general, the linear relation between the input, which represents the desired shaking table displacement $x_d(t)$ and the output, which represents the actual shaking table displacement $x_m(t)$ is obtained through different subsystem relationships that are: the servovalve transfer function between the input signal $\Delta x(t)$ and the servovalve oil flow rate $q_s(t)$; the actuator transfer function between the servovalve oil flow rate $q_s(t)$ and the shaking table measured displacement $x_m(t)$ and a shaking table standard feedback controller where the input signal $\Delta x(t)$ is computed based on the error signal between the desired shaking table displacement $x_d(t)$ and the measured shaking table displacement $x_m(t)$.

An early study has developed a linear analytical dynamic of a uniaxial shaking table that was able to predict well the observed dynamic performance of the shaking table for a wide range of operating conditions [24]. The proposed model has consisted of a total transfer function in Laplace domain between the desired and measured table displacements, taking into account the effects of actuator oil compressibility, oil leakage across the sealed joints within the actuator, time delay in the servovalve response, compliance of the actuator reaction mass, and dynamic characteristics of

the payload. The mathematical relationships that have been developed could be divided into different subsystems:

- A three-stage-servovalve transfer function, expressed by:

$$H_{sv}(s) = \frac{q_s(s)}{x_c(s)} \tag{2.1}$$

Where $x_c(s)$ is the servovalve command signal and q_s is the oil flow rate. In their work, the authors have confirmed that this expression, even if it was widely used, may not be sufficient to predict accurately the shaking table behaviour. Therefore, the improved three-stage-servovalve transfer function could incorporate a time delay that could physically interpreted as the time necessary to overcome the mechanical and hydraulic inertia of the servovalve, as expressed in the following equation:

$$H_{sv}(s) = k_t e^{-\tau s} \tag{2.2}$$

And k_t has been defined as a table gain factor.

- A servovalve-actuator transfer function is expressed by :

$$S(s) = \frac{H_{sv}(s)}{sA + k_{le}\left(\frac{F_a(s)}{x_t(s)}\right) + s\left(\frac{V}{4\beta A}\right)\left(\frac{F_a(s)}{x_t(s)}\right)} \tag{2.3}$$

$F_a(s)$ is the actuator force, A is the piston effective area, β is the bulk modulus of the fluid, V is the total volume of both chambers of the actuator, K_{le} is the flow pressure coefficient and $x_t(s)$ is the relative actuator displacement.

This servovalve-actuator mathematical expression assumes a linear relationship between the fluid leakage through the actuator seals and the pressure of the fluid in the actuator chamber.

- A servo-hydraulic system transfer function given by:

$$H(s) = \frac{S(s)\left(\frac{1}{s}K_i + K_p + s(K_{ff} + K_d)\right)}{1 + S(s)\left[\frac{1}{s}(K_i + K_p) + sK_d - \left(\frac{K_{dp}}{A}\right)\left(\frac{F_a(s)}{x_t(s)}\right)\right]} \tag{2.4}$$

The gains K_p, K_i, K_d, K_{ff} and K_{dp} are the user-set gains of the controller.

- A total shaking table transfer function T(s) expressed by:

$$T(s) = \mathrm{H}'(\mathrm{s})[1 + \mathrm{B}(\mathrm{s})] \tag{2.5}$$

Where B(s) is the base transfer function defined as a transfer function between the relative actuator displacement x_t(s) and the displacement of the reaction mass relative to the laboratory floor x_b(s).

The developed model has been used to perform a sensitive analysis of the shaking table dynamics and useful to understand the dynamics of a shaking table system and how it is influenced by characteristics of the test structure, control gain parameters and base compliance.

The linearization of the shaking table dynamics and/or the actuator has been often seen in the literature for a simplified shaking table modelling purpose. In a more recent work [108], a linear parameter varying model control methodology has been proposed where the modes of vibration of the system have been controlled individually by applying to the control loop a partial nonlinear dynamic inversion to account for parameter variations. In this work, the servovalve flow rate output is assumed to be proportional to the control input U as given in the following equation:

$$q_m = K_{sv}\, U \tag{2.6}$$

Where K_{sv} is the gain of power of the amplifier and the servovalve.

A mathematical model of the cylinder can be expressed as:

$$q_m = A_a \frac{dy_d}{dt} + K_a \frac{dP_m}{dt} + C_{al} P_m \tag{2.7}$$

Where y_d is the displacement of the piston; P_m is the differential pressure in the cylinder; A_a is the piston area; K_a is the internal stiffness of the cylinder and C_{al} is the leakage coefficient in the cylinder.

A common block diagram of the actuator is presented in Figure 2.3.

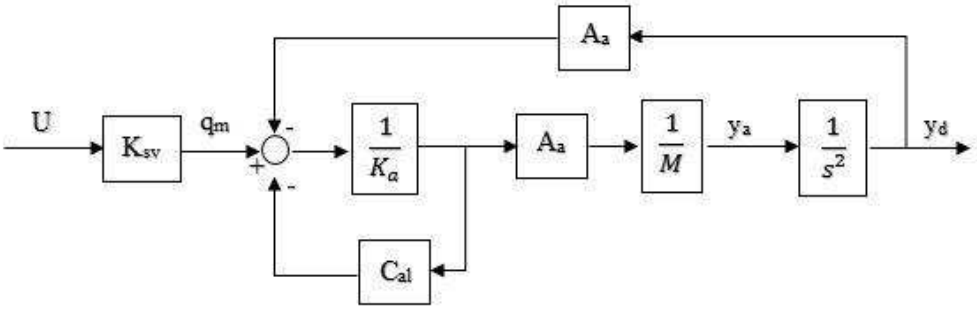

Figure 2.3: Block diagram of an actuator.

For more detailed equations, an entire single actuator model, including the flow-velocity relationships, fluid compressibility, and the leakage across the piston as well as the valve orifice equations could be found in [108].

A simplified open-loop dynamic model of an electro-servo-hydraulic shaking table EHST has been used to model a 6-DOF shaking table actuated by eight servo-controlled hydraulic actuators [127]:

$$G(s) = \frac{K_0}{s(\frac{s^2}{\omega_{sv}^2}+\frac{2\xi_{sv}}{\omega_{sv}}s+1)(\frac{s^2}{\omega_h^2}+\frac{2\xi_h}{\omega_h}s+1)} \tag{2.8}$$

Where K_0 is the open-loop gain of the EHST given by:

$$K_0 = \frac{K_{sv}K_q}{A_p} \tag{2.9}$$

K_{sv} is the servovalve gain; K_q is the linearized flow gain; A_p is the effective area of the hydraulic actuator.

ω_{sv} and ξ_{sv} represent the natural angular frequency and the damping ratio of the actuator, respectively. ω_h and ξ_h represent the natural angular frequency and the damping ratio of the servovalve, respectively.

Similar work has been developed to model a six-DOF shaking table, where the linearized model of the system has been achieved by the DOF decomposition transforming the multi-axis motion to the single actuator displacement [158]. The expression of the natural angular frequency and the damping ratio of the servovalve were given by:

$$\omega_h = \sqrt{\frac{4\beta A^2}{V_t m}} \tag{2.10}$$

$$\xi_h = (K_c + C_{tc})\sqrt{\frac{\beta m}{V_t}}/A \tag{2.11}$$

K_c represents the flow pressure coefficient, C_{tc} is the total leakage coefficient, including the internal leakage coefficient and the external leakage coefficient, m is the mass of the piston and V_t is the total volume of the actuator.

In more global point of view of a standard shaking table, a simplified block diagram of the different transfer function components of the shaking table system, incorporating the dynamics of the platform as well as the specimen are depicted in Figure 2.4.

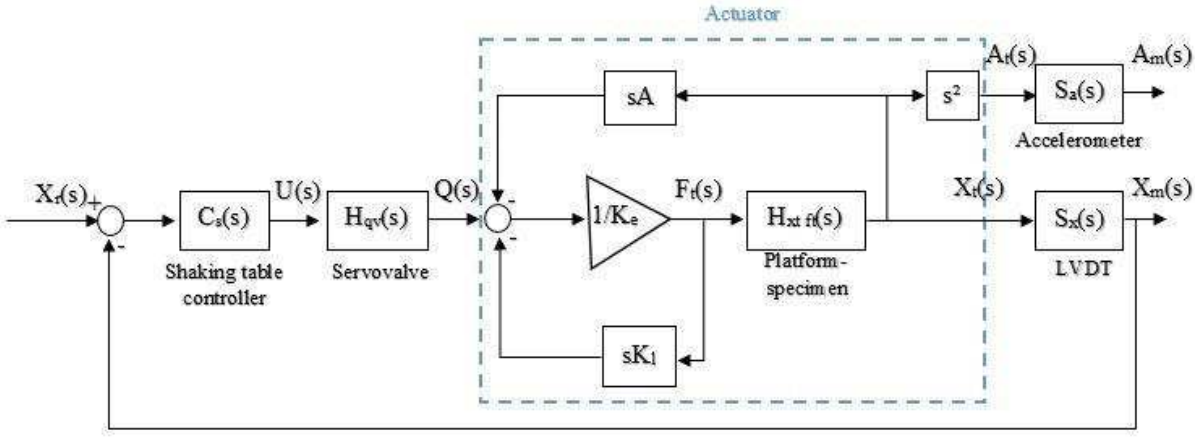

Figure 2.4: Block diagram of standard shaking table.

The resulting table displacement from the input actuator force can be represented by equation 3.1 [144]:

$$F_t(s) = H_{xt\,ft}(s)X_t(s) \tag{2.12}$$

Where $H_{xt\,ft}(s)$ represents the force-displacement transfer function. $H_{qv}(s)$ represents the servovalve transfer function from actual command signal to oil flow through the actuator chambers. K_e represents the force-flow coefficient; K_l represents the system constant defined by the properties of the hydraulic fluid. C(s) is a standard feedback controller. U(s) is the command signal sent to the actuator servovalve. $X_t(s)$

and $A_t(s)$ represent the true displacement and acceleration of the table, respectively. $X_m(s)$ and $A_m(s)$ are the measured displacement and measured acceleration, respectively; while $S_a(s)$ and $S_x(s)$ are the transfer functions of the shaking table accelerometer and the LVDT, respectively.

In this section, only few works of linearized EHST models have been reported. The most used models found in the literature are linear [105, 109, 120, 133]. For example, a three-DOF planar model has been developed including a linear relationship between actuator and table co-ordinates [135]. A linear modelling of Japan's E-defense shaking table has enabled the six hydraulic modal resonances to be predicted [58, 95].

Nevertheless, the fidelity of these linear models to reproduce the real shaking table behaviour is generally verified when the shaking table system and the tested structures are linear (behave as elastic systems) with known characteristics and unchanged parameters and suitable to apply a classic control laws. However, this linear/linearized methodology to simulate the shaking tables behaviour has shown numerous limitations due to many high order dynamics and time-varying aspect of the shaking table that are not taken into account, the interaction between the shaking table components as well as the table-specimen interaction, which make the shaking table testing a real challenge and the reproduced signal distortions unavoidable. The need to include nonlinear characteristics in shaking table testing models has become necessary.

2.4. Advanced models of servo-hydraulic shaking table

Nonlinearity is the difficult problem which exists universally in servo-hydraulic systems that has not been solved effectively yet. The nonlinearities of servo-hydraulic systems are generally caused by the dynamic characteristics of the servo-hydraulic components, the mutual influence of the mechanical, hydraulic and electronic subsystems, as well as the inherent nonlinearities of hydraulic power mechanism such as hysteresis, dead zone, fluid leakage, limiting properties and so on.

In addition to these high nonlinearities, there are numerous model uncertainties which cannot be known and modelled accurately. Therefore, an exhaustive understanding of the dynamic characteristics of a shaking table and a thorough model of the system

not only allow its limitations to be assessed, but also enables its control algorithm to be optimized. Incorporating nonlinear models such as the servovalve, actuator and specimen nonlinearities has attracted a lot of research attention [105, 169, 191].

2.4.1. Servovalve modeling

In many studies, it has been recognized that the servovalve response has a significant impact on the system dynamics. For this reason, many attempts for modelling and studying the dynamic characteristics of servovalves and their components have been carried out. Generally speaking, the servovalve, which transforms the control input signal into oil flow, is a complex system where several parameters may only be estimated within a specified frequency range, or even completely unknown. The servovalve nonlinearities have always relied on the flow-pressure characteristics, change of control volumes and the friction force equation [87]. Furthermore, several dynamic uncertainties are due to leakage flow, dry friction and so on.

The simplest model of the single-axis positional response to a valve control signal input has been represented by a series gain and integrator and had shown that it could be improved by the addition of an empirical first-order lead/lag, identified from experimental data, has been proposed [15]. More commonly, however, a second order lag term is added to model the table mass interacting with the hydraulic “oil-column” compressibility, e.g., Shimizu et al., 2004 [135], Iwasaki et al., 2005 [55], Kakegawa et al., 2003 [58] with a time delay and taking into account the maximum spool displacement and the slew rate limit [105].

Even if these simplified models are valuable from a theoretical point of view, the values of several parameters are not possible to be determined by direct measurements or by parametric identification which is laborious and often burdened with a large degree of uncertainty. The identification issue is mostly not addressed, while the adopted models do not properly reflect the underlying physical behaviour of the servovalve.

Number of published works continue to focus on the development and validation of advanced models, taking into account some of commonly ignored nonlinear sources in servo-hydraulic systems. A nonlinear non-dimensional

mathematical model has been developed to fully describe the dynamic performance of a two-stage electrohydraulic servovalve [32]. The system nonlinear model governing equations have included the mean flow rate equation, first stage governing equations, spool governing equations, first stage and second stage output pressures equations. The valve dynamic performance has been obtained through its transient response and its frequency response using Matlab software package.

A detailed nonlinear model of a servo-hydraulic system has been developed to take into account the presence of unknown parameters such as the pressure drop caused by the interface block between the actuator and the servovalve [138]. The simulation model of the system has been described as a second order model, designed on the AMESim software. It includes some components generally neglected: two pipes between the cylinder chambers and the servovalve in order to represent the intermediary block in a simplified way, two accumulators and some lines respectively on the supply and exhaust pressure way. The viscous, stiction and coulomb friction force have been taken into account as well.

A mathematical model of a hydraulic servo system for a manipulator robotic arm and its essential components has been developed comprising the most relevant dynamics and nonlinear effects encountered in hydraulic servo systems [177]. The model consisted of three parts: the valve dynamics, the pressure dynamics and the mechanical part. A comparison of the steady state displacement errors between the nonlinear, linear and simplified linear models has been carried out, proving that the simulated nonlinear model shows better accuracy than the linear and the improved linear models.

A nonlinear Hammerstein model has been developed for a servo-hydraulic system modeled by a static nonlinear block and a dynamic linear block, showing that the nonlinear dynamics of the system have been well captured [172].

A nonlinear dynamic of the different hydraulic actuator subsystems, the servo-valve and the cylinder, have been developed and the most nonlinearities of the system, which arise from compressibility of the hydraulic fluid, the complex flow properties of the servovalve, valve overlap and friction in the hydraulic cylinder, have been simulated [162]. Friction models have been developed to

simulate accurately the system responses. It has been shown that for simulating the behaviour of the system, nonlinear modelling of the friction is not enough, and therefore, by adding position and acceleration measurements of the real system, two new nonlinear dynamic models have been presented for simulating the system position, velocity and acceleration responses.

2.4.2. Actuator modeling

The hydraulic actuator is the basic functional element of the hydraulic servo-system. It includes a load mass, with the driving oil flows Q_A and Q_B as inputs, and correspondingly the actuator pressures P_A and P_B, and position x_p or velocity $\dot{x_p}$ as outputs. In shaking table systems, hydraulic actuators are still the most used, because the technology of electrical actuators does not (yet) provide the performance achieved by hydraulic actuators in generating high power to weight ratio [162]. The aim job of the actuator is to transform the hydraulic energy in terms of flow and pressure into mechanical energy in terms of velocity and force. However, with increasing the accuracy requirements of complex motion systems, the limits of performance of hydraulic servo-systems, due to the nonlinear and dynamic characteristics of these systems, come into the picture.

The theoretical modelling of the hydraulic actuator is less involved than that of the servo-valve. Essentially, the problem of modelling hydraulic actuators has been well established in early studies, among others, by Merritt [87] and the principal model relations have been developed here in. In the basic actuator model, internal leakage and friction of the actuator have to be taken into account. Many hydraulic actuators in servo applications are provided with hydrostatic bearings, and for this type of bearings theoretical relations for the leakage and friction are available. Moreover, the physical modelling of the hydraulic actuator is well-known and well-defined in the literature. Generally, the actuator model consists of a mass balances between for each chamber and an equation of motion of the piston. The mass balances of the respective actuator chambers give state equations for the actuator pressures at both sides of the piston allowing these equations [162]:

$$\dot{P_A} = \frac{E}{V_A}(Q_A - Q_{el,A} - Q_{il} - A_A \dot{x_p}) \quad (2.13)$$

$$\dot{P_B} = \frac{E}{V_B}(Q_B - Q_{el,B} - Q_{il} - A_B \dot{x_p}) \quad (2.14)$$

Where A_A and A_B are the respective piston areas; Q_{il} and Q_{el} represent the internal and external leakage flow respectively; V_A and V_B are the volume of the respective actuator chambers. x_p and $\dot{xp}$ are the position and velocity of the piston, respectively, obtained by the following equation:

$$M_p \ddot{x_p} = A_B P_B - A_A P_A - F_f + F_e \quad (2.15)$$

Where M_p is the inertia of the piston including the inertia of the load. F_f is the friction force on the piston which in the next subsection different models of the friction in the literature have been discussed. The external force F_e is the sum of the forces acting on the piston.

In the cited work, several friction models have been simulated in order to compensate for hydraulic nonlinearities that are present and that affect the dynamic characteristics of the servo hydraulic system.

A dynamic model of a hydraulic servo-rotary actuator has been developed including the external disturbances, the unmodeled disturbances, the time-variant disturbances as well as the nonlinear friction effects modelled as known nonlinear functions [185]. The dynamics of the inertia load have been expressed as follows:

$$m\ddot{y} = P_L A - B\dot{y} - A_f S_f(\dot{y}) - d_n + f(t) \quad (2.16)$$

Where m and y represent the moment of inertia and the angular displacement of the load, respectively; P_L=P_1-P_2 is the load pressure in the hydraulic actuator; A is the radian displacement of the actuator; B is the viscous friction coefficient of the system; $A_f S_f$ represents the approximated nonlinear Coulomb friction, in which the amplitude A_f and the continuous shape function S_f should be identified for controller implementation. d_n is the time-invariant or changing slowly part of the unmodeled disturbances, that is the direct current (DC) value

of the unmodeled disturbances; and f(t) represents other time-variant disturbances such as the unconsidered nonlinear frictions as well as external disturbances.

Taking the basic nonlinearities of the actuator into account, namely the valve flow nonlinearity, and leakage flow, another dynamics actuator model has been developed.

The nonlinear actuator dynamics have been described in detailed equations [162].

Recently, with increasingly exacting performance demands in terms of robust tracking with high accuracy and fast response, several recent works are still dedicated to develop nonlinear accurate models of servo hydraulic actuators [84, 190] by modelling parametric uncertainties and time-varying disturbance [182] that represent the main problem in developing high-performance closed-loop controllers.

2.4.3. Specimen modeling

Shaking table tests are a powerful tool to reproduce realistic earthquake scenarios through dynamic base excitations in order to provide valuable knowledge of seismic behaviour of structures, mostly the complex ones. When a test specimen is mounted on the table, the interaction between the shaking table and the specimen affects the entire system dynamics, leading to undesirable distortion in the reproduced earthquake record and deteriorating the control system performance as well. This interaction between shake tables and linear structures was addressed by Blondet and Esparza (1988) [11], Rinawi and Clough (1991) [115], and Conte and Trombetti (2000) [24]. Designing a robust and successful control technique that aims to replicate faithfully the desired signal commonly relies of many linear assumptions, transfer functions representations and unvarying parameters of the shaking table. However, most of the shaking tables testing needs to push the tested structure to high nonlinear states in order to understand its complex nonlinear behaviour, analyse some collapse mechanisms, and so on.

A number of developed studies have targeted the development of control methodologies that are able to reproduce target signals on a shaking table

platform by reducing the effects of nonlinear structures. However, many applications including the experimental evaluation of non-structural components such as suspended ceiling systems [113] or the qualification testing of complex equipment (IEEE, 2006) it is often required to simulate a floor/roof motion at a specific location (such as roof corners or mid spans) of a structure mounted on a shake table [116].

As the objective of the control system of the shake table–structure is to determine the desired excitation input $x_d(t)$ such that the response output y(t) of the shake table, or the mounted structure will follow the pre-defined target motion $y_d(t)$, the table-structure interaction needs to be taken into account and an advanced model of the tested structure is required.

The acceleration transfer function described by the ratio of the output structural total acceleration response to a shake table motion in frequency domain can be expressed, for a SDOF structure, as follows:

$$H_s(\omega) = \frac{2s\xi_s\omega_s + {\omega_s}^2}{s^2 + 2s\xi_s\omega_s + {\omega_s}^2} \tag{2.17}$$

Where ω_s and ξ_s are the natural frequency and the damping ratio of the structure.

Considering a typical nonlinear hysteretic SDOF system illustrated in figure 2.5, the equations of motion of the table-structure system can be expressed as follows:

$$m_s\ddot{x}_s(t) + c_s\dot{x}_s(t) + f_s(x) = -m_s\ddot{x}_t(t) \tag{2.18}$$

$$m_t\ddot{x}_s(t) - \{c_s\dot{x}_s(t) + f_s(x)\} = -f_a(t) \tag{2.19}$$

Where m_s and m_t represent the structure mass and the table mass, respectively; c_s is the damping coefficient of the structure; $f_s(a)$ is the nonlinear restoring force; x_s is the structure response displacement and x_t is the shaking table displacement; f_a is the actuator force applied to the table.

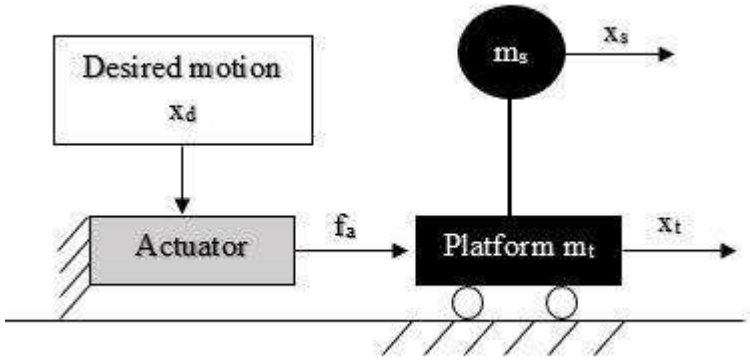

Figure 2.5: Schematic of a shaking table loaded with a SDOF specimen.

The actuator force can be expressed as [100]:

$$f_a(t) = m_e\ddot{x}(t) + K_e x(t) + (C_e|\dot{x}(t)|^{\alpha} + f_{\mu e})sign(\dot{x}(t)) \quad (2.20)$$

Where m_e is the total mass, x is the table displacement, C_e is the damping coefficient, K_e is the effective horizontal stiffness and $f_{\mu e}$ is the Coulomb friction force.

In many works, nonlinear specimens have been tested on shaking tables. Numerical and experimental examination of the control performance has been carried out for a shaking table loaded with a nonlinear SDOF structure [34]. The results presented in this study show the tracking performance of the shaking table in presence of a nonlinear specimen modelled with a nonlinear spring expressed by tri-linear hysteresis loop.

2.5. Electric shaking tables (case study: QUANSER STIII)

2.5.1. Overview

A general description of servo-hydraulic shaking tables has been given previously for sizable facilities. A more detailed presentation of a second type of shaking tables which has been extensively used in this study is given in this section.

QUANSER shaking table III (ST III) is an electric high-powered bi-axial shaking table, composed of two moving steel stages: a bottom stage, actuated with two linear motors along the horizontal x-axis and a top stage and one linear motor along the transversal y-axis. The stages can move with a maximum load of

100Kg at high accelerations and velocities with a maximum stroke displacement of 21.6 cm. The table is actuated by linear electric motors which increases the reliability of the system and keeps the process quiet.

Figure 2.6 shows an overview of a QUANSER ST III (University of Djelfa) and its different components and the nomenclature of the components labelled in Figure 2.7 are listed in Table 2.1. Figure 2.8 illustrates the relevant interaction diagram of the entire shaking table system.

Table 2.1: QUANSER ST III Components.

No.	Component	No.	Component
1	Ground support stage	7	Top axis linear motor
2	Bottom axis linear motor	8	Top axis hard stops
3	Bottom axis hard stops	9	Top axis stage
4	Bottom axis linear bearing guide	10	Encoder scanning head
5	Bottom axis stage	11	Encoder scale tape
6	Top axis linear bearing guide	12	Magnet for limit switch

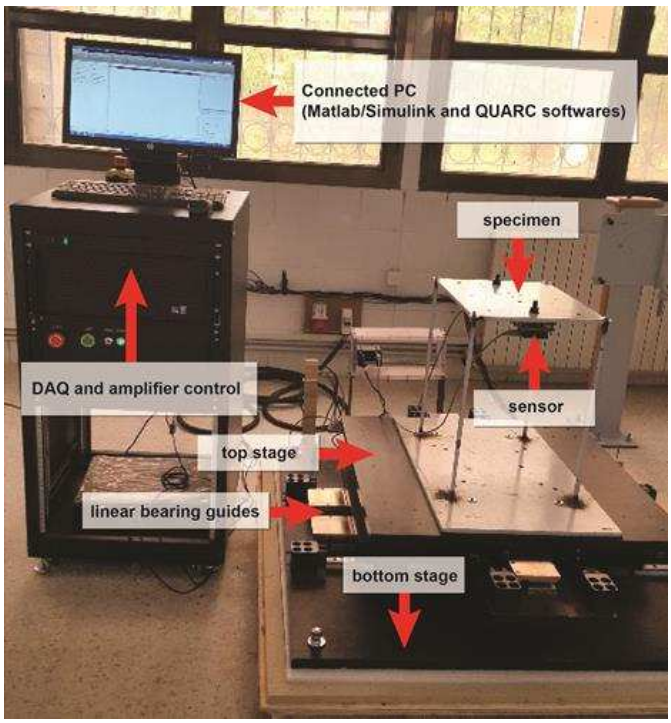

Figure 2.6: Overview of the QUANSER STIII (university of Djelfa).

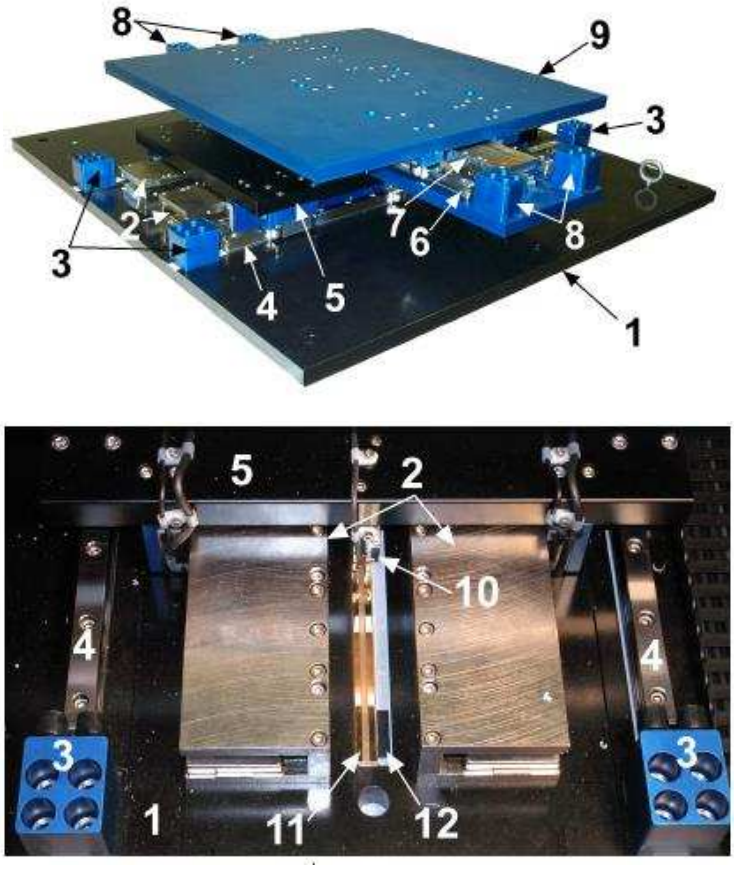

Figure 2.7: QUANSER ST III components (a) Top view (b) Top corner view.

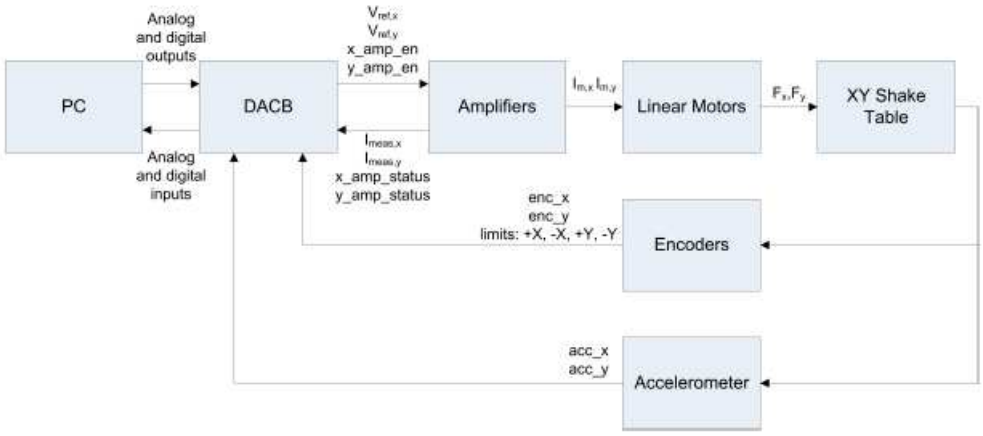

Figure 2.8: Diagram interaction between the QUANSER STIII components.

The current needed to move the stage at the desired position, which is the named command signal, is calculated by the real-time control software (QUARC) and sent to the power amplifier through the analog output channel of the DAQ device. The amplifier applies the current and drives the motor on the XY Shake Table III. The table tracking the commanded signal and the resulting displacement and acceleration of the stage are measured by the on-board encoder (LVDT) and the accelerometer sensors. The encoder and accelerometer are connected to the DAQ and their signals can be displayed and processed further.

The sliding system is composed of a pair of linear guides using ball bearings. They enable the two stages to move with a total stoke of ±21.6cm. The peak acceleration with a maximum payload of 100Kg is 1.1g and 1.5g along x axis and y axis, respectively. The displacement and acceleration measured by encoders and accelerometers are acquired through a DAQ card by a control program implemented in MATLAB software on a PC.

2.5.1.1. Bottom and top stage

The top axis stage weighs a total of 95.22Kg and the moving mass is 47.61Kg. The bottom stage axis weighs a total of 175.48Kg and the moving mass is 175.48Kg.

The bottom stage, shown in Figure 2.7, is 106.7x106.4 cm^2. The bottom linear motor drives are installed onto this plate. The plate has 4 large screw holes at each corner and smaller screw holes along the sides. These can be used to fasten the shake table onto a ground floor support to prevent the shake table system from moving, or at least reduce the amount of vibration. Although this is not necessary, it is recommended in order to yield more precise results when, for instance, measuring acceleration.

The top stage, shown in Figure 2.7 is 71.1x71.1 cm^2. The top stage has many screw holes that can be used to mount structures and other objects.

2.5.1.2. Motors

The QUANSER ST III is actuated using three linear motors with identical specifications: two linear motors actuating the bottom axis and a single linear motor actuating the top axis. The linear motor specifications are given in Table 2.2.

Table 2.2: Linear motor specifications.

Description	Value
Max peak current	36A
Max continuous current	12A
Max peak force	2642N
Max continuous force	880.7N
Max peak power	4554W
Max DC voltage	330V

2.5.1.3. Amplifiers

The linear motors are driven using current-controlled PWM amplifiers from Advanced Motion Controls (AMC). The amplifiers for the two axes are different: the x-axis uses the AMC B060A400AC drive and the y-axis uses the B30A40AC drive. The main specifications for the x-axis amplifiers and the y-axis amplifiers are given in Tables 2.3 and Table 2.4, respectively. The current reference pin on each amplifier has a maximum output of ±7.25V (i.e., command signal to current loop). This is used to calculate the amplifier gain.

Table 2.3: X-axis amplifier specifications.

Description	Value
Max peak power	7600A
Max peak current	40A
Max continuous current	20A
Motor current-force constant	5.52A/V
Current monitor scaling	5.7A/V

Table 2.4: Y-axis amplifier specifications.

Description	Value
Max peak power	5700A
Max peak current	30A
Max continuous current	15A
Motor current-force constant	4.14A/V
Current monitor scaling	4.2A/V

2.5.1.4. Linear bearing guides

The bottom and top stages ride along a pair of linear guides using ball bearings. They enable the stages to have a total travel length of 8.50 inches, or 21.59 cm. Both are shown in Figure 2.7.

2.5.1.5. Encoders

There is a LIDA 477/487 Heidenhain encoder mounted on the ground stage base plate that measures the bottom axis or x-axis position. The encoder read head scans along the scaling strip and outputs 250,000 counts per meter in 1X mode. The encoder resolution is therefore 250 nm/count. Similarly, there is an encoder setup on the top stage to measure the y-axis position.

2.5.1.6. Accelerometers

A dual-axis ADXL210E accelerometer is mounted underneath the stage of the Shake Table II to measure the acceleration of the stage in both the x and y directions. The sensor has a range of ±10g and its noise, in the operating range of the shake table, is approximately ±5.0 mV, i.e., ±5.0 mg. The analog sensor is calibrated such that 1V equals 1g, or 9.81 m/s^2.

2.5.1.7. Limit switches

There is a total of four limit switches installed to detect when the bottom or top stage approaches the limit of their travel the safety hard stops. There is a +X and -X limit switch at each end of the bottom x-axis stage and a +Y and -Y limit switch at each end of the top y-axis stage. The

limit sensors are magnetically triggered. They are located approximately 1 cm from all the safety hard stops which limits the x-axis and y-axis travel distance between limit sensors to 20.15cm. Thus, when the stage goes over the +X switch, it outputs 0. However, when +X is not being pressed down (i.e., triggered) it normally outputs 1. This signal can then be used to calibrate the stage to center or to stop the control software and prevent the table from hitting the hard stops.

2.5.2. Theoretical model

The x-axis of the QUANSER shaking table model can be represented by the transfer function expressed in the following equation:

$$X(s) = \frac{1}{K_{f,x}s^2} I_{m,x}(s) \quad (2.21)$$

Where X(s) = L[x(t)] is the Laplace of the stage position along the x-axis, $I_{m,x}(s)$ is the Laplace of the applied current and $K_{f,x}$ is the model gain. The model gain, for the x-axis, is given by:

$$K_{f,x} = \frac{M_{t,x}}{K_{t,x}} \quad (2.22)$$

Where $M_{t,x}$ is the total mass being moved by the motor (i.e., both pre-load and payload) and $K_{t,x}$ is the current-force constant of the motor.

Similarly, for the y-axis, the expression of the transfer function is given by:

$$Y(s) = \frac{1}{K_{f,y}s^2} I_{m,y}(s) \quad (2.23)$$

$$K_{f,y} = \frac{M_{t,y}}{K_{t,y}} \quad (2.24)$$

$M_{t,y}$ is the moving mass along the y-axis, $I_{m,y}$ is the applied current to motor y, and $K_{t,y}$ is the force current constant of linear motor y.

2.5.3. Running QUARC controller of the QUANSER STIII

In order to run the controllers of the QUANSER STIII, the real-time control software QUARC, MATLAB/Simulink with the real time workshop and the Control System toolbox as well as the LabVIEW run-time software are required. The shaking table test procedure assumes that the shaking table is

connected to the same PC that the software is running on. The advantage of the QUANSER STIII controllers as they are implemented in MATLAB/Simulink environment is that it provides the possibility to the users to design their own controller and to run it using QUARC.

Before running any of the experiments the stage of the XY Shake Table III should be in the center position, which is in the middle of the left and right limit switches. The Simulink diagram for the calibration process is shown in Figure 2.9.

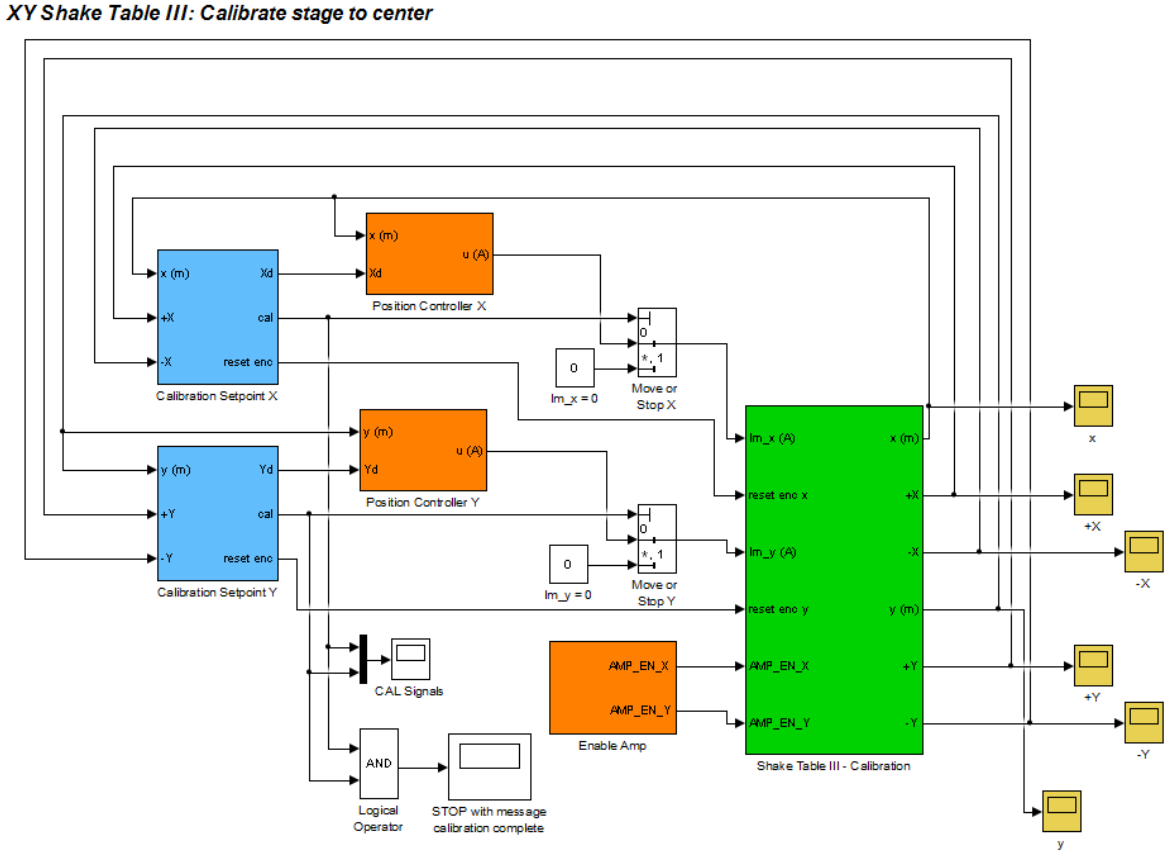

Figure 2.9: Simulink diagram of the QUANSER STIII calibration.

Once the calibration is completed, different types of signals can be selected to be tracked by the platform such as sine wave signal, sine sweep signal (chirp signal) and earthquake records.

Figures 3.10 to 3.12 show the Simulink diagram that is used for sine wave command signal, sine sweep command signal and earthquake record, respectively.

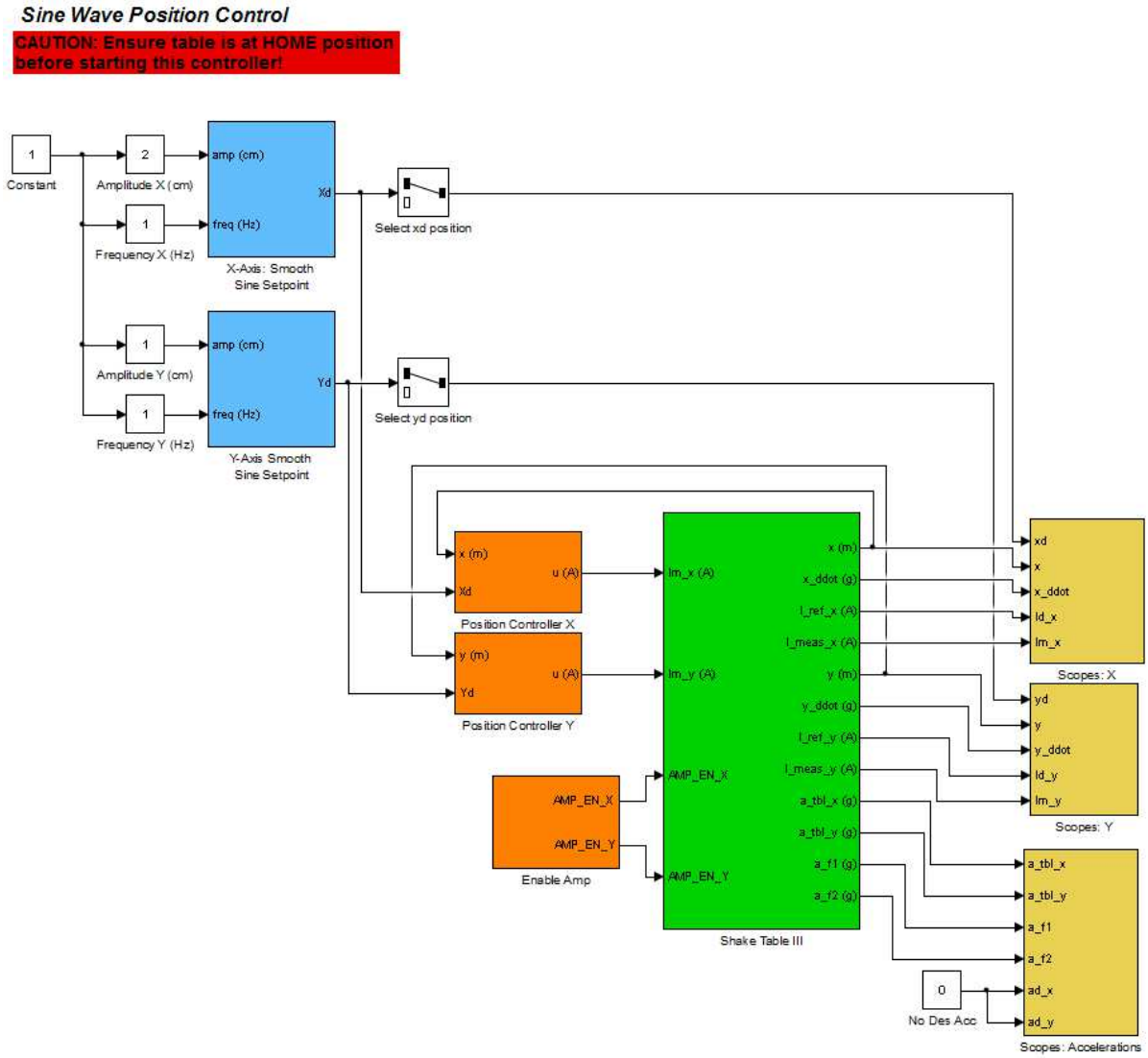

Figure 2.10: Simulink model used to command a sine wave to the XY Shake Table III using QUARC.

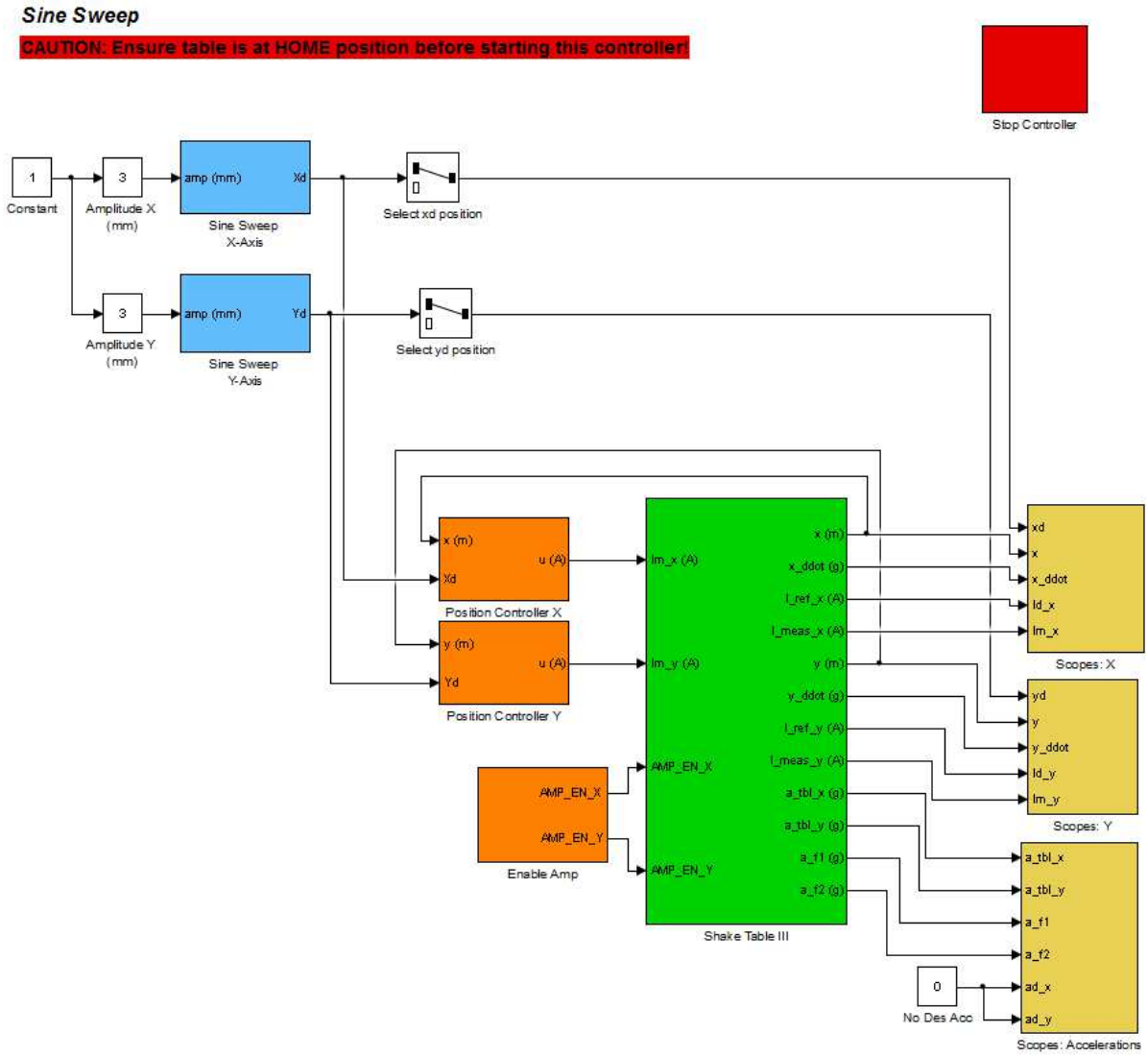

Figure 2.11: Simulink model used to command a sine sweep to the XY Shake Table III using QUARC.

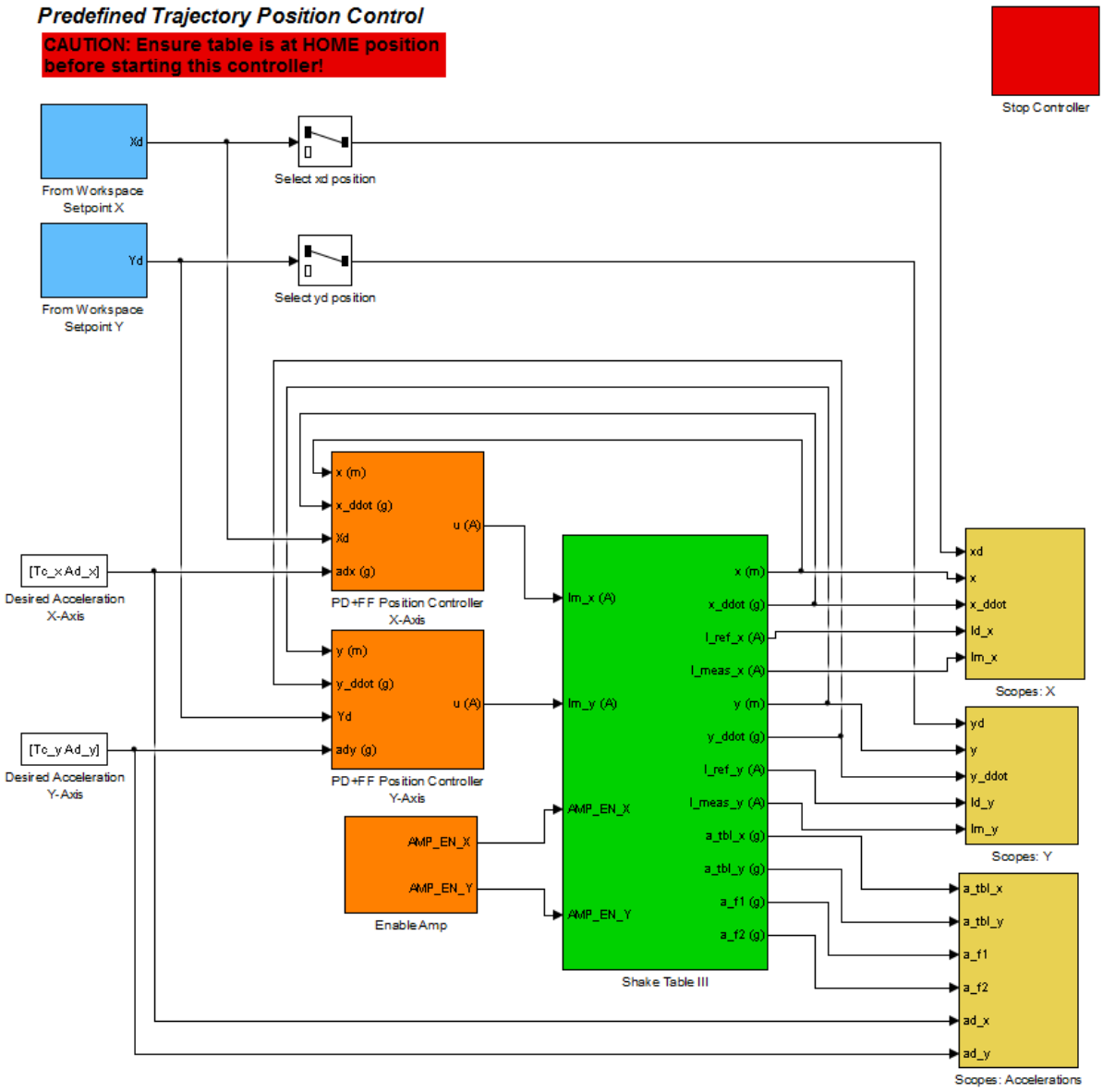

Figure 2.12: Simulink model used to command an earthquake record to the XY Shake Table III using QUARC.

2.6. Conclusion

A shaking table is a technique in experimental earthquake engineering that provides base excitation to the structures under test in order to evaluate their seismic behaviour. Due to the shaking table dynamics, the nonlinear components and the number of varying parameters during the experimental process, the shaking table system behaviour is usually unpredictable and the users can usually only tune the controller parameters via trial and error. However, the efficiency and stability of the control techniques are not guaranteed. Therefore, a realistic model of the shaking table system is required for any control design.

In this chapter, the standard shaking table modelling methodologies that could be found in the literature have been reviewed. Various studies have developed analytical representations of the shaking table system's behaviour and simplified models of the system's components through the linearization of the actuator, the servovalve, SDOFs decoupling and so on. These works have recognized that there is a compromise between the degree of accuracy of the developed model and its complexity to be used afterward in the design of an appropriate control algorithm.

Other studies have presented advanced accurate models of shaking table subsystems that take into account as many nonlinearities as possible, such as nonlinear models of the actuator, the servovalve and/or the tested specimen in order to reproduce a realistic behaviour of the real shaking table system.

The last part of this chapter describes in details the QUANSER Shaking Table III, with a brief presentation of its components, capacities, and limitations. A theoretical model of the shaking table, developed according to the manual given by the manufacturers, is used as a primary numerical model of the system to test the validity of the proposed control scheme designed to enhance the performance of the original PDFF shaking table controller.

CHAPTER 3

NUMERICAL IMPLEMENTATION OF THE NN-PDFF CONTROLLER

3.1. Introduction

Shaking tables are intended to reproduce reference accelerations especially earthquake records at the base of the tested structures. They are generally driven by the classical controllers, usually performing in displacement, velocity or acceleration mode.

The aim of this chapter is to apply a NN control algorithm and test its efficiency to simulated shaking tables. The NN is implemented in two strategies to overcome some shortcomings inherited to conventional PDFF shaking table controller. The NN is designed to provide an auxiliary control to the primary control function provided by the PDFF controller. The global performance of the proposed control technique is assessed through the measure of the RMSE that is computed between the desired accelerations and the shaking table output. Further assessment is carried out by comparing the results of the proposed control algorithm with those of the original PDFF controller in term of signal distortion in the time domain.

3.2. PID-based NN control

In most cases, the inner-loop controller of shaking tables is a PID controller due to its versatility and tuning simplicity. However, in many dynamic and seismic tests, the PID controller fails to meet some requirements, such as wide frequency bandwidth, high tracking performance and high power spectral density (PSD) replication precision. Its performance is severely deteriorated because of the complexity of the real shaking table system, the nonlinear parameters, the nonlinear behaviour of the specimen and many other causes cited previously in the second and third chapters of this theses. Consequently, the PID becomes an auxiliary part of the entire shaking table control system and usually it is associated to other control methodologies and compensation techniques to improve its performance for different shaking table testing conditions. For this reason, instead of implementing a new upgraded control system, which is usually a complex and difficult task, various research works have suggested improvements of existing PID controllers by combining them with artificial intelligent

algorithms such as neural networks (NNs). The purpose of this combination is to take advantages of the simplicity of the standard PID control and the NN's powerful capabilities to deal with nonlinearities.

Beside the shaking table control, an extensive research work on the use of PID and NNs controllers has been developed for several industrial systems such as DC motor systems for example. A PID controller and a NN controller have been designed and implemented in parallel to speed control a Permanent Magnet motor [25]. The objective was to follow the speed trajectory generated by a speed reference generator and results have been improved. The position control of a servomotor of a 3-Dimensional laser processing system has been enhanced using NN controller in terms of good positioning accuracy, fast-tracking accuracy, strong robustness and nonlinear cancellation [167]. A nonlinear controller based on NNs has proven to be efficient considering set point tracking performance on a nonlinear DC motor system [92]. A similar work has been achieved by designing a feedforward NN as a DC motor control driver [89]. In dynamic robot control, a PID-based NN controller has been proposed to control a two-links robotic manipulator system [6].

Recently, several researchers have provided a wide literature concerning the use of combined PID-NN methods, mostly focused on the use of NNs to auto-tune the PID controller. Abundant published research works can be found in the literature, however, only few are briefly mentioned in this section. A combination of a PID and a three-layer NN has been proposed and verified for a complex nonlinear MIMO system exhibiting strong coupling [60]. An online self-tuning method using neural networks has been designed for a nonlinear PD computed torque controller of a 2DOF planar parallel manipulator [71]. The PD gains have been tuned online using NNs and results have showed the improvement of the control performance in terms of minimizing the error in tracking trajectories. Similarly, a NN-based PID (NNPID) like controller which is tuned when the controller is operating in an online mode for high performance permanent magnet synchronous motor (PMSM) position control has been proposed [67]. In this proposed control methodology, online gradient free training algorithm is proposed for training NNPID controller which requires almost no parameter to be determined prior to the implementation. The development of an adaptive PID controller has been proposed for an air supply channel of a coal-gas furnace [20]. The NN controller has been used for auto-tuning the PID in a parallel scheme, based on the control error signal and the sensor data. The proposed control algorithm has been

executed through three phases: recording the system response to a test signal, performing an identification of the system, setting up the PID gains for the initialization of the auto-tuning NN block controller, training the auto-tuning NN block to finally operate on the controlled plant. A Neural Network based intelligent PI controller and Neural Network based PID controller have been designed and simulated to increase the position accuracy in a pneumatic servo actuator [50]. The well-trained NN has been able to provide the PI and the PID controllers with the suitable gains according to each feedback that contains the change in error in position and the change in external load force. These gains have kept the position response within minimum overshoot, minimum rise time and minimum steady state error. The presented results have been satisfied without and with the effect of applying external variable load force.

3.2.1. Feedforward neural networks with Lavenberg-Marquardt training algorithm

The NN used in this study is a feedforward NN using the powerful Lavenberg-Marquardt as a training algorithm. This algorithm presents a good balance between the complexity and simplicity of networks used for the improvement of the shaking table PDFF control system. Most of the applications of nonlinear least squares to NNs have focused on sequential implementations, where the weights are updated after each presentation of an input/output set. However, the standard algorithms are performed in batch mode, where the weights are only updated after a complete sweep through the training set. In the following, the application of a standard Lavenberg-Marquardt algorithm to the batch training of multi-layer NN is presented.

Considering a two-layer feedforward NN, the net input to unit *i* in layer *k+1* is given as follows:

$$a^{k+1}(i) = \sum_{j=1}^{Sk} w^{k+1}(i,j) y^{k}(j) + b^{k+1}(i) \tag{3.1}$$

The output of unit *i* can be expressed as:

$$y^{k+1}(i) = f^{k+1}(a^{k+1}(i)) \tag{3.2}$$

The task of the network is to learn associations between a specified set of input-output pairs {(x_1,T_1), (x_2,T_2), … (x_Q, T_Q)}. The performance index of the network is presented in the following equation:

$$V = \frac{1}{2}\left(\sum_{q=1}^{Q}\left(T_q - Y_q{}^M\right)^T\left(T_q - Y_q{}^M\right)\right) = \frac{1}{2}\sum_{q=1}^{Q} e_q^T e_q \tag{3.3}$$

Where $Y_q{}^M$ is the output of the network when the q^{th} input x_q is presented and e_q is the error computed between the q^{th} output and target. For the standard backpropagation algorithm an approximate steepest descent rule is used. The performance index is approximated as:

$$\hat{V} = \frac{1}{2} e_q^T e_q \tag{3.4}$$

Where the total sum of squares is replaced by the squared errors for a single input/output pair. The approximate steepest (gradient) descent algorithm is then expressed as follows:

$$\Delta W^k(i,j) = -\mu \frac{\partial \hat{V}}{\partial W^k(i,j)} \tag{3.5}$$

$$\Delta b^k(i) = -\alpha \frac{\partial \hat{V}}{\partial b^k(i)} \tag{3.6}$$

Where α is the learning rate.

3.2.2. PID-NN control schemes

Neural networks are used in conjunction with more conventional controllers in order to help or enhance the controller performance. The NN control algorithm can be used as a controller in two different ways: direct control and indirect control. In the direct control, the NN represents the main system controller which performs an adaptive control through online learning process. Its hidden layer neurons simply work as PID controller terms through their activation functions thus it simultaneously utilizes advantages of both PID controller and neural structure [63, 111]. In this type of control, the PID controller parameters are

automatically and continuously tuned in accordance with the changes of the system parameters. The effectiveness of this type of control has been proven in few applications in terms of nonlinear control, tracking capabilities and disturbance robustness.

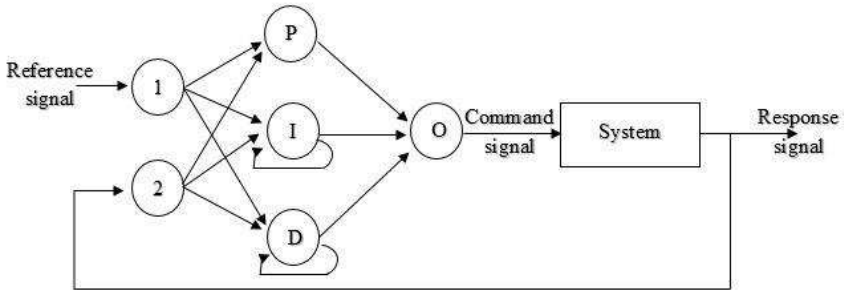

Figure 3.1: Structure of PID-NN direct control [Shahraki et al., 2009].

Indirect NN control means that a NN controller uses a NN model of the system for compensation purposes. In this case, the NN is not the main controller but it is used to model the system to be controlled in order to assist the main controller. The NN in this case is usually trained offline. Figure 3.2 illustrates an example of an indirect NN control.

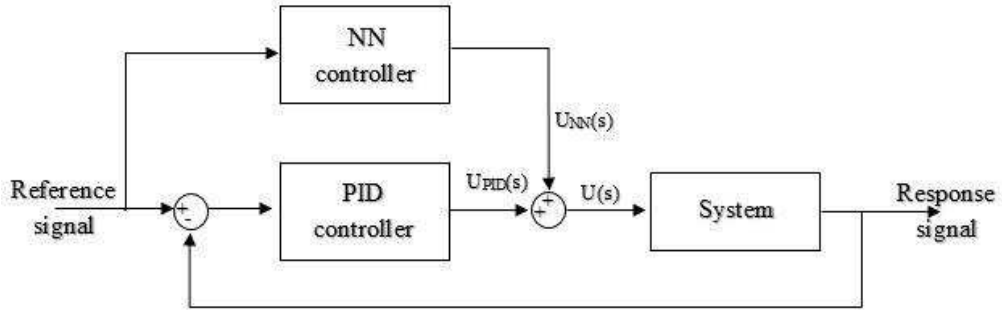

Figure 3.2: Indirect example of NN, Feedforward with NN inverse model control [Norgaard et al., 2002].

Most of the applications of NNs involve indirect control scheme where the NN is used as a compensator [154]. An early study [13] published some comparison results of three different implementation of NN controllers tested for a hydraulic actuator system: 1) simple open loop profile follower, 2) PID neural controller (NN as compensator) and 3) NN controller.

3.3. Shaking table numerical model 01

3.3.1. Description

Modelling of the shaking table is a real complex task due to the several nonlinear parts of the system and its time varying parameters. Many studies have been done to modelling the shaking table system using experimental parameters identification [100] or linearization methods of the dynamic system to develop analytical model of the system [161].

As a starting point, a simplified model of a shaking table has been developed in an early work in form of finite element models to model the global behavior of a typical shaking table in unloaded and loaded conditions [68]. Some details of the finite element model are as follows:

- The platform of the shaking table has been modeled in a shell element with a defined effective mass and stiffness;
- the actuators have been modeled by link elements with a given rigidity, natural frequency, damping ratio and a nonlinear viscous damping coefficient;
- A nonlinear tested structure modeled by plastic link elements at its bases.

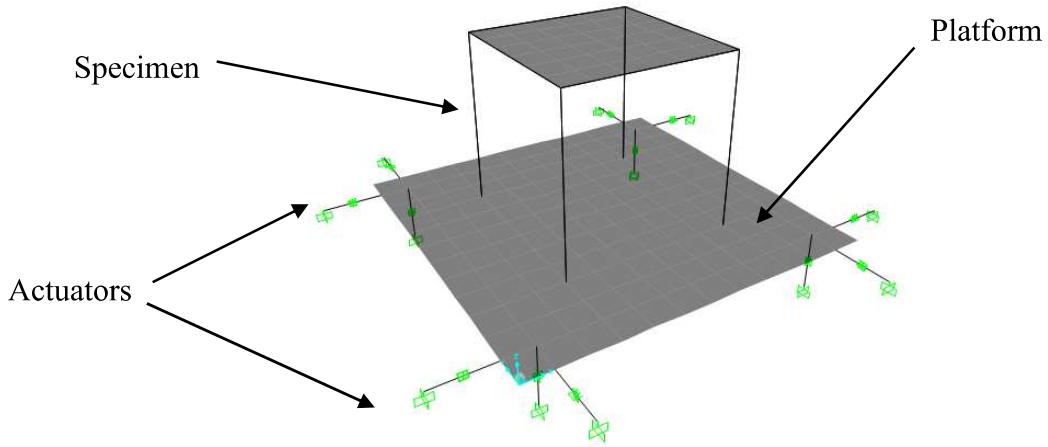

Figure 3.3: FE model of the shaking table and a mounted specimen [Larbi et al., 2015].

Several nonlinear dynamic simulations have been performed to collect input/output time histories used to carry out an estimation of the total transfer function of the system. The second order transfer function is estimated using the MATLAB system identification toolbox, based on the input signal that represents the desired acceleration earthquake record and the output signal that

represents the acceleration response signal measured at the platform of the shaking table. The most accurate results have been produced using sine sweep excitation signal.

The expression of the estimated transfer function is given in the following equation [69]:

$$T(s) = \frac{2.8912\ s+383.9521}{s^2+2.6485\ s+524.642} \tag{3.7}$$

The magnitude and the phase of the shaking table transfer function are shown in Figure 3.4.

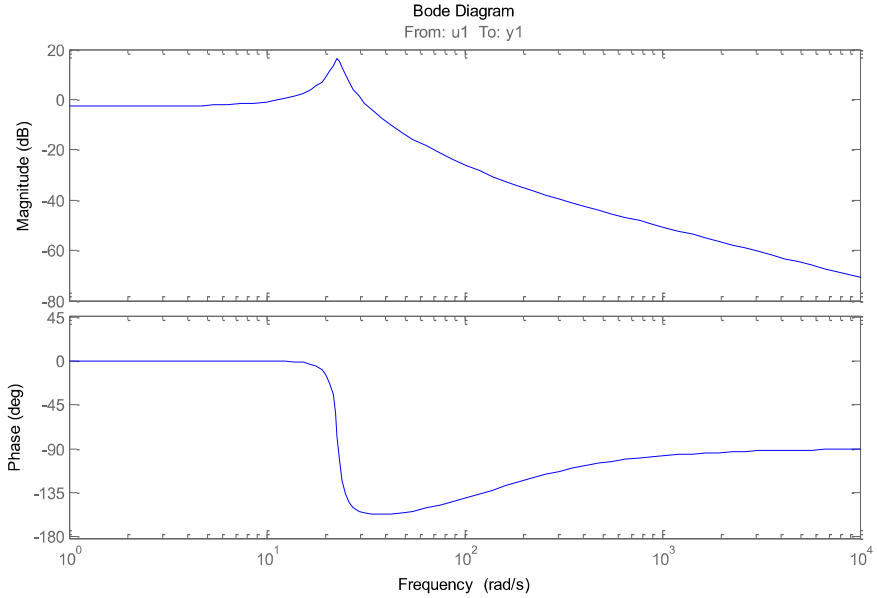

Figure 3.4: Magnitude (a) and phase (b) of the shaking table transfer function.

In order to develop a realistic model of a shaking table with an optimal tuned controller, a conventional PID controller has been added. In order to model the behavior of the shaking table with an online control system, the above transfer function is implemented in Matlab/Simulink with an online PID controller. The tuned gains of the controller i.e. P, I and D parameters are equal to 0.717, 0.013 and 3.32 respectively. The Simulink model of the shaking table is shown in Figure 3.5.

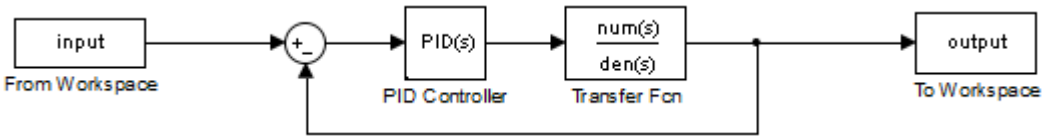

Figure 3.5: Schematic of the Shaking Table with a PID controller (Matlab/Simulink).

3.3.2. NN control strategy

In order to reduce the signal distortion between the desired and the measured signals, two NN control strategies that combine the optimal PID controller and the designed NN control algorithm are proposed. The first control strategy intends to implement the NN in an offline mode. Figure 3.6 represents the Simulink model of the shaking table with the offline NN controller. The NN algorithm is implemented through a MATLAB function. The aim of this control scheme is to produce the appropriate command signal to the shaking table, so as to obtain a closed loop response as close to the desired accelerations as possible. The predefined earthquake record that is presented to the NN as an input data. The second control strategy that is proposed is to use the NN as an additional improvement of the signal replication achieved by the PID controller. The Simulink model of the proposed online control loop is represented in Figure 3.7.

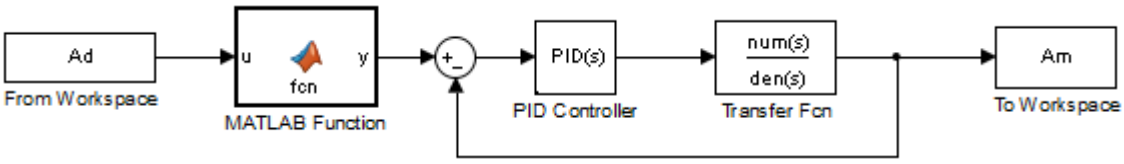

Figure 3.6: Simulink model of the shaking table with offline NN controller.

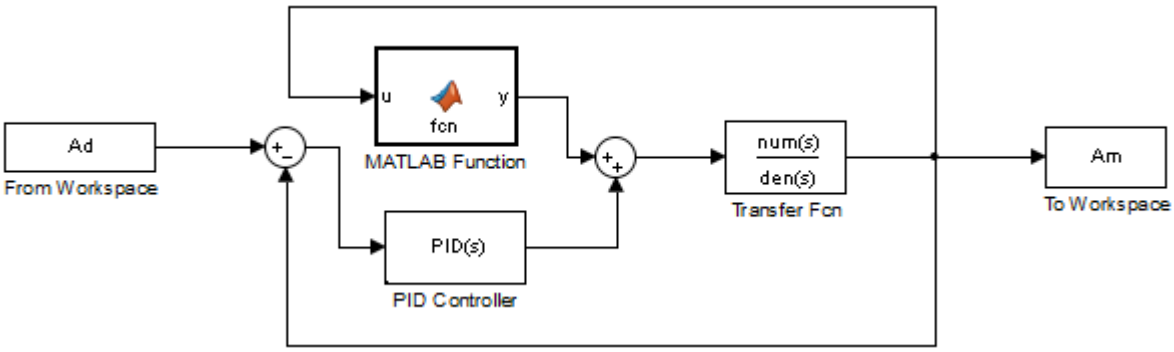

Figure 3.7: Simulink model of the shaking table with online NN controller.

Several existing types of NNs could be found in the literature. The simplest multilayer NN is the most used to enhance the performance of conventional controllers such as the PID [67]. The chosen NN is the Layer-Recurrent Network (LRN) which is a new version of the Elman Network. The number of nodes and hidden layers are determined via a routine optimization procedure of the proposed NN. The chosen structure was established based on the best NN performance in terms of coefficient of correlation, number of epochs, and mean-square-error (MSE) values. Results have led to the choice of the final NN architecture constituted by 21 hidden neurons with sigmoid function.

A number of simulations are carried out to collect input/output acceleration signals of the shaking table with a PID controller that is represented in Figure 3.6 and Figure 3.7. These acceleration data are used to constitute a database to train the NN in offline mode. The training data points are treated with a sampling time of 0.2 millisecond, creating more than 70000 training points. These training data aim to train the NN to predict the appropriate or the additional command signal so that the system responses tend to be as close to the target as possible. The training procedure has three stages: training, validation and testing. In general, the training and testing data are generated from a selected earthquake record by assigning percentages, that is, 70% for training and 30% for validation, while testing requires a data set that the NN had never seen before. The stop criterion of number of epochs for checking the increase of error on the validation data set is selected 1000 and the value of performance goal sets 10^{-4}.

After training, the proposed NN is implemented through a MATLAB Function in the Simulink model of the shaking table as shown in Figure 3.6.

3.3.3. Performance of the NN control

The database to train the NN is constituted using inputs and output signals from the shaking table model controlled by the PID, represented in Figure 3.6 and Figure 3.7. The Lavenberg-Marquardt backpropagation algorithm is used in the training process of the NN. The error in the prediction of the target signal is estimated using the mean square error formula (MSE) formula expressed in Equation 3.8, with a target value around 10^{-4}, as illustrated in Figure 3.8.

$$MSE = \frac{\sum_{i=1}^{N}(A_d(i)-A_{m,NN}(i))^2}{\sum_{i=1}^{N}A_d(i)^2} \tag{3.8}$$

Where $A_d(i)$ is the target acceleration value and $A_{m,NN}(i)$ is the acceleration predicted by the NN at step i. N is the number of data points which is 70000 for El Centro earthquake record used to train the NN.

A linear regression between the network response and the target is performed and a correlation coefficient between the response and the target R is calculated using the following equation:

$$R_{xy} = \frac{\sum_{i=1}^{N}(x_i-\bar{x})(y_i-\bar{y})}{\sqrt{\sum_{i=1}^{N}(x_i-\bar{x})^2\sum_{i=1}^{N}(y_i-y)^2}} \tag{3.9}$$

In this case, the signal x represents the output of the NN and the signal y represents the target. The coefficient of correlation is computed to evaluate the degree of similitude between the output and the desired signals, for several real ground motions.

The fitting line shown in Figure 3.9 is practically superposed with the diagonal and the correlation coefficient R obtained is very close to unity. An example of a time-domain comparison between the NN output and the target signal for Northridge earthquake record is illustrated in Figure 3.10. As it is shown, the NN is capable to produce the desired acceleration with high accuracy.

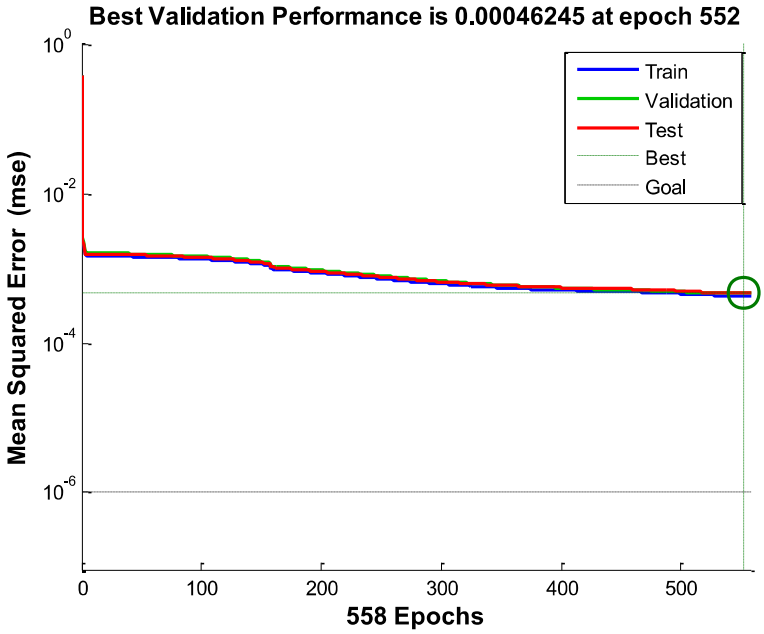

Figure 3.8: Mean Square Error (MSE) in the NN prediction of the target signal.

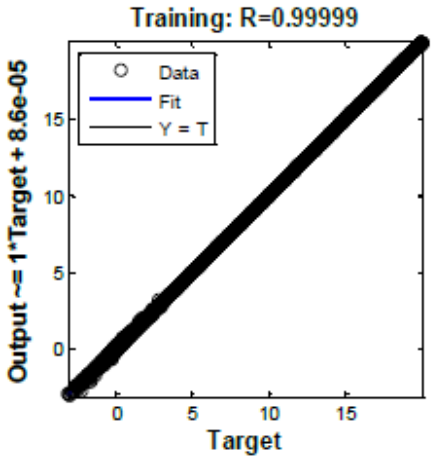

Figure 3.9: Linear regression between the NN output and the target signal.

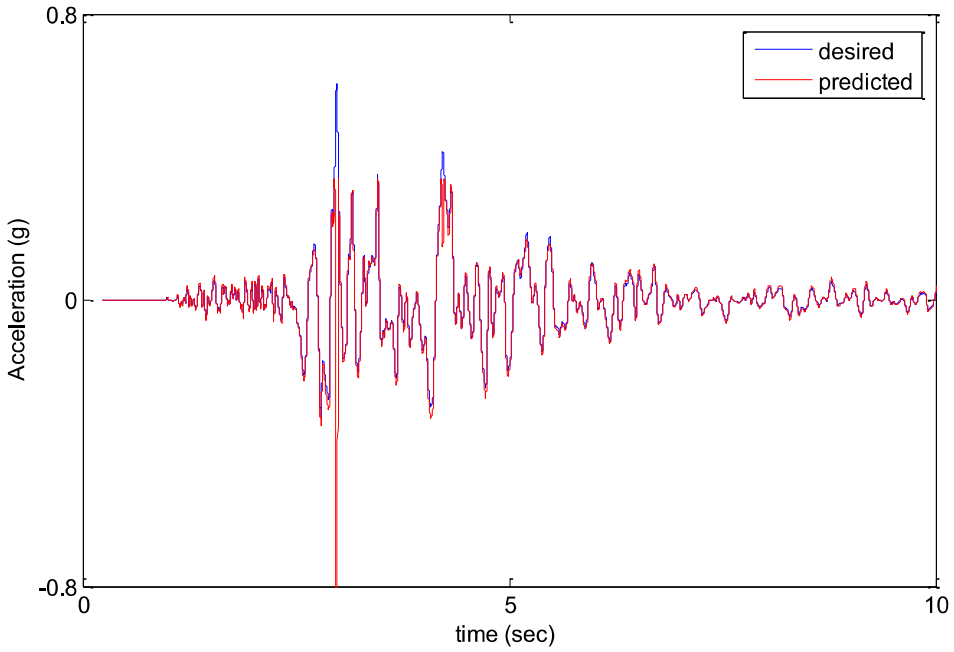

Figure 3.10: Time domain comparison between the target and the NN output (Northridge earthquake record).

Then, the trained network is implemented in the model to represent an additional control function in conjunction with the PID controller in two different ways: offline and online. The performance of the combined control is evaluated by comparing the closed loop responses and the target signals. This comparison is quantified through the computation of the Root Mean Square Error (RMSE) between the reference signals and the reproduced accelerations. For this purpose, several earthquake records are simulated using the PID controller alone and the combined PID-NN controller.

Table 3.3 resume the RMSE values, computed using equation 3.10, obtained before and after implementing both the offline and the online NN controllers.

$$RMSE = \frac{\sum_{i=1}^{N}(A_d(i)-A_m(i))^2}{\sum_{i=1}^{N}A_d(i)^2} \tag{3.10}$$

Where $A_d(i)$ is the desired acceleration at step i, $A_m(i)$ is the acceleration system output at step i and N is the total number of data points.

It is found that the online control scheme produced more accurate response signals than the offline control. This is due to the fact that the NN that takes into

account the response data to readjust its parameters and provide the appropriate command signal at each time step when it performs online.

Table 3.1: RMSE between the response and reference accelerations for PID and PID+NN controllers.

Earthquake record	RMSE (%) PID	RMSE (%) PID+NN	
		offline	online
El-Centro	07.92	07.47	06.58
Cape-Mendocino	12.67	12.12	12.05
Northridge	07.56	07.13	06.39

Figure 3.11 to Figure 3.13 show the time-domain comparison between the target signals and the response signals achieved with the PID controller alone and with the combination of the PID and the online NN controller. As it can be seen through the plots, the NN enhances the signal reproduction on the shaking table, where the time delays in the system responses are significantly reduced and the entire output signals with the additional neural control correction follows the target signal more accurately, especially at the peak values.

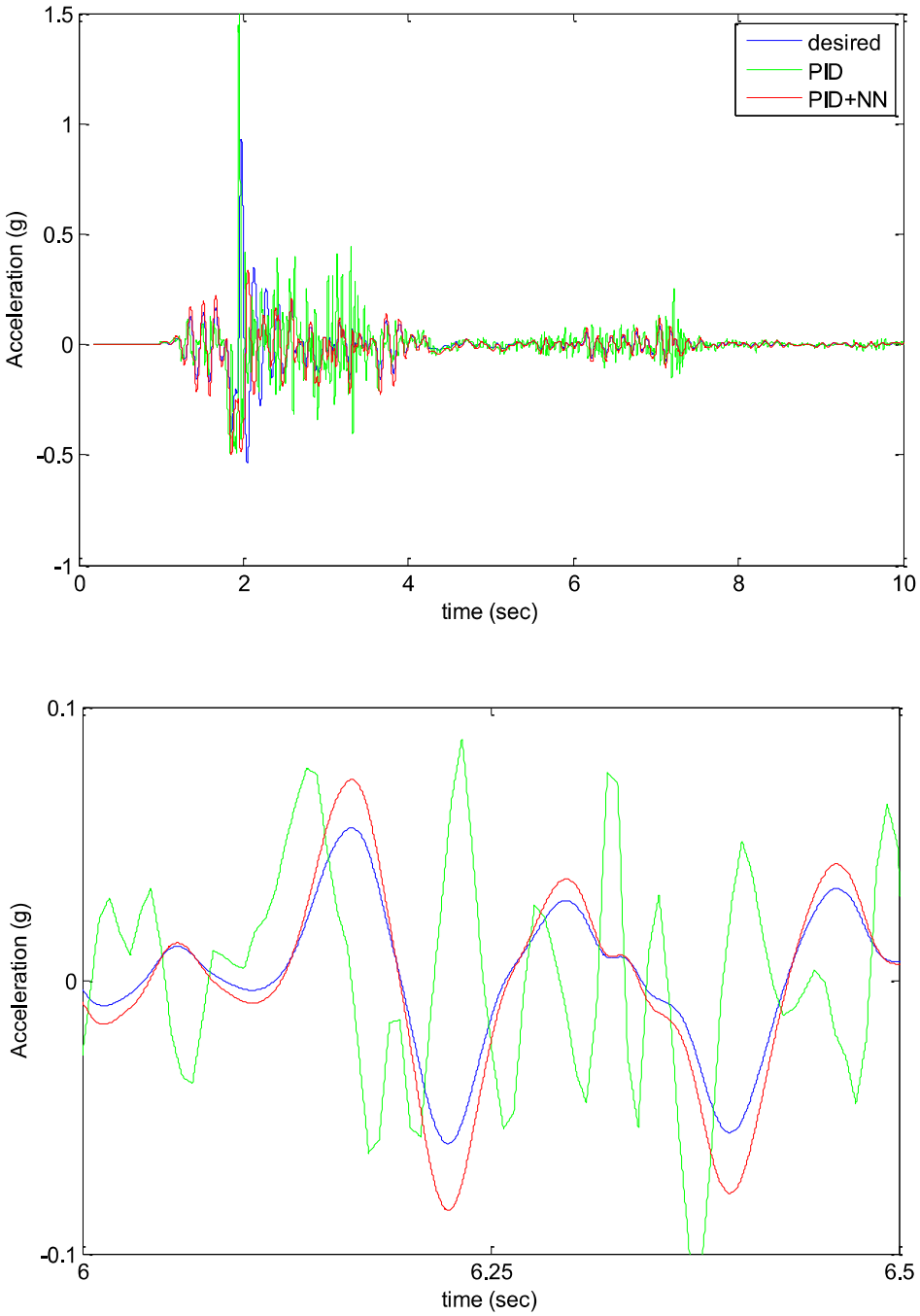

Figure 3.11: Time domain comparison between the desired signal and the reproduced signal with the PID and the PID-NN (Cape-Mendocino earthquake record).

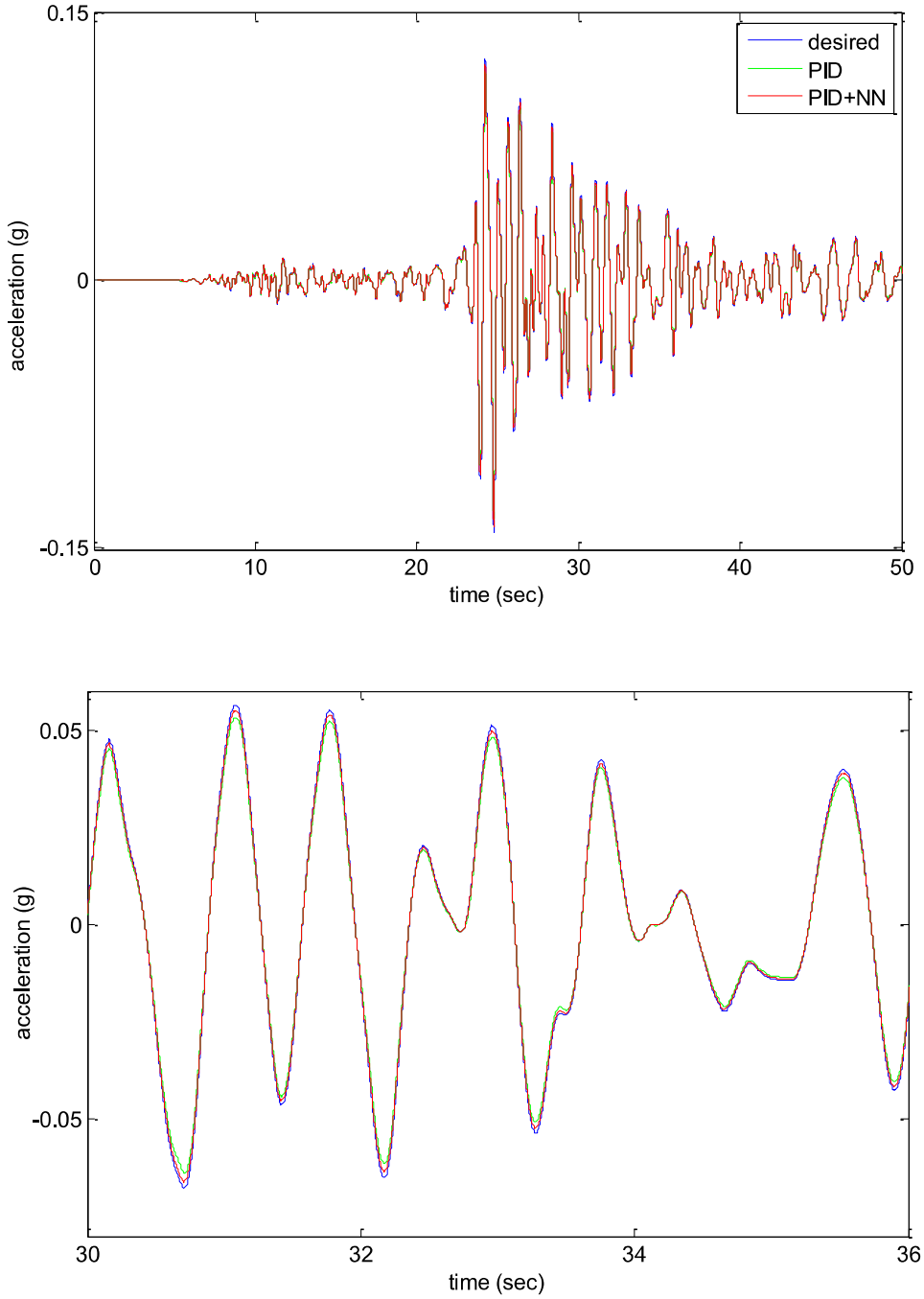

Figure 3.12: Time domain comparison between the desired signal and the reproduced signal with the PID and the PID-NN (Kobe earthquake record).

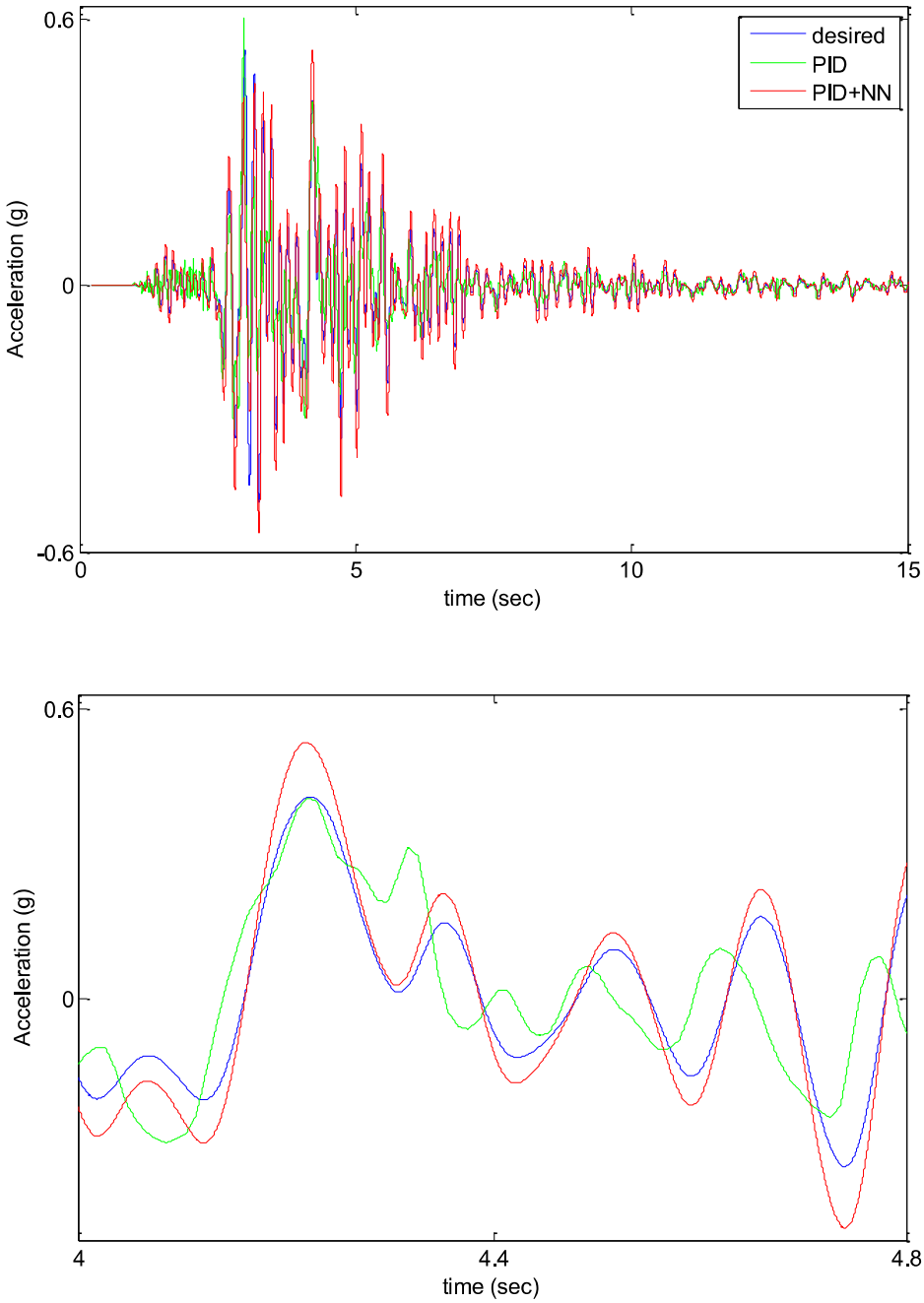

Figure 3.13: Time domain comparison between the desired signal and the reproduced signal with the PID and the PID-NN (Northridge earthquake record).

3.4. Shaking table numerical model 02

3.4.1. Description

This model is a representative model of the QUANSER Shaking Table III, described in details in Chapter 3. The QUANSER STIII is an electric bi-axial electro-hydraulic earthquake simulator. The control system is a PD-Feedforward (PDFF) Simulink-based controllers that run in real-time through the real-time control software QUARC. The advantage of these controllers is the possibility to simulate several real earthquake records and also, to perform analysis through the Matlab environment. The bloc diagram used to control the stage position is depicted in Figure 3.14.

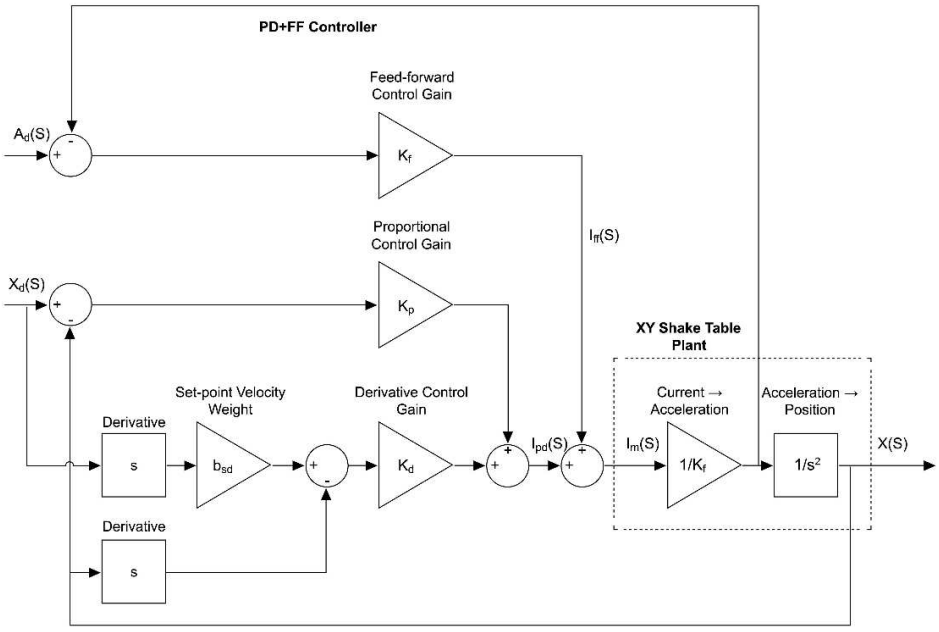

Figure 3.14: Bloc diagram of the shaking table position control.

Where $A_d(s)$ is the desired acceleration, $X_d(s)$ is the desired position, X(s) is the measured position, b_{sd} is the set-point velocity weight, $I_{ff}(s)$ and $I_{pd}(s)$ are the command signals provided by the FF and the PD controllers, respectively.

The current motor signal $I_m(t)$ used by the PDFF controller to regulate the stage position along the horizontal x axis is represented in the following equation:

$$I_m(t) = K_p\big(x_d(t) - x(t)\big) + K_d\big(\dot{x_d}(t) - \dot{x}(t)\big) + K_f(\ddot{x_d}(t) - \ddot{x}(t)) \qquad (3.11)$$

K_p is the proportional control gain, K_d is the derivative control gain. The gains values are fixed by default in the controller software for each axis. The PD gains are obtained allowing the two following expressions:

$$K_p = K_f \omega_n{}^2 \tag{3.12}$$

$$K_d = 2K_f \xi \omega_n{}^2 \tag{3.13}$$

The values given in the user manual are as follows: ω_n=62.8 rad/s which represents the natural frequency and ξ=0.8 which represents the damping ratio of the closed loop control.
The default gain values are given in Table 3.2.

Table 3.2: Controller gains values.

DOF	K_p	K_d	K_f
X	7533 A/m	191.8 A-s/m	1.91 A/(m/s)²
Y	2577 A/m	191.8 A-s/m	0.653 A/(m/s)²

Even if the control system of the Quanser STIII is implemented in Simulink with an accessible and easy way, replicating the entire model as faithfully as possible and obtaining responses similar to the experimental signals is still a great challenge. First, several dynamic tests have been carried out on the Quanser STIII to collect a database constituted by input-output real signals. A realistic model of the shaking table is developed and validated, as represented in Figure 3.15. As shown in this figure, the simulated acceleration can track the experimental results with a good performance. It indicates that the model that is built represent a decent environment to simulate the real behaviour of the real shaking table. The experimental and the simulated response of the shaking table to El-Centro earthquake record are compared in Figure 3.16.

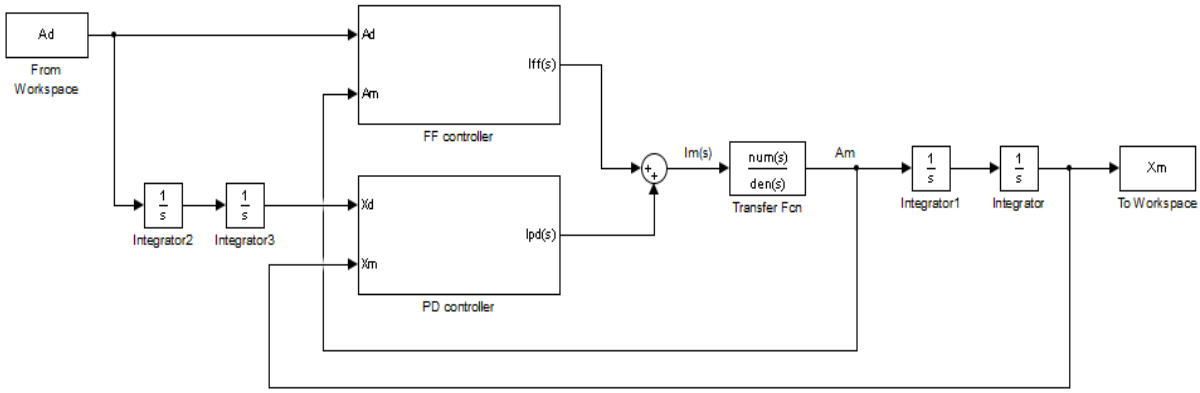

Figure 3.15: Numerical model of the QUANSER STIII in Simulink.

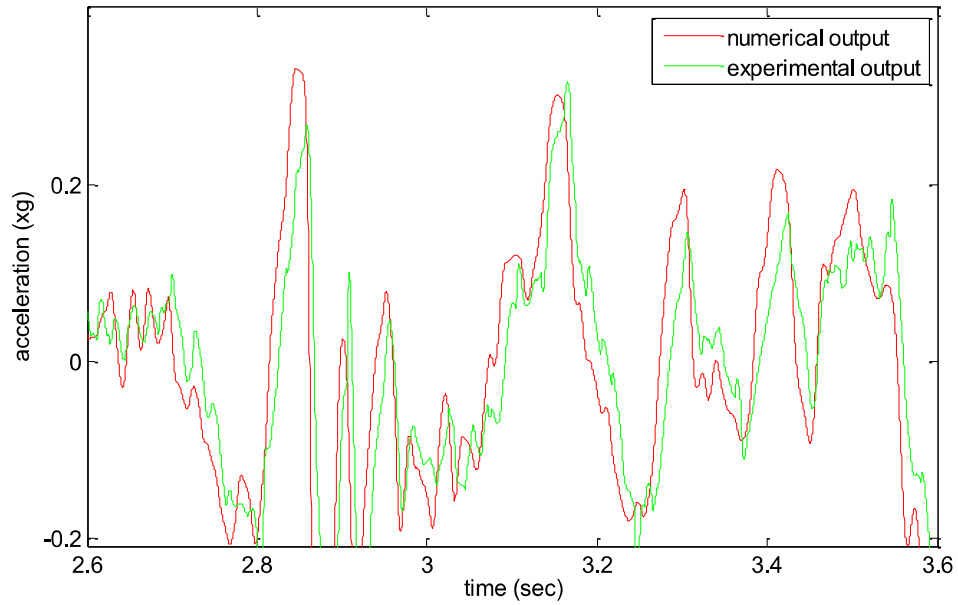

Figure 3.16: Degree of similitude between the numerical and the experimental responses (El-Centro earthquake record).

3.4.2. NN Control strategy

While shaking tables are designed to reproduce reference accelerations, inner-loop controllers are in most cases performing in displacement mode. In practice, the displacement controllers fail to replicate accelerations signals accurately. As for the Quanser Shake Table III, the actual control system which is the PD-Feedforward (PDFF) controller, provides a quasi-perfect matching between the measured position and the desired position. However, the control is not as efficient in the reproduction of acceleration signals. This distortion problem is obtained for different types of signals such as sinusoidal signals, random

acceleration signals and acceleration earthquake records. The performance achieved by the actual PD-FF controller for both displacement and acceleration are shown respectively in Figure 3.17 and Figure 3.18.

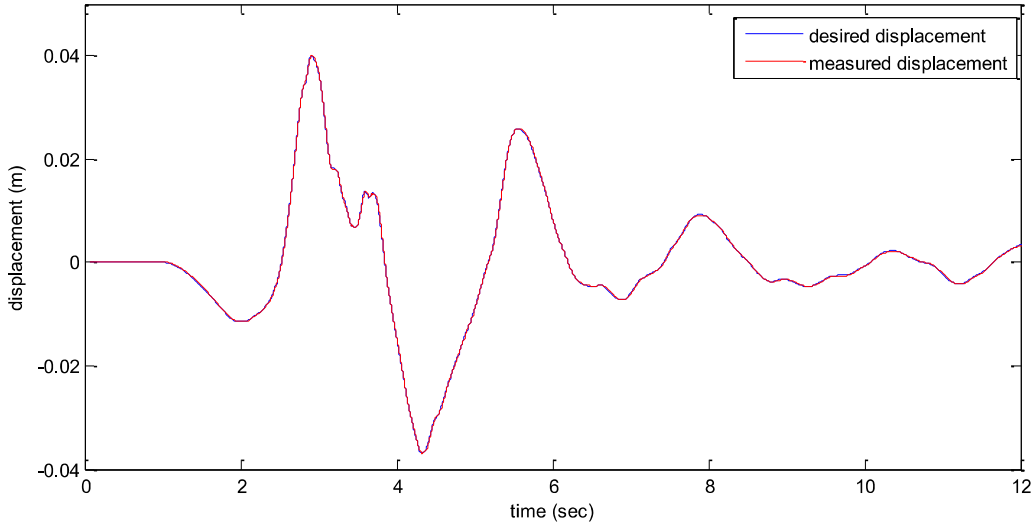

Figure 3.17: Comparison between the desired and measured position with the original PDFF controller (El-Centro earthquake record).

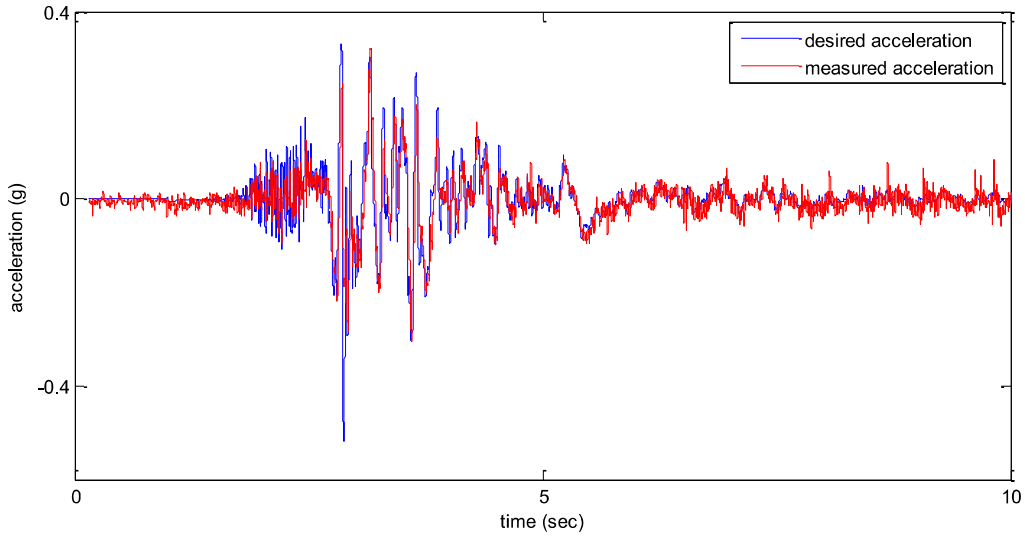

Figure 3.18: Comparison between the desired signal and experimental response acceleration with the original PDFF controller (El-Centro earthquake record).

The numerical model of the shaking table QUANSER STIII is simulated under a number of selected earthquake records. Similarly to the first proposed NN

control methodology for the first model of the shaking table, the structure of the NN in terms of type, number of hidden layers and the number of hidden neurons is kept unchanged.

The feedforward NN is trained offline using data that are collected from the simulated input and output signals of the numerical shaking table model using the Lavenberg Marquardt training algorithm.

Number of implementations of the NN controller combined with conventional controllers such as PID controllers could be found in the literature. Many advantages and disadvantages could be examined. However, as the shaking table system a unique dynamic system, the optimal configuration of the combination of the designed NN control function with the PDFF controller could only be determined via trial-and-error. In this case, two methodologies for the NN implementation are investigated: an offline and an online NN control. In order to choose the optimal implementation of the NN block in the numerical model, a routine optimization procedure is performed based on the values of the computed RMSEs between the reproduced signals and the desired signals. The smaller error is reached, the best matching results are obtained.

Three different block diagrams of three NN implementations are presented in Figure 3.19 where Figure 3.19(a) represents the offline control scheme and Figure 3.19(b) and Figure 3.19(c) represent two different online control schemes.

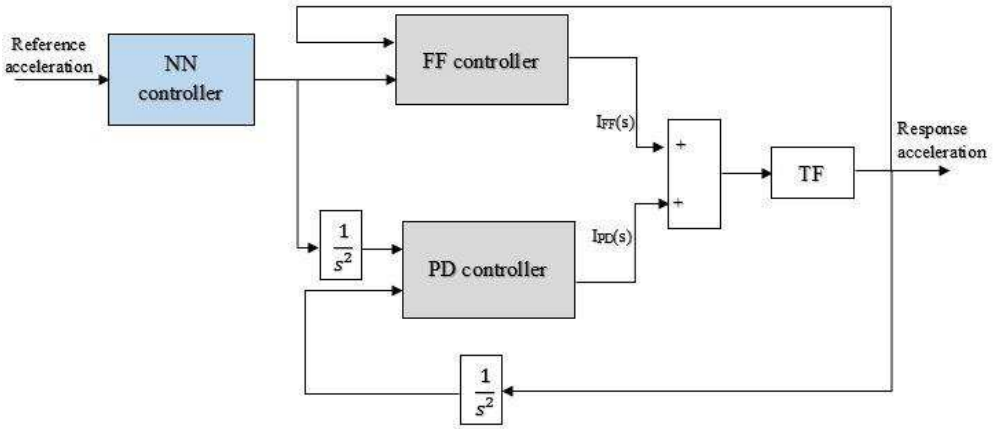

(a)

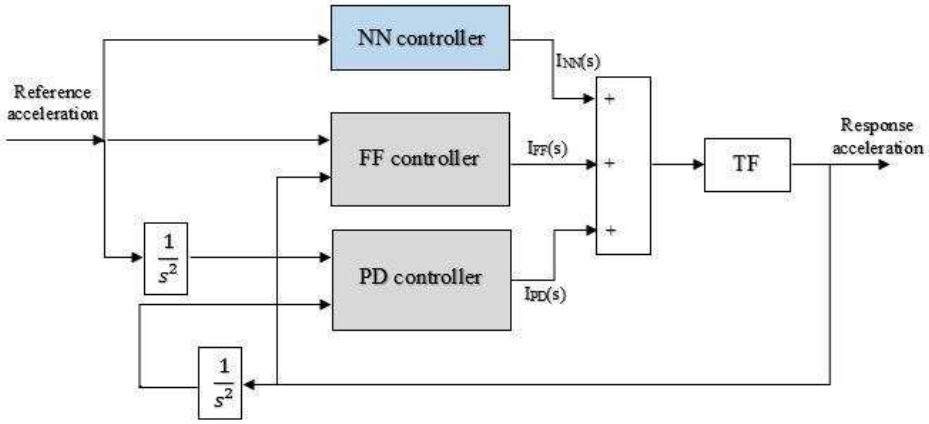

(b)

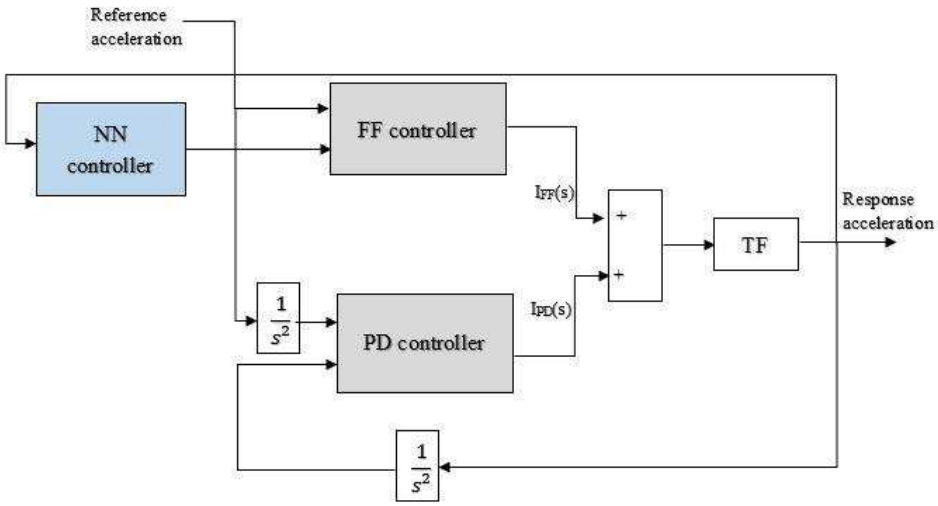

(c)

Figure 3.19: Variation of the implementation of the NN block (a) offline (b) and (c) online.

For each implementation scheme of the NN, the RMSE value is computed and compared with the RMSE obtained with the original PDFF controller alone. These values are summarized in Table 3.3. The results have led to select the final implementation that is represented in Figure 3.20. As it can be observed, the optimal online control scheme that has provided the smallest error in acceleration reproduction is the scheme (b).

Table 3.3: RMSE between the response and reference accelerations for different NN block implementation.

Earthquake record	RMSE (%) PDFF	RMSE (%) PDFF + NN		
		Scheme (a)	Scheme (b)	Scheme (c)
El-Centro	06.86	06.53	05.94	07.28
Cape-Mendocino	12.10	12.53	10.69	12.89
Northridge	06.37	06.72	05.83	07.38

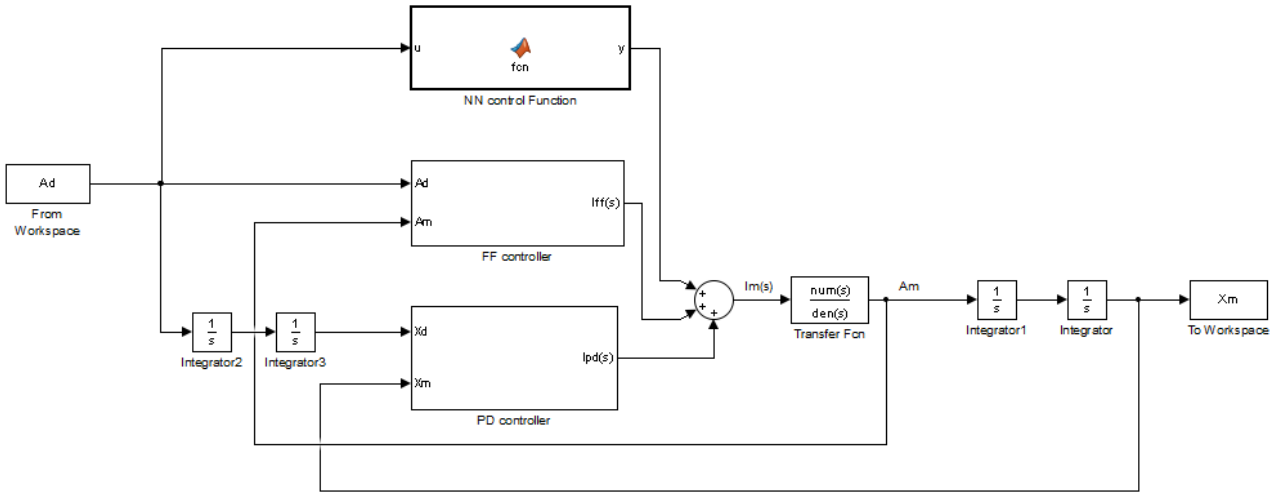

Figure 3.20: Simulink model of the shaking table with the proposed NN based PD-Feedforward controller.

3.4.3. Performance of the NN control

The database to train the NN is constituted by acceleration signals collected via several simulations of the shaking table model controlled by the PDFF controller. The error in the prediction of the target signal is estimated using the mean square error formula (MSE) with a target value around 10^{-4}, as illustrated in Figure 3.21. A linear regression between the network response and the target is performed and a correlation coefficient between the response and the target R is calculated. The fitting line shown in Figure 3.22 is practically superposed with the diagonal and the correlation coefficient R obtained is very close to unity. An example of a time-domain comparison between the NN output and the target signal for Northridge earthquake record is illustrated in Figure 3.23.

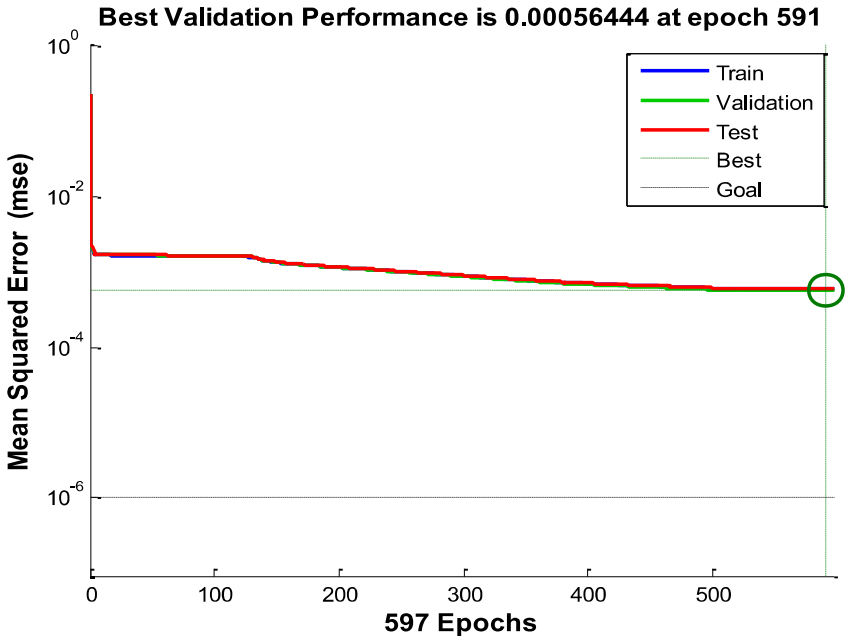

Figure 3.21: Mean Square Error (MSE) in the NN prediction of the target signal.

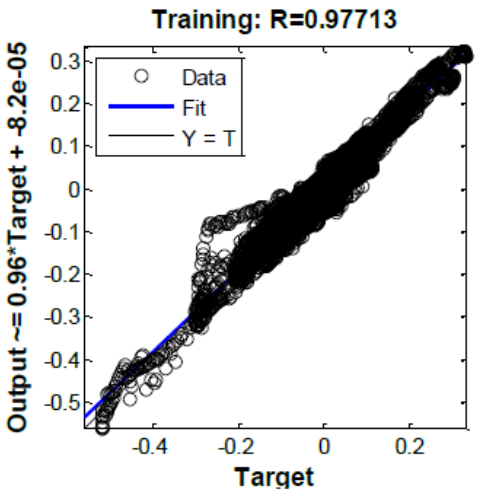

Figure 3.22: Linear regression between the NN output and the reference signal.

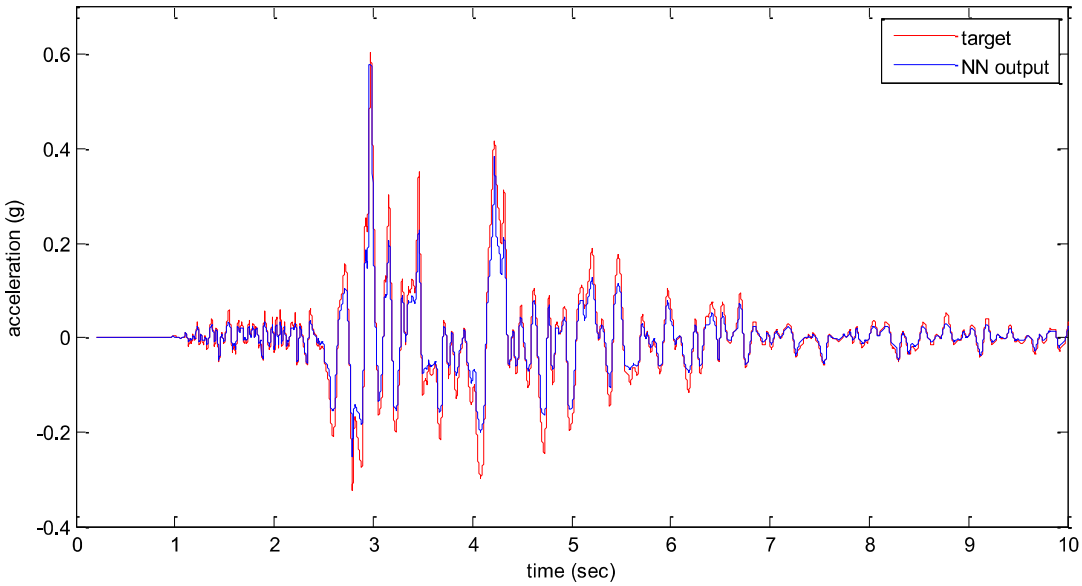

Figure 3.23: Time domain comparison between the target and the NN output (Northridge earthquake record).

After good performance in the training process, the NN is implemented and simulated online with the actual PDFF controller. Numerous simulations using real earthquake records are carried out. The results prove that the NN outperforms the PDFF controller in terms of signal distortion. In fact, the acceleration responses of the numerical shaking table model to different earthquake records are closer to the target with the additional NN-based controller, especially in peak values. As showed in Table 3.3, the RMSE between the output and the desired signals, which is computed for several

ground motions, has reached smaller values. This highlights to the capabilities of the additional NN control function to improve the acceleration tracking accuracy of the shaking table system.

Figure 3.24 to Figure 3.26 show comparisons in time-domain between the desired accelerations and the measured accelerations produced with both the PDFF and the PDFF+NN controllers for few of the used earthquake records.

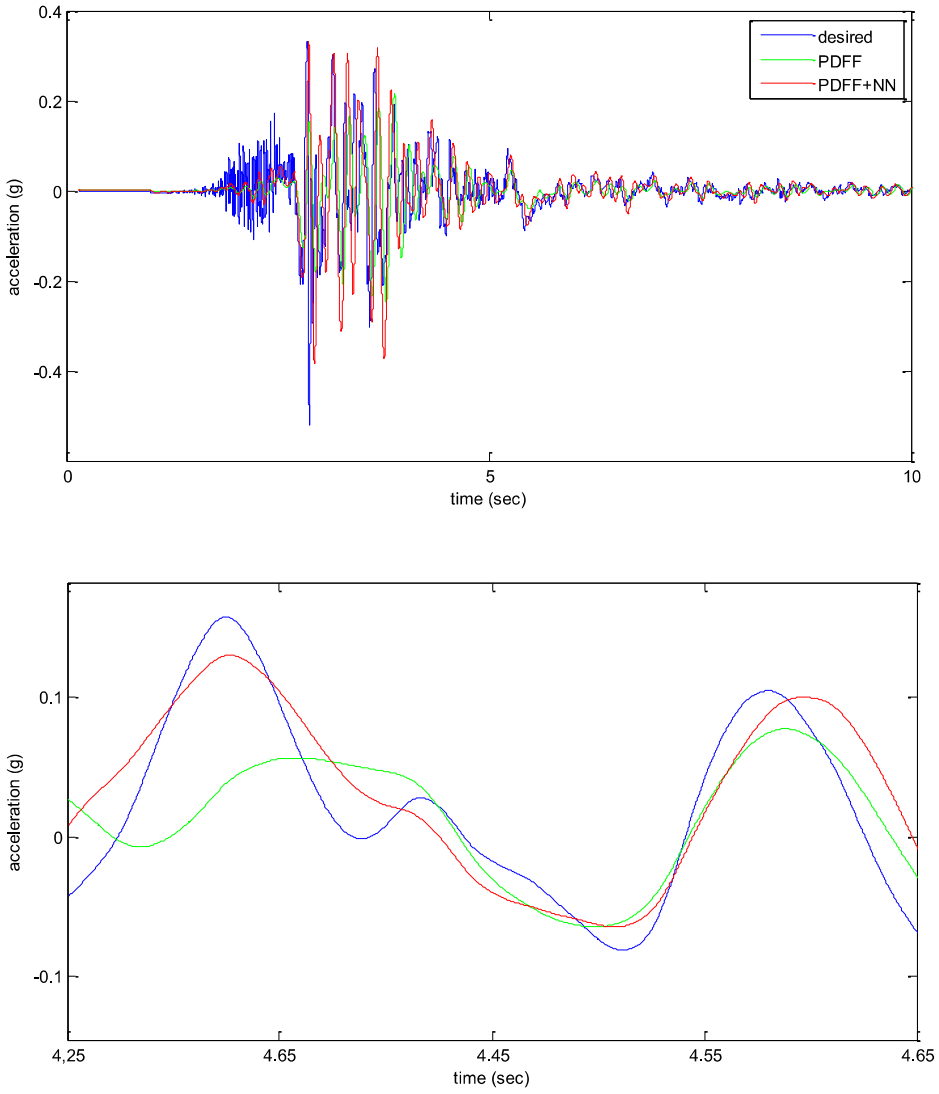

Figure 3.24: Time domain comparison between the desired signal and the reproduced signal with the PID and the PID-NN (El-Centro earthquake record).

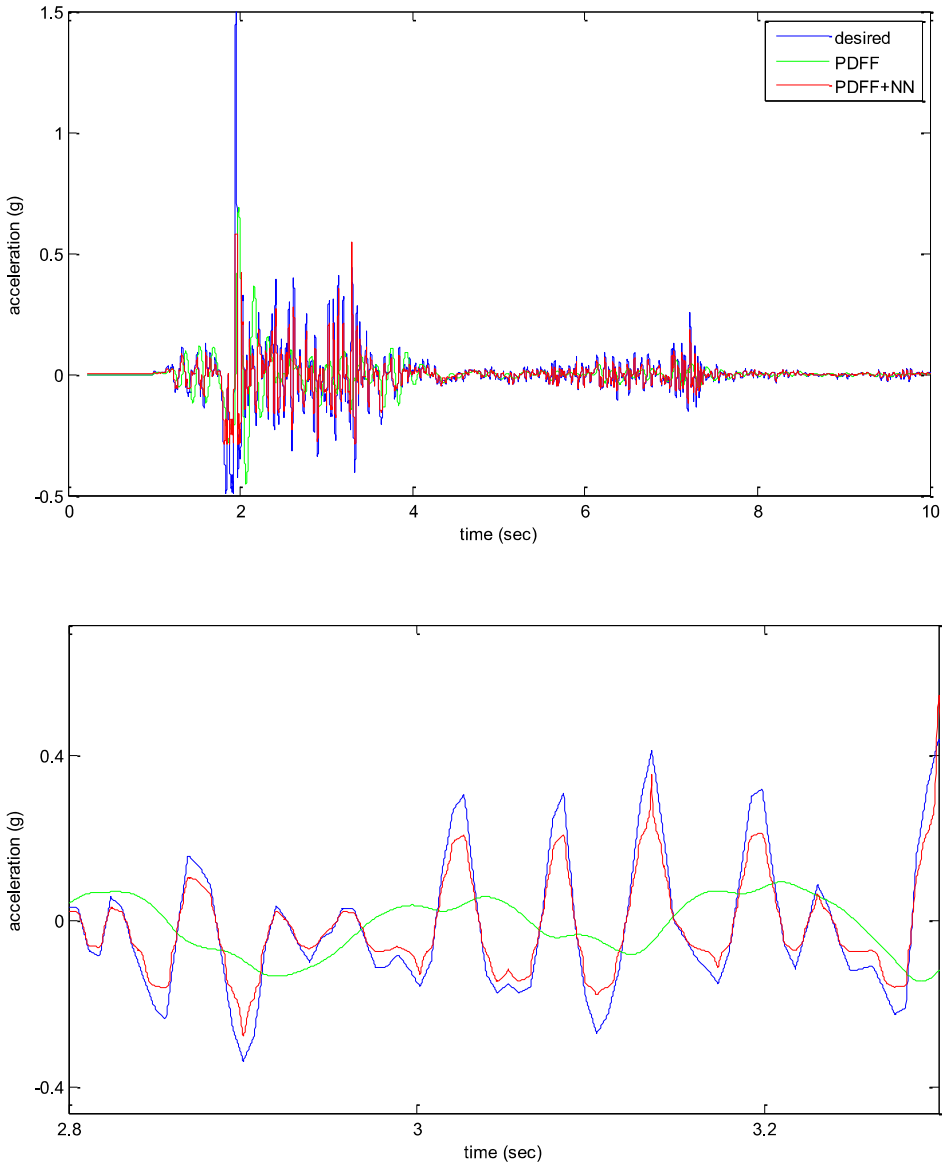

Figure 3.25: Time domain comparison between the desired signal and the reproduced signal with the PID and the PID-NN (Cape-Mendocino earthquake record).

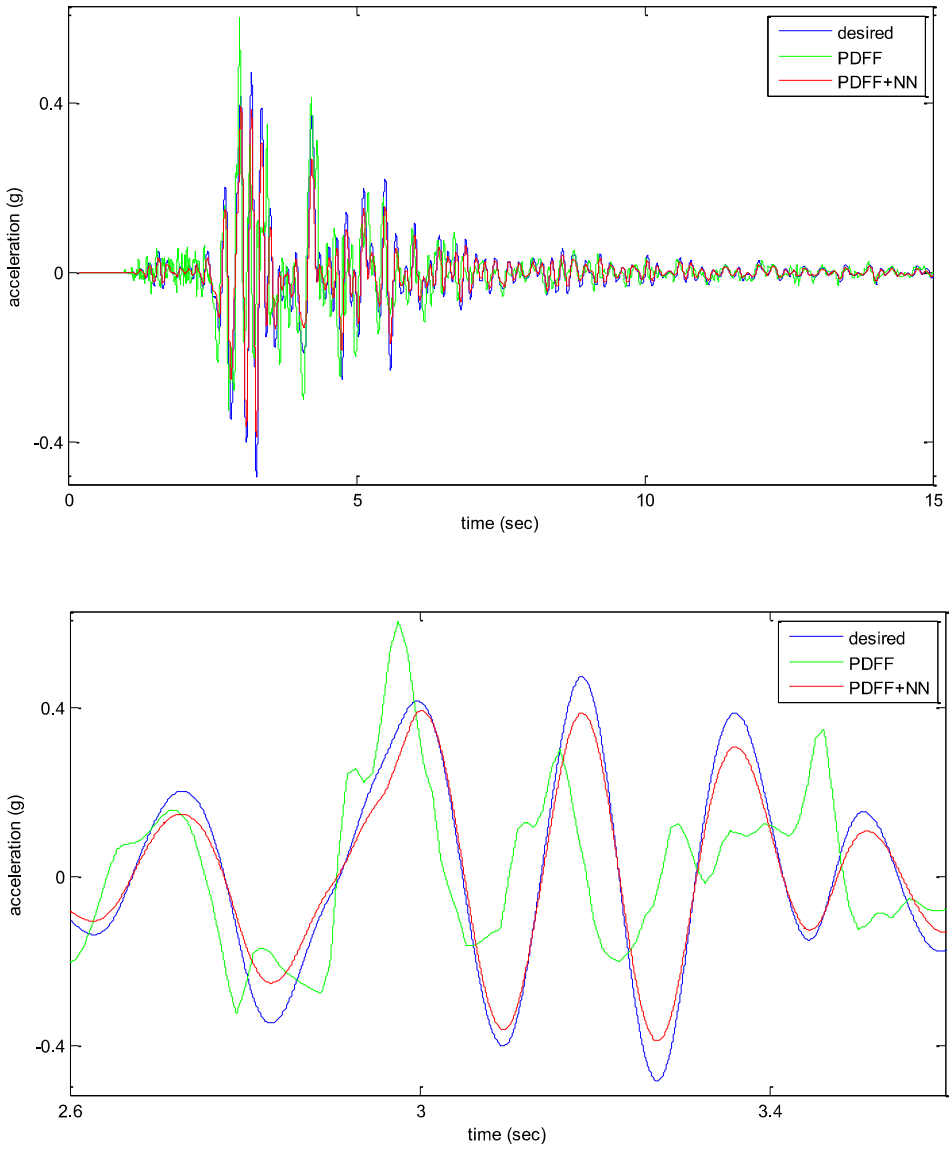

Figure 3.26: Time domain comparison between the desired signal and the reproduced signal with the PID and the PID-NN (Northridge earthquake record).

3.5. Conclusion

This chapter provides evidence of potential enhancement of the acceleration tracking accuracy of shaking tables controlled by conventional controllers using NNs. For this purpose, two models of shaking table are developed in MATLAB/Simulink environment to reproduce the shaking table's behaviour as faithfully as possible. The first model represents an estimated transfer function of a Finite Element model capable to replicate the global behaviour of a standard shaking table controlled by an optimal PID tuned controller. The second model is a realistic Simulink model of an electric bi-axial shaking table which is the QUANSER STIII controlled by a Simulink-based PD-Feedforward controller. These two models produce the input and output data that is used to train the NN. After training of the NN, different implementation schemes of the neural control algorithm are tested and investigated in order to obtain the optimal control loop that provides the best matching performance. For several simulations using real earthquake records, the output signal produced by the numerical shaking table model is closer to the target with the additional NN controller. Through this numerical validation, the designed NN shows prominent control features. Therefore, an experimental implementation to reduce the observed signal distortion on the QUANSER STIII is carried out in the next chapter.

CHAPTER 4

EXPERIMENTAL IMPLEMENTATION OF THE NN-PDFF CONTROLLER

4.1. Introduction

The utility of shaking table tests to study the effects of dynamic vibrations on structures highly depends on the ability of the shaking table, on which the structure is mounted, to faithfully reproduce signals whose effects are important to analyse. In order to track reference signals with the lowest distortion possible, accurate control of such devices is fundamental to ensure the reliability of the shaking table tests. In the previous chapter, the numerical model of the QUANSER STIII provided a simulated environment to implement a designed NN control function and to assess its performance when associated with the original PDFF controller in term of reducing the signal distortion in measured accelerations.

In this chapter, as a result of the simulation study, the NN control algorithm is implemented online in the acceleration closed-loop of the real QUANSER STIII control system to experimentally evaluate the robustness of the designed controller. The NN acts on the command signal and compensate for acceleration distortions due to the system nonlinearities as well as the dynamic table-specimen interaction. Several comparisons are undertaken to assess the performance of the PDFF-based NN controller over the original PDFF controller.

4.2. Experimental facility description and test procedure

The experimental part of this thesis has been conducted on a QUANSER Shaking Table III located at the Laboratory of the Faculty of Civil Engineering of the University of Djelfa, Algeria. An overview of the facility with a mounted specimen is shown in Figure 4.1. The detailed components of the shaking table are presented in Chapter 2. As mentioned previously, the shaking table is a bi-axial high-powered planar stage that can move a maximum payload of 100Kg at a maximum of 1g acceleration. The stage has a total stroke of ±21 cm along either x-axis or y-axis. In order to increase the system performance and to keep the tests quiet, the shaking table is actuated using three linear motors. Two motors mounted on the bottom stage of the shaking table

operate in parallel and power the x-axis. A single motor mounted to the top stage actuates the y-axis.

The shaking table system contains a power amplifier (PWM current-controlled amplifiers), Data acquisition (DAQ) device (QUANSER Q8) and a connected PC (a common commercial PC) to run the real-time software (QUARC software).

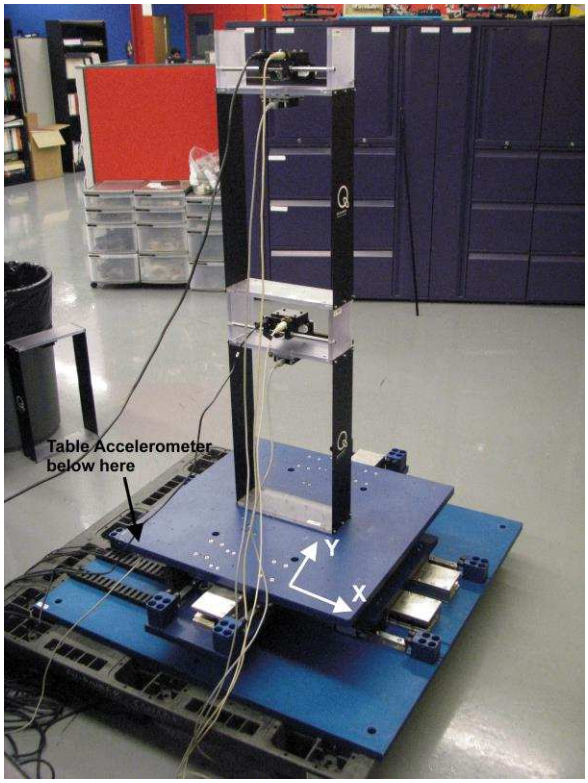

Figure 4.1: View of the QUANSER Shaking Table III with a mounted specimen.

The desired command signal to be reproduced on the shaking table platform (sine wave, sine sweep, earthquake record, etc.) is selected by the user via the connected PC. Then, the current needed is computed using the QUARC software and sent through the analog output channel of the DAQ device to the power amplifier. Therefore, the amplifier applies the current and drives the motor on the shaking table to move the platform along the command signal.

The resulting displacement and acceleration of the stage are measured by the on-board encoders (LIDA 477/487 Heidenhain encoders) for displacement measurements and the accelerometer sensors (A dual-axis ADXL210E accelerometer) for acceleration measurements in a range of ±10 g and a noise's range of ±5.0 mg.

The encoders and accelerometers are connected to the DAQ and their signals can be displayed and processed further on the connected PC. The x-axis and y-axis differential encoders are connected to a line driver to output a single-ended signal.

These signals are then connected to the DAQ. The limit switch output is connected directly to the digital inputs on the data acquisition system.

The system hardware contains an Emergency-Stop switch (E-Stop switch) and an ARM button on the front panel of the amplifier/control box, presented in Figure 4.2. It is important to note that the amplifiers can only be enabled if the E-Stop switches are in the released position and the ARM button has been pressed.

Figure 4.2: Front panel of the amplifier/control box.

The shaking table test can be performed following this procedure:

1. System power
    a. Turn ON the main power supply that is connected to the amplifier (three-phase or single-phase).
    b. Release the E-Stop button located on the front panel of the amplifier/control box, shown in Figure 4.2, by turning it clockwise ;
    c. Release the switch on the remote E-Stop (the red button) shown in Figure 4.2;
    d. Press on the green ARM button on the front panel of the amplifier box, shown in Figure 4.2;
    e. The POWER and ARMED LEDs should both be ON. If the PC was just turned ON, then the amplifiers will be enabled. Otherwise (e.g, if a controller was just ran), the amplifiers are ready-to-be-enabled.
2. Calibration

    Before running the shaking table test, the top stage should be in the middle stroke position on both x-axis and y-axis. The calibration of the stage could be performed following these steps:

    a. Run the "*q_cal_xy.mdl*" Simulink model of the shaking table calibration, shown in Figure 2.9 (Chapter 2) once the model is built;
    b. After the controller has been ran, the stage begins to move towards the center and stops at the middle of the left and right limit switches (the

center position) and the message showing “table calibrated” then appears.

This indicates that the calibration of the table has been successfully done and the shaking table test can be carried out.

3. Shaking table tests

In order to carry out the shaking table tests, the user needs to select the type of the excitation signal to be sent via the command PC. The Simulink block diagrams to command a sine wave signal, a sine sweep signal or an earthquake record are presented in Figures 2.10 to 2.12 of chapter 2. In order to command a reference signal, the user specifies the desired amplitude and frequency for the sine signal, the initial and final frequencies along with the amplitude for the sweep signal, and the name of the earthquake record for the earthquake replication.

The procedure of running a shaking table test is presented by these steps:

a. Run the Matlab script “*setup.m*” in order to compute the controller gains, the filters parameters, the sensor calibration constants, and all the parameters used in all supplied Simulink models;
b. Open the appropriate Simulink model (*q_sine_xy.mdl*, or *q_sweep_xy.mdl* or *q_quake_xy.mdl*);
c. Build the QUARC controller;
d. Run the QUARC controller; therefore, the shaking table tracks the defined command signal and the measured positions and/or accelerations can be displayed, saved and analyzed.
e. The controller stops by itself when the duration defined by the user for the sine and sweep signals or the duration of the earthquake record is reached.

The maximum acceleration of the command signal that the table is capable to track for a given frequency or range of frequencies, can be defined from the bandwidth curve represented in Figure 4.3 for both x-axis and y-axis. These bandwidth curves take into account the limitations of the shaking table in position, velocity and acceleration for unloaded conditions. For the x-axis, low frequencies between 0-2.1Hz are limited by the table stroke. Beyond this range, commands are limited by the acceleration. For the y-axis, low frequencies between 0-1.9Hz are limited by the table stroke. For frequencies in the range of

1.9-3.3Hz, commands are limited by the velocity. For frequencies higher than 3.3Hz, commands are limited by the acceleration.

The bottom plot shows the acceleration of the load when the stage is tracking a sine wave at varying frequencies with an amplitude specified by the combined limit.

Figure 4.4 presents the bandwidth curves for both x-axis and y-axis with a 100Kg payload.

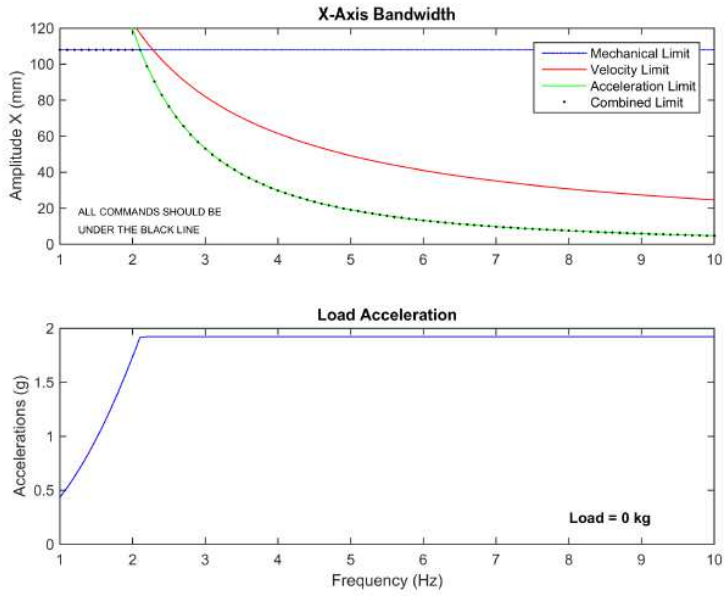

(a)

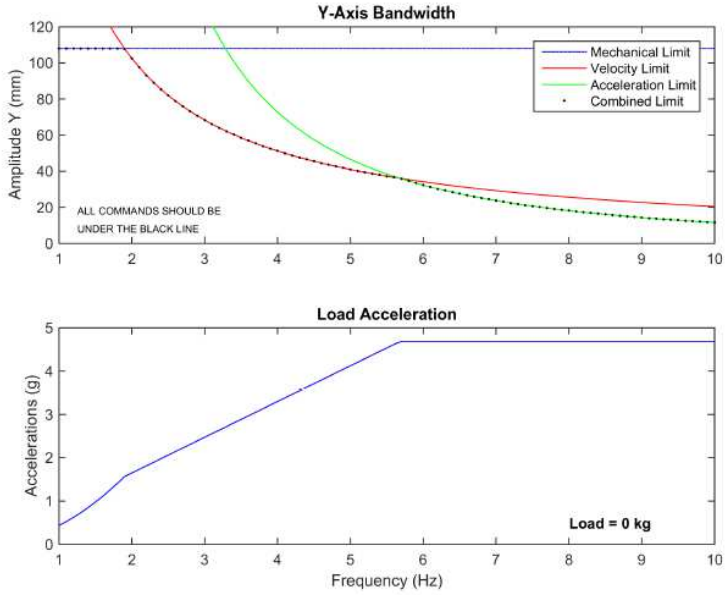

(b)

Figure 4.3: Shaking table bandwidth curve (a) x-axis (b) y-axis (unloaded table).

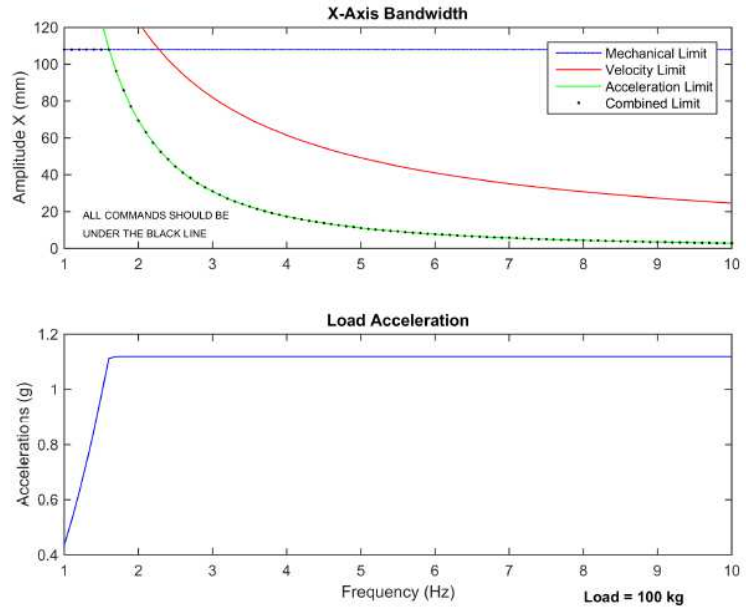

(a)

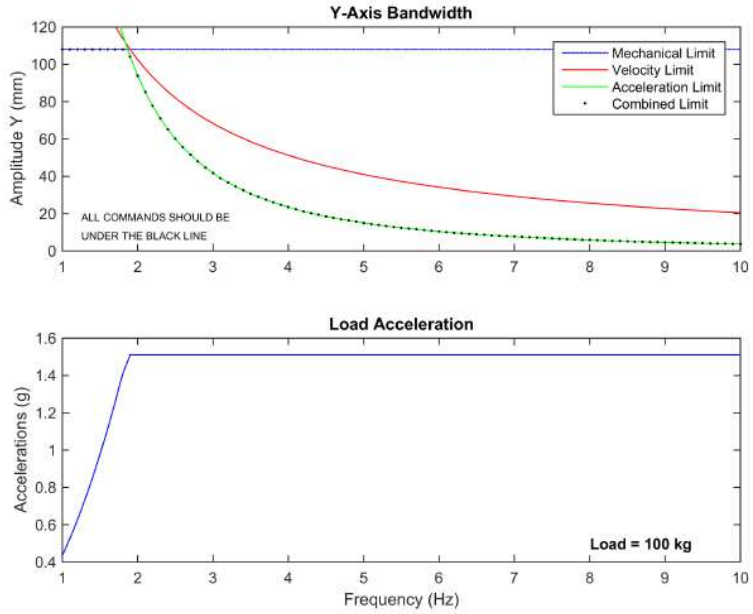

(b)

Figure 4.4: Shaking table bandwidth curve (a) x-axis (b) y-axis (with an additional 100Kg payload).

4.3. Performance of the original PDFF controller

The control system of the QUANSER STIII is a Simulink-based proportional derivative and feedforward (PDFF) controller which drives time history signals through QUARC real-time software. Originally, the PDFF controller is designed to control the shaking table position following the control scheme described in section 2.5.2 of chapter 2. The PD controller aims to regulate the stage position and velocity while the FeedForward controller tends to track the reference acceleration. This section presents the acceleration tracking performance of the original control system of the shaking table and shows its limitations. For this purpose, an experimental investigation is performed by analysing different acceleration responses of the table under different excitation signals, for both unloaded and loaded table conditions. The information about the real acceleration output of the system in the frequency domain indicates the real behaviour of the shaking table system and leads to a better system identification.

4.3.1. Sine wave input signal

In order to evaluate the dynamic behaviour of the shaking table system at different amplitudes and frequencies, several sinusoidal tests are carried out within the system performance range. For a first stage, the sinusoidal shaking table tests are carried out with no payload mounted on the platform in order to collect data information about the bare shaking table system by eliminating the effect of the table-specimen interaction. Figure 4.5 shows the time history acceleration responses to a sinusoidal vibration test of a 1Hz frequency for a variation of amplitudes: 10mm, 40mm and 50mm, respectively. Undesirable peak amplitudes in the acceleration responses of the table indicate the large signal distortion of the system output due to the nonlinearities of the shaking table system. It can be seen on the time history of the acceleration responses that the distortion decreases when the amplitudes of the input increase.

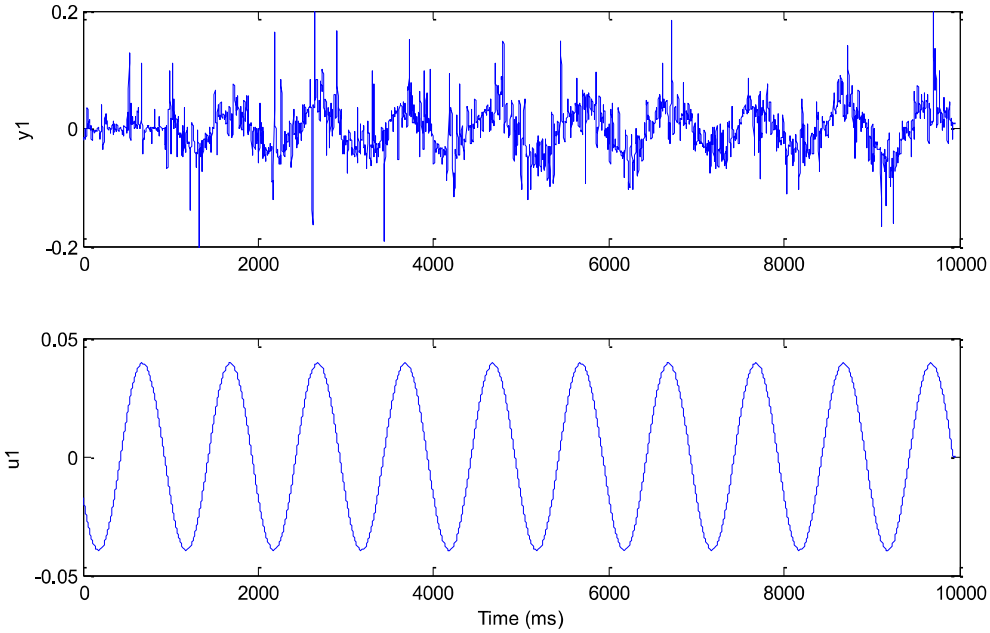

Figure 4.5: (a) Time history response for a sine wave signal of a frequency of 1Hz and amplitude of 10mm for an unloaded table.

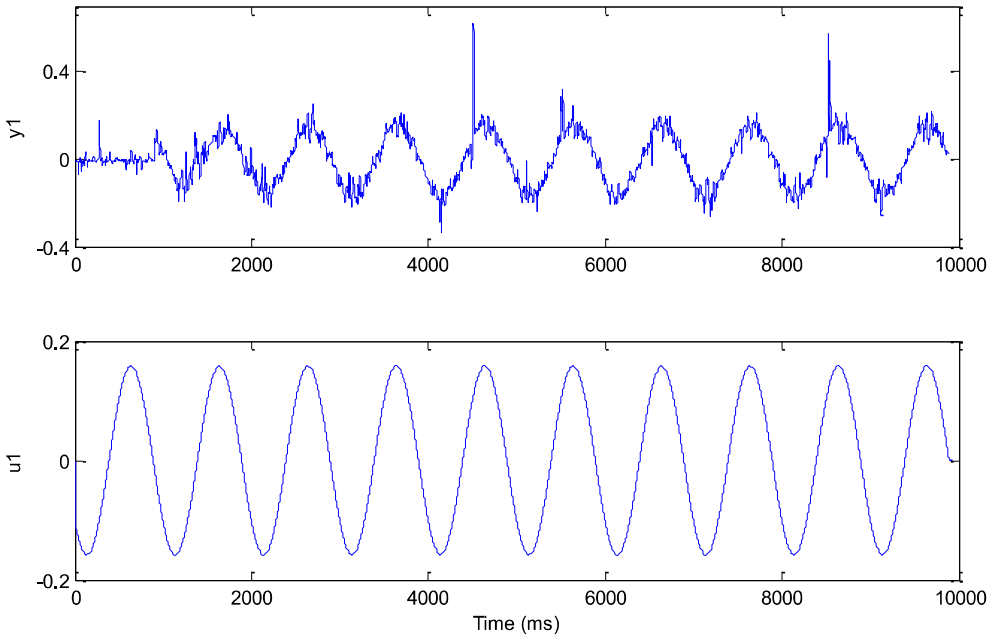

Figure 4.5: (b) Time history response for a sine wave signal of a frequency of 1Hz and amplitude of 40mm for an unloaded table.

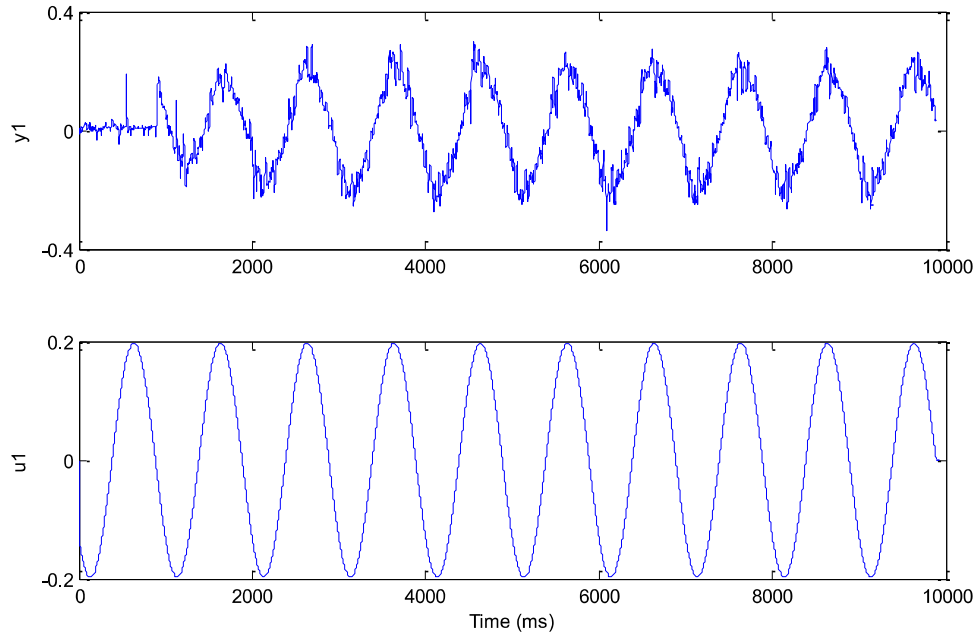

Figure 4.5: (c) Time history response for a sine wave signal of a frequency of 1Hz and amplitude of 50mm for an unloaded table.

In order to assess the degree of distortion of the system output, further analysis of the acceleration responses is carried out in the frequency domain as well. Figure 4.6 represents the FFT of the acceleration system outputs as responses to sine wave inputs. Several sinusoidal tests are performed, only three are presented in this study. The shaking table attends to track three sine waves with the same signal amplitude of 10mm and three different frequencies of excitations: 1Hz, 3Hz and 5Hz. The frequency response of the table under a sinusoidal input of 1Hz exhibits a large band of measured amplitudes observed after the frequency of excitation. For higher frequencies of excitation, the curves are improved, showing few harmonics whose number decreases by increasing the frequency of excitation. Through the results displayed in the frequency range of interest of [0-20Hz], the lower the frequency of signal excitation is, the more important the distortion of the output signal becomes.

A further analysis is achieved through sinusoidal tests applying to a loaded table. A mounted 69Kg steel payload with a frequency of 3.5Hz is positioned on the top stage of the shaking table.

In order to study the effect of the amplitude variation on the frequency response of the table, three sinusoidal tests with a frequency of 1Hz and three different

amplitudes: 10mm, 40mm and 50mm are executed. The FFT of the acceleration responses of the table are presented in Figure 4.6. Therefore, the effect of the frequency of the signal excitation on the acceleration response of the table is investigated and the results are illustrated in Figure 4.7. The sine waves have the same amplitude of 10mm and the three selected frequencies are 1Hz, 3Hz and 5Hz.

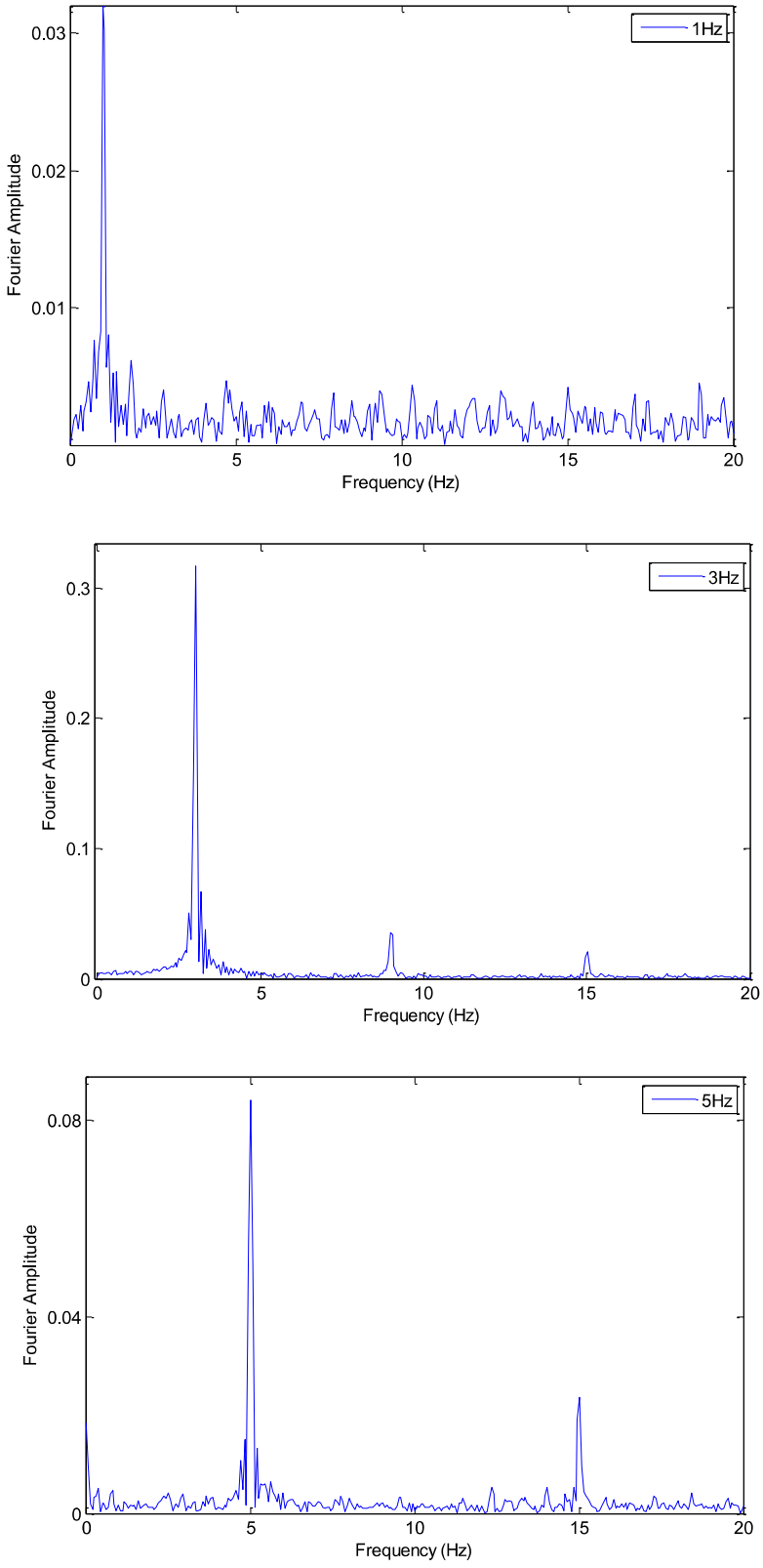

Figure 4.6: FFT of the acceleration response for a sine wave signal of an amplitude of 10mm and different frequencies for an unloaded table.

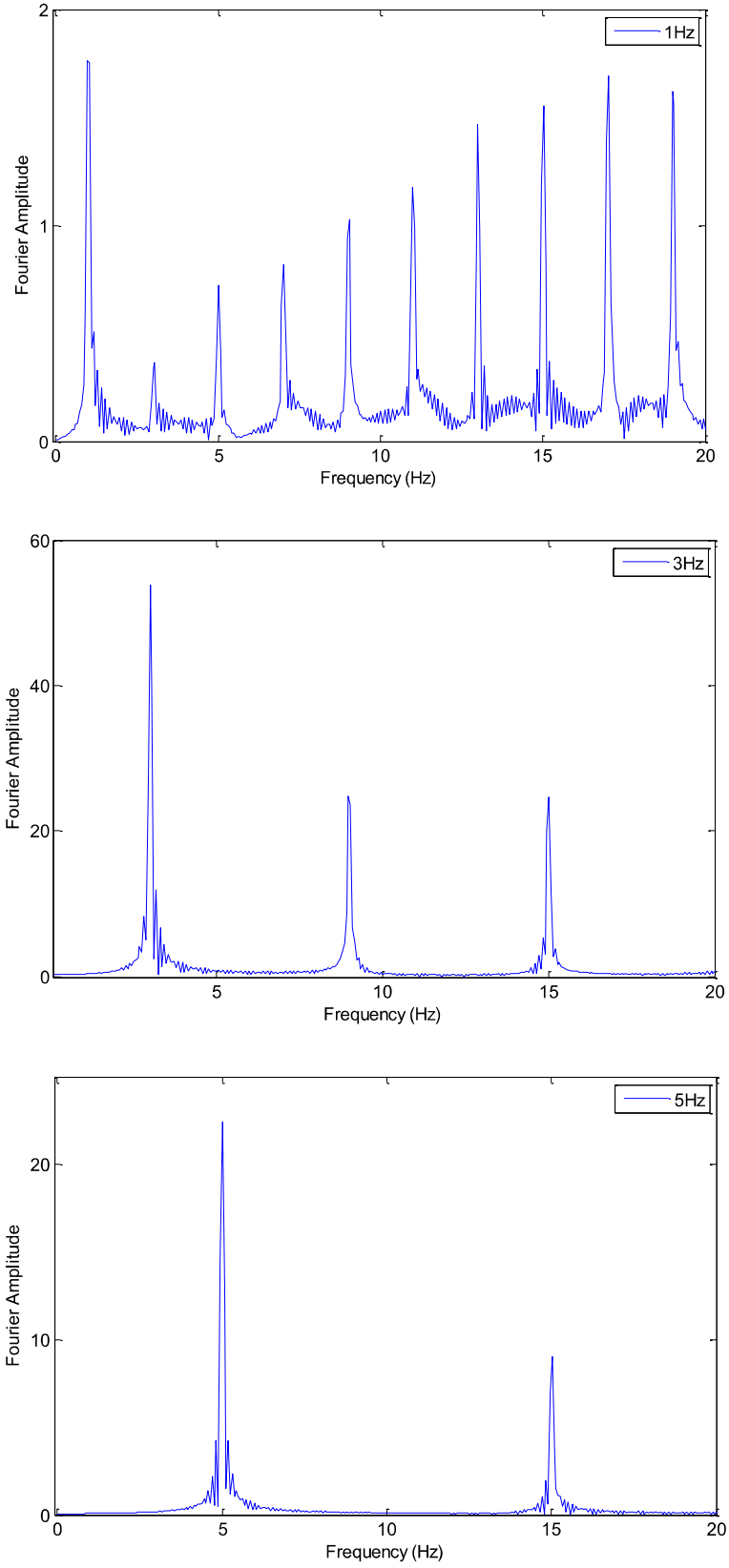

Figure 4.7: FFT of the acceleration response for a sine wave signal of an amplitudes of 10mm and different frequencies for a table + payload.

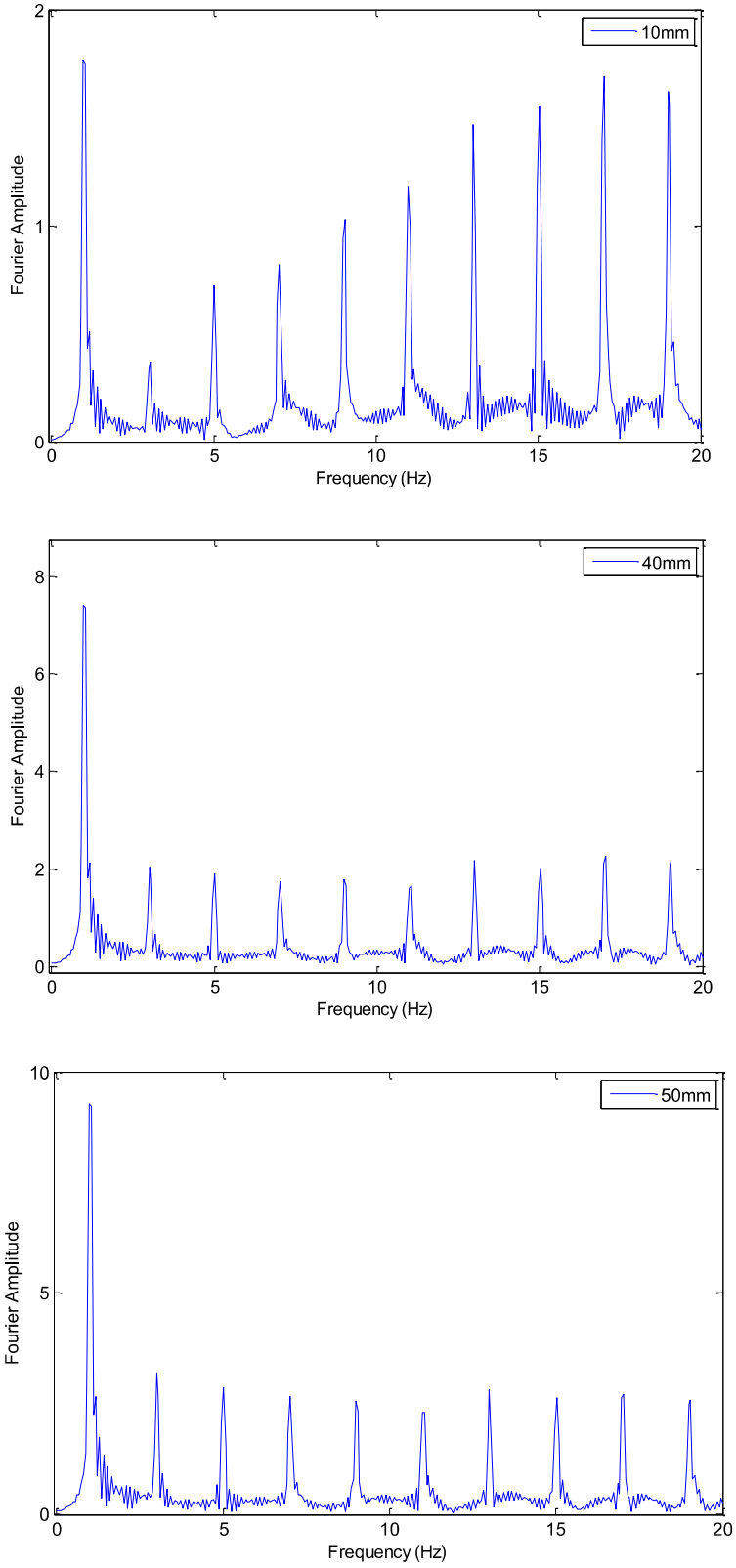

Figure 4.8: FFT of the acceleration response for a sine wave signal of a frequency of 1Hz and different amplitudes for a table + payload.

Based on the presented results of the acceleration responses in the frequency domains, several harmonic distortions clearly exist in the shaking table output and demonstrate the nonlinearity of the system.

For analysing the results, total harmonic distortion (THD) criterion is used to evaluate harmonic distortion. The THD criterion can be computed from the following equation [162]:

$$THD = \frac{\sqrt{A_2{}^2 + A_3{}^2 + A_4{}^2 + \cdots}}{A_1} \tag{4.1}$$

Where A_1 is the fundamental amplitude, A_2 is the amplitude of second harmonic, A_3 is the amplitude of the third harmonic, and so on.

A first study of the effect of the frequency on the acceleration response is investigated, using sinusoidal tests with the same amplitude (10mm) and three frequencies: 1Hz, 3Hz and 5Hz. The values of the THD computed using equation (5.1) are presented in Table 4.1, computed in the frequency range of [0-20Hz].

A second study focuses on the effect of the amplitude of the sine wave input and uses sinusoidal excitations with the same frequency of 1Hz and three different amplitudes: 10mm, 40mm and 50mm. The obtained THD values are presented in Table 4.2.

Table 4.1: THD analysis results for different sinusoidal frequencies.

	1Hz	3Hz	5Hz
Fundamental amplitude	1.766	53.85	22.43
THD (%)	210.49	65.03	40.13

Table 4.2: THD analysis results for different sinusoidal amplitudes.

	10mm	40mm	50mm
Fundamental amplitude	1.766	7.406	9.212
THD (%)	210.49	88.31	80.16

The THD values show that the acceleration response of the loaded table is highly distorted. They indicate that with the same amplitude of the sinusoidal input, the harmonic distortion decreases by increasing the frequencies of the excitation.

The time and frequency representations of the table responses presented in Figure 4.5 to Figure 4.8 prove that the acceleration output of the shaking table system is highly distorted.

THD values presented in Table 4.1 and Table 4.2 demonstrate that the harmonic distortion decreases when the amplitude and frequency of the excitation signal increase. However, the signal distortion is still seriously significant which indicates the nonlinear behaviour of the shaking table that the original PDFF control system is unable to compensate.

4.3.2. Earthquake record input signal

As it has been proved through the experimental responses of the table under sinusoidal excitations, the shaking table is highly nonlinear which affects the control system performance. In this section, the capabilities of the original PDFF controller to replicate historical earthquake records are presented. Three typical far-field and near-field earthquake records, the 1940 El-Centro, the 1992 Cape-Mendocino and the 1994 Northridge ground motions are used in this test.

In order to demonstrate the behaviour of the shaking table in time and frequency domains, representative comparisons between the desired and the achieved acceleration responses are illustrated in Figures 4.9 to 4.14 for a bare table, and in Figures 4.15 to 4.20 for a loaded table. A time window of [0-10sec] is chosen for a comparison aspect. The figures below show the effect of the interaction between the table and the specimen as well, in which it is seen that the degree of distortion is larger when the table is loaded, especially in peak values.

The Root Mean Square Error (RMSE) is chosen as an assessment index of the degree of distortion observed between the desired acceleration and the response. Table 4.3 and Table 4.4 give the computed RMSE values for unloaded and loaded table conditions, respectively. The $RMSE_T$ indicates the error acceleration in the time domain and $RMSE_F$ indicates the error

acceleration in the frequency domain are computed using the following equations:

$$RMSE_T\,(\%) = \sqrt{\frac{\sum_{k=1}^{N}(a_d(k)-a_m(k))^2}{\sum_{k=1}^{N}a_d(k)^2}}x100\% \quad (4.2)$$

$$RMSE_F\,(\%) = \sqrt{\frac{\sum_{k=1}^{NF}(S_d(k)-S_m(k))^2}{\sum_{k=1}^{NF}S_d(k)^2}}x100\% \quad (4.3)$$

Where $a_d(k)$ and $a_m(k)$ are the desired and the measured acceleration at the step k, respectively. N is the number of data points. $S_d(k)$ and $S_m(k)$ are the desired and measured Fourier magnitude at the k-th frequency, respectively. N_F is the number of frequencies in Fourier Transform that cover the frequencies of interest. In this study, the frequency range of 0-100 Hz is adopted.

Another important assessment index of the shaking table tracking performance is the degree of fidelity in reproducing the PGA of the earthquake record $\varepsilon_{(PGA)}$. In fact, the shaking table test could be totally controversial with a reproduced PGA at the base of the tested structure that is different from the PGA of the real ground motion. In this study, the error in signal reproduction is calculated according to the equation (4.4). It is clear that the acceleration responses of the shaking table system under earthquake records is highly distorted and requires to be enhanced for more reliable shaking table tests.

$$\varepsilon_{PGA} = \frac{|achieved\ PGA - desired\ PGA|}{desired\ PGA} \quad (4.4)$$

Table 4.3: RMSE between desired and measured acceleration of an unloaded table under earthquake records.

	$RMSE_T$ (%)	$RMSE_F$ (%)	ε (%)
El-Centro	63.62	35.33	02.56
Cape-Mendocino	54.80	28.20	33.70
Northridge	54.31	22.78	09.48

Table 4.4: RMSE between desired and measured acceleration of a loaded table under earthquake records.

	$RMSE_T$ (%)	$RMSE_F$ (%)	ε (%)
El-Centro	68.02	53.62	14.14
Cape-Mendocino	69.80	31.60	67.32
Northridge	63.04	55.86	22.30

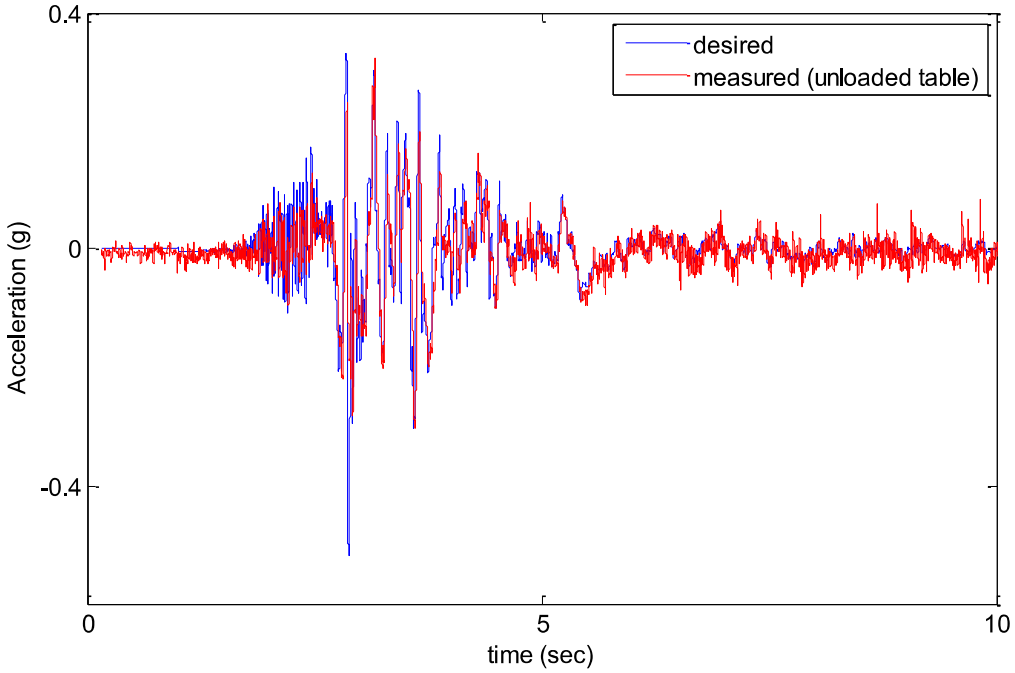

Figure 4.9: Acceleration time-history of the measured response for unloaded table under El-Centro earthquake record.

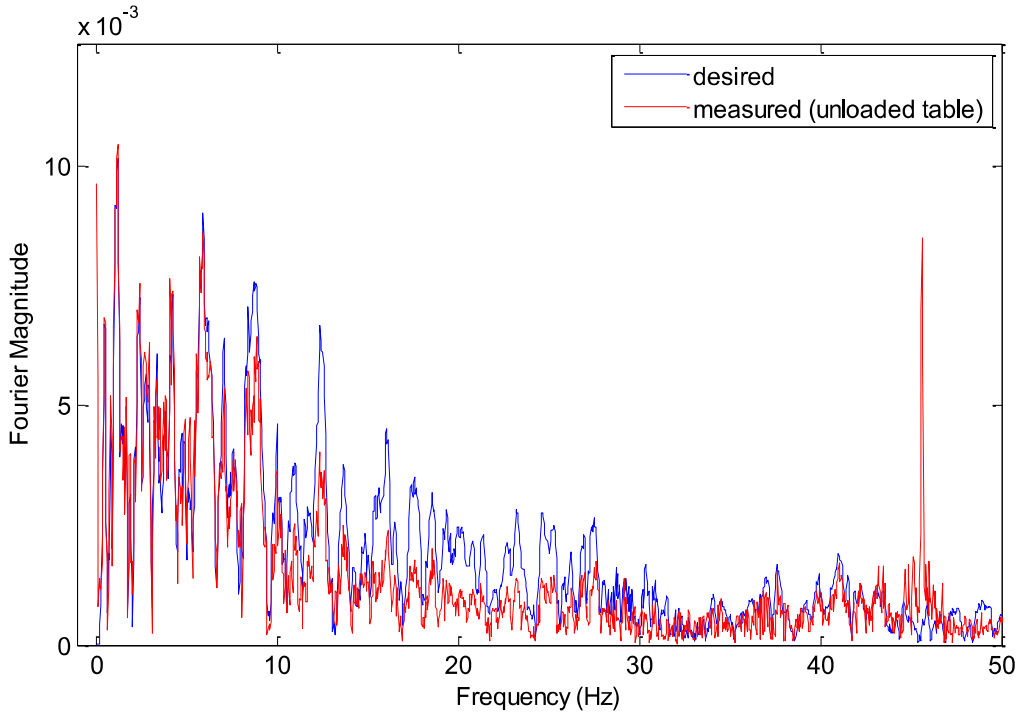

Figure 4.10: FFT of the acceleration response for unloaded table under El-Centro earthquake record.

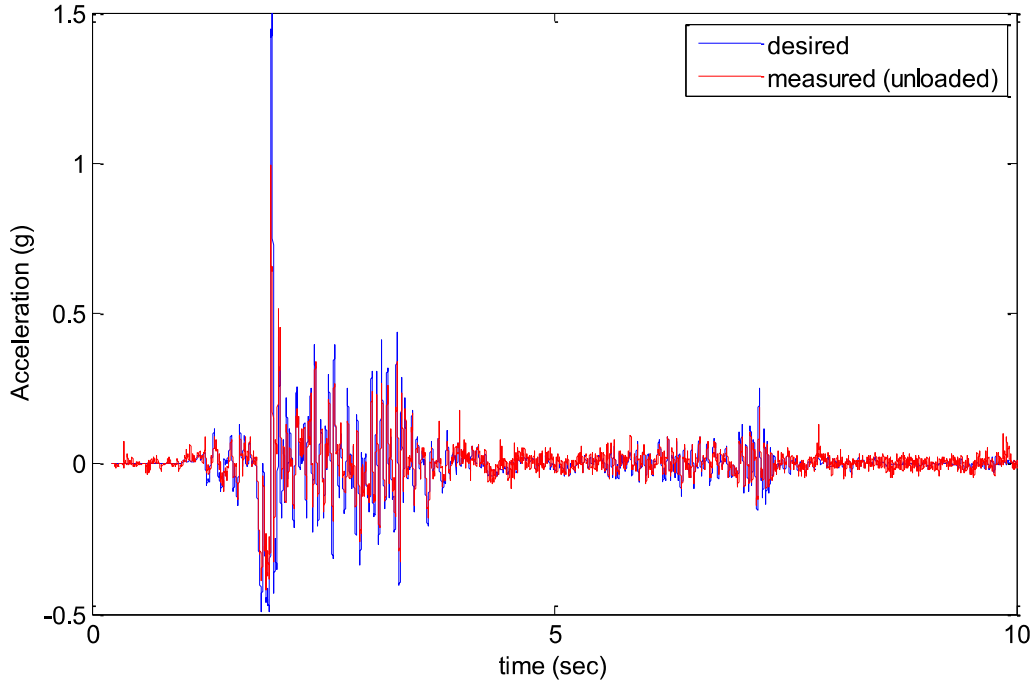

Figure 4.11: Acceleration time-history of the measured response for unloaded table under Cape-Mendocino earthquake record.

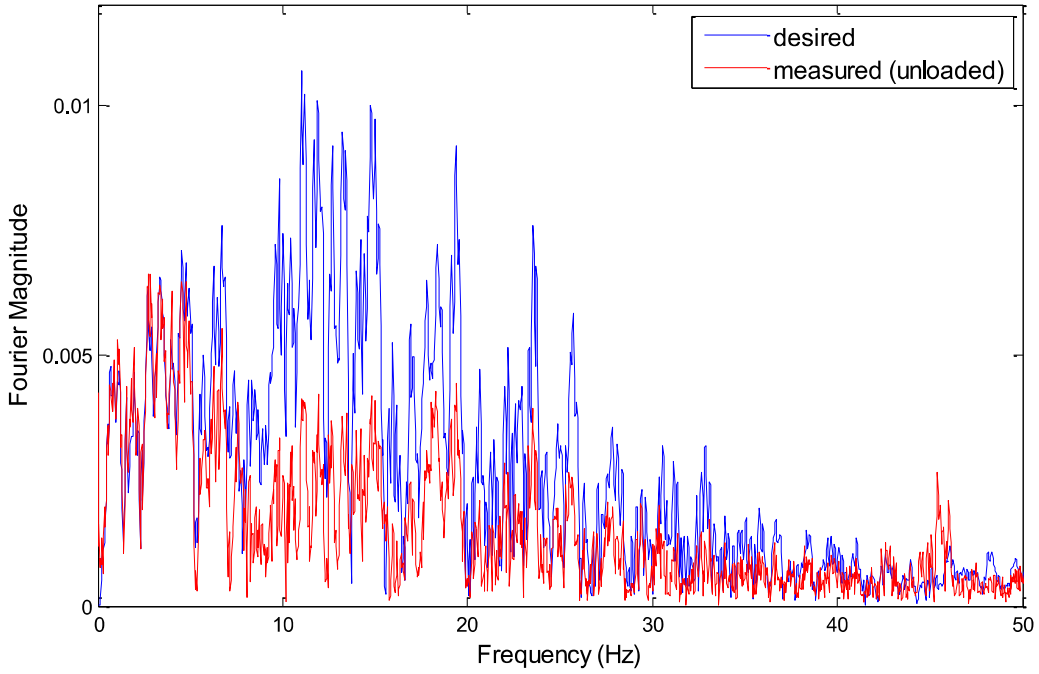

Figure 4.12: FFT of the acceleration response for unloaded table under Cape-Mendocino earthquake record.

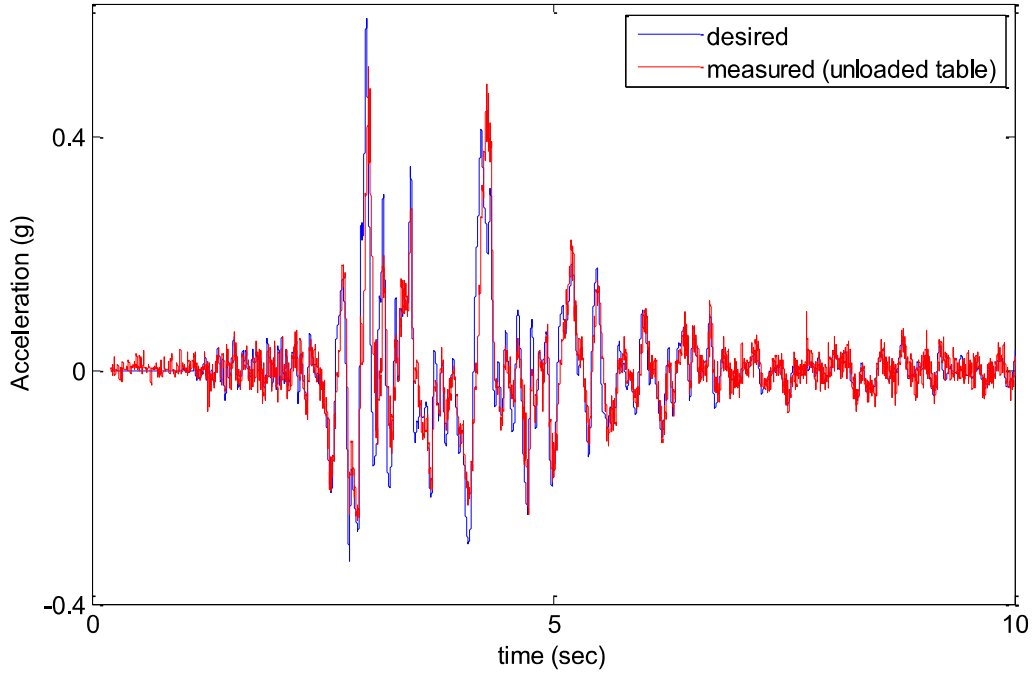

Figure 4.13: Acceleration time-history of the measured response for unloaded table under Northridge earthquake record.

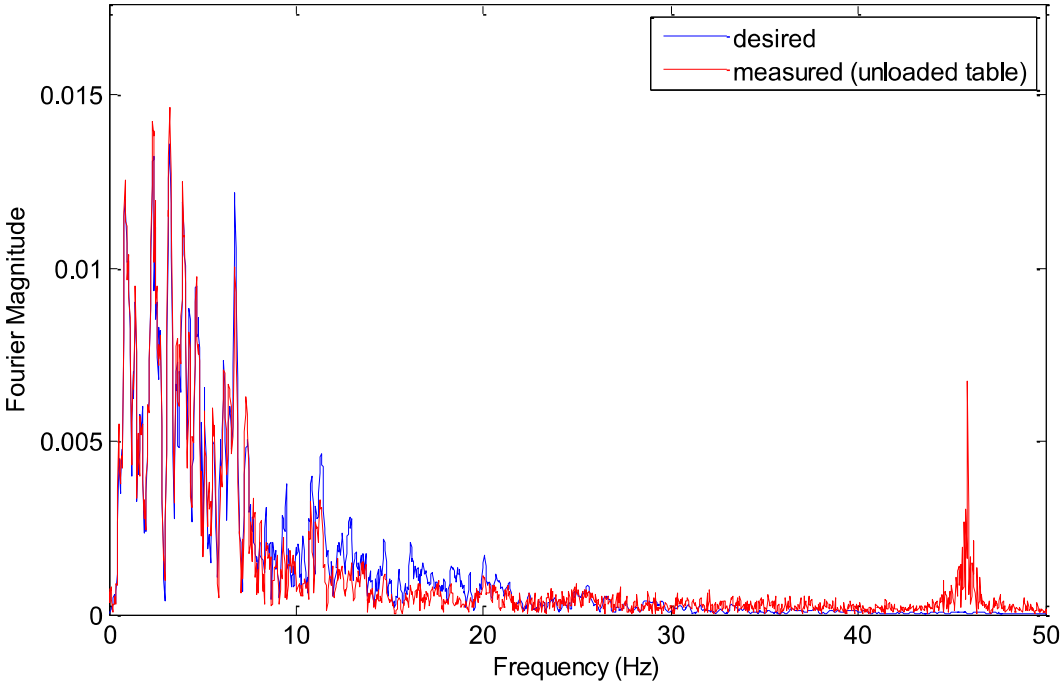

Figure 4.14: FFT of the acceleration response for unloaded table under Northridge earthquake record.

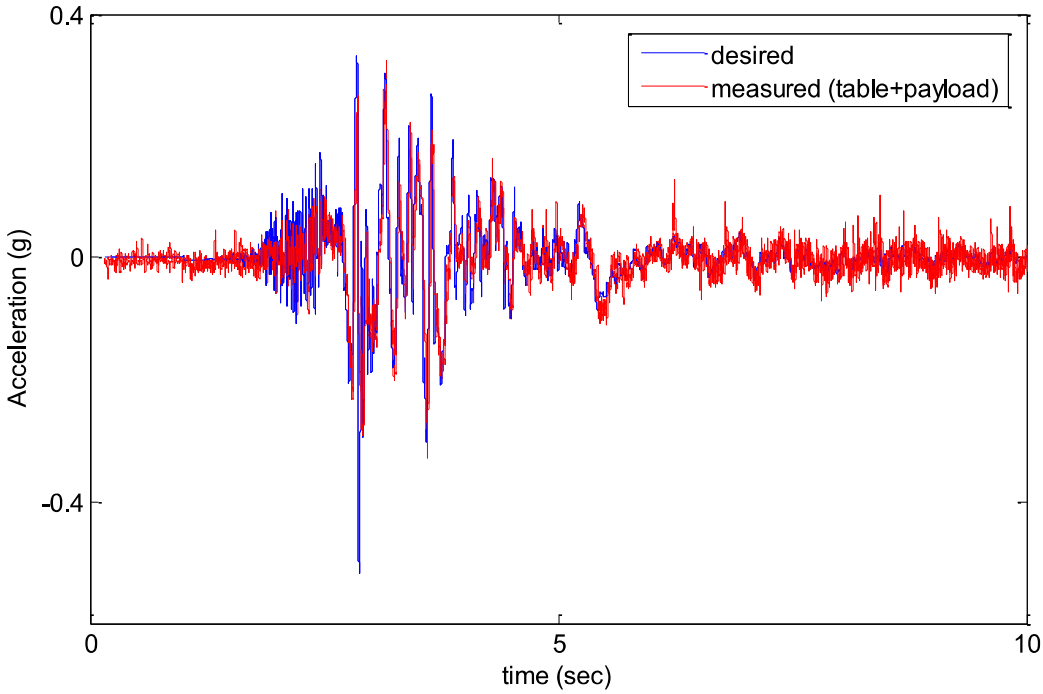

Figure 4.15: Acceleration time-history of the measured response loaded table under El-Centro earthquake record.

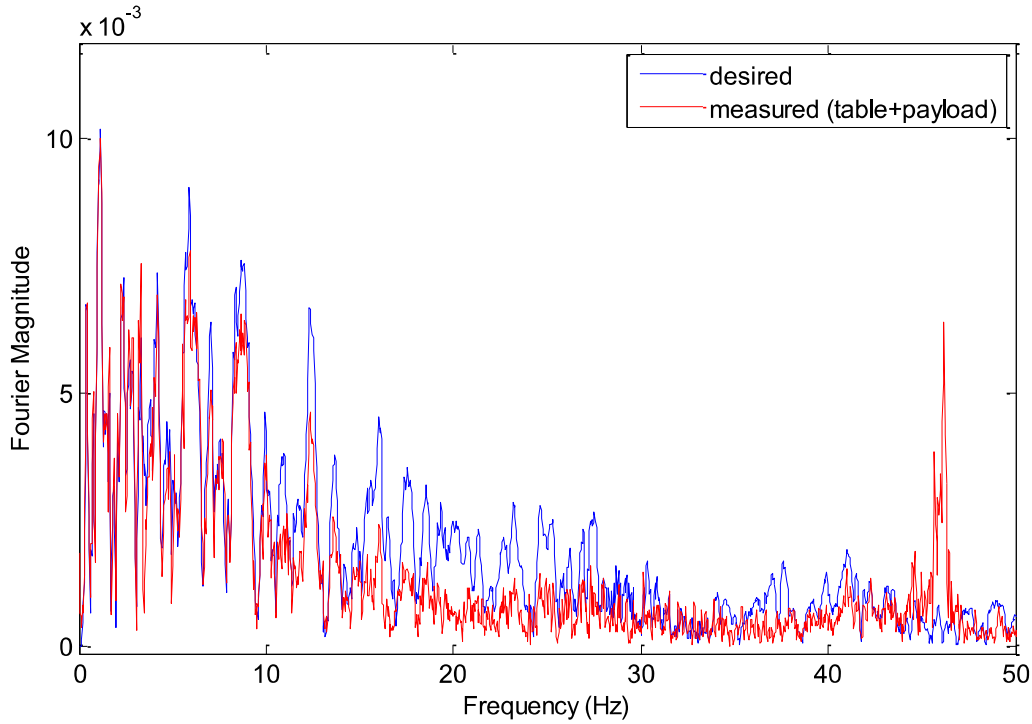

Figure 4.16: FFT of the acceleration response for a loaded table under El-Centro earthquake record.

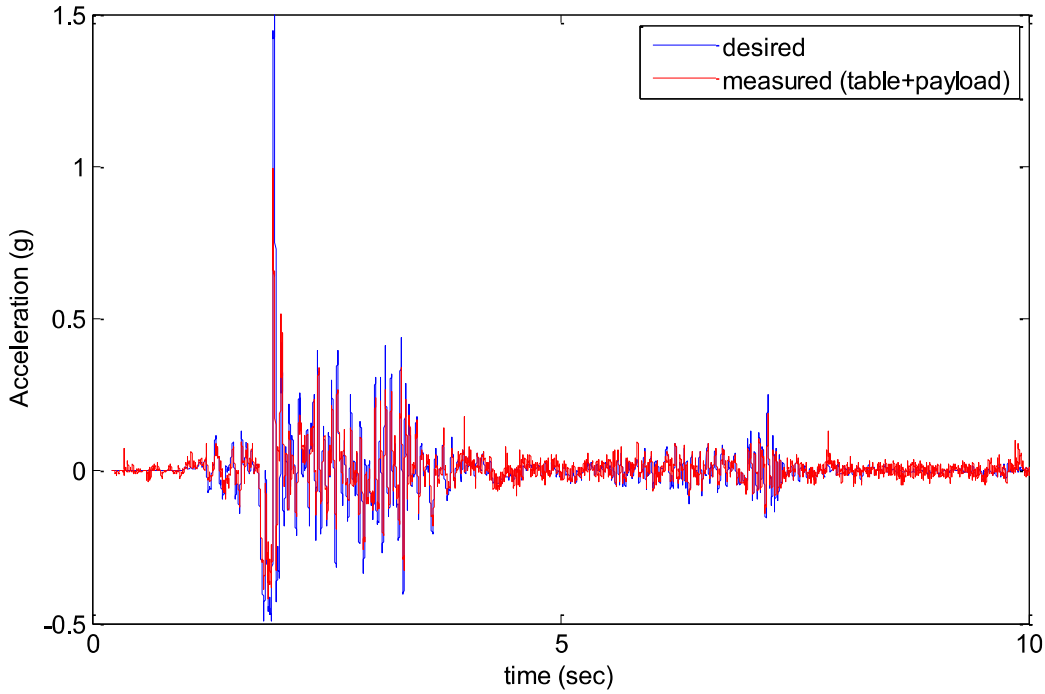

Figure 4.17: Acceleration time-history of the measured response loaded table under Cape-Mendocino earthquake record.

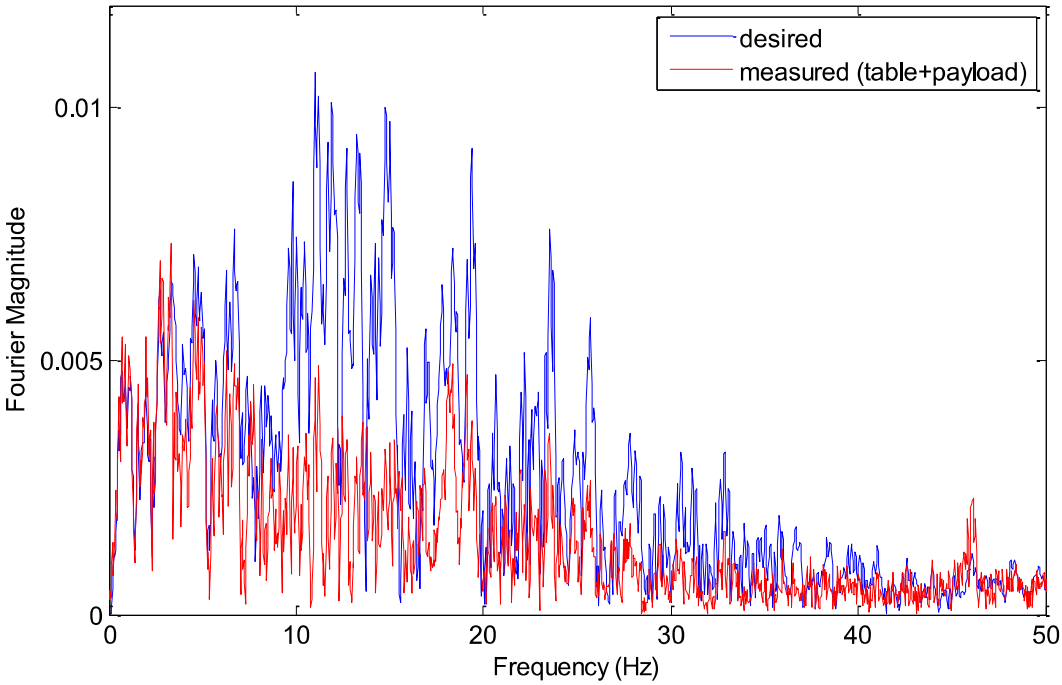

Figure 4.18: FFT of the acceleration response for a loaded table under Cape-Mendocino earthquake record.

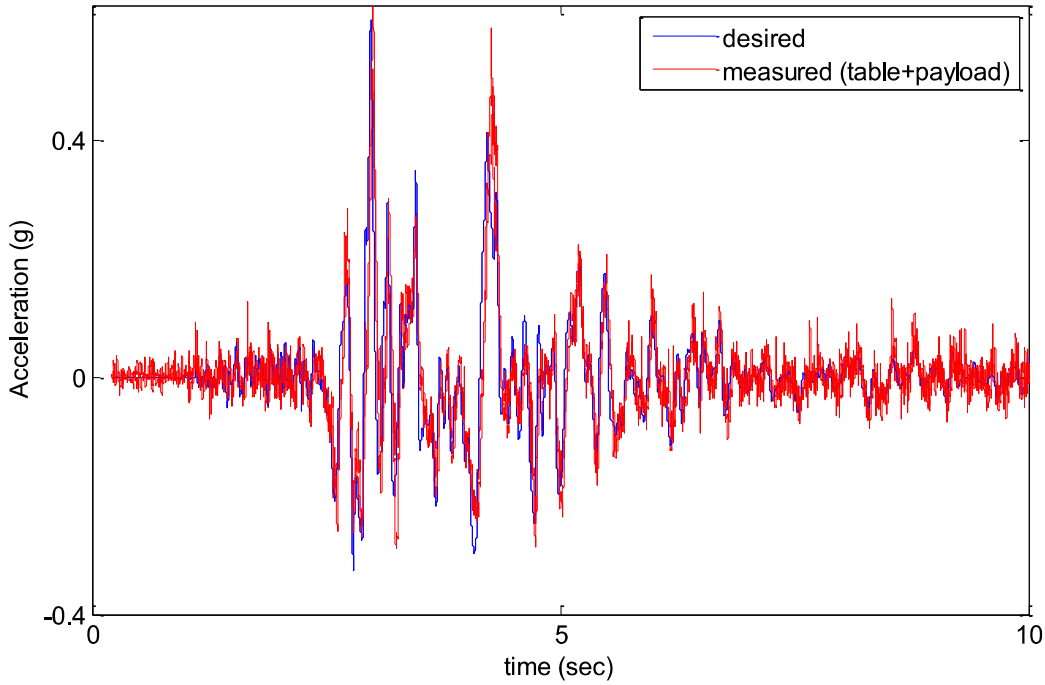

Figure 4.19: Acceleration time-history of the measured response loaded table under Northridge earthquake record.

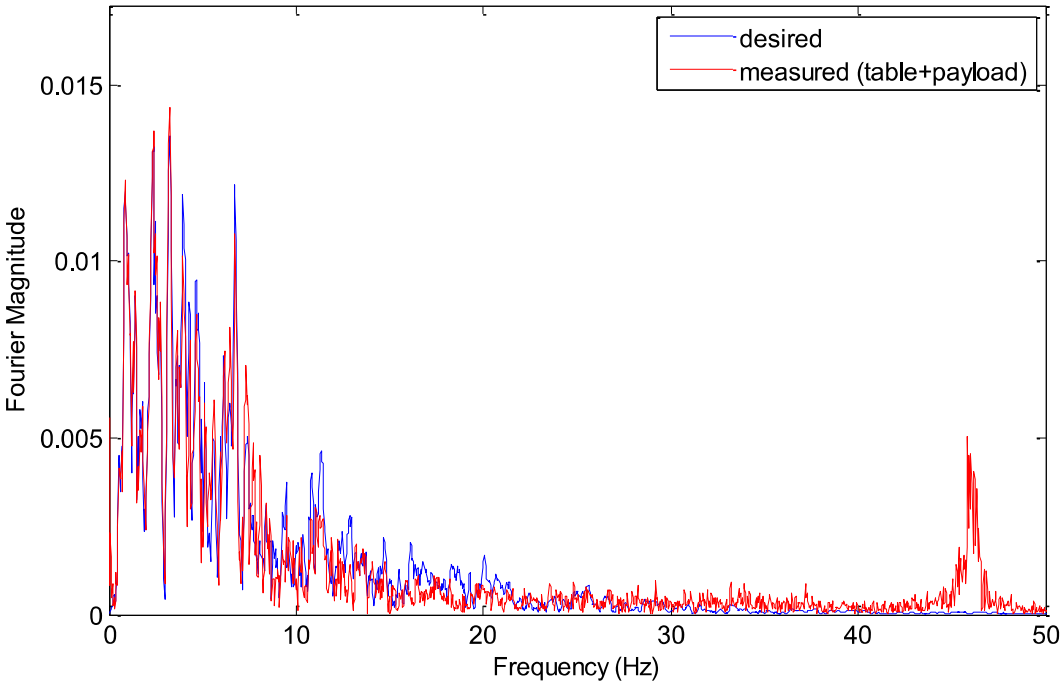

Figure 4.20: FFT of the acceleration response for a loaded table under Northridge earthquake record.

4.4. Design of the NN control function

As mentioned previously, the simplest multilayer feedforward network is the most used NN while combined with classic linear controllers. Therefore, the proposed NN is a three-layer feedforward NN. In order to determine the structure of the NN, a routine optimization procedure is carried out based on the best NN performance in terms of coefficient of correlation, number of epochs, and mean-square-error (MSE) values. Results presented in Table 4.5, led to the choice of the final architecture presented in Figure 4.21, constituted of 8 neurons in the hidden layer with sigmoidal activation function and one neuron in the output layer with pureline activation function.

Table 4.5: Performance of the NN with variation of the number of the hidden neurons.

Number of hidden neurons	Number of epochs	MSE values	Coefficient of correlation
5	15	1.16×10^{-3}	0.80
8	666	1.35×10^{-4}	0.96
10	489	1.83×10^{-4}	0.96
15	613	4.54×10^{-4}	0.95
25	236	5.41×10^{-4}	0.88
35	833	4.20×10^{-4}	0.91

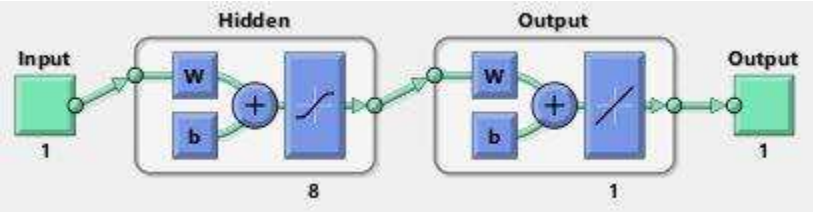

Figure 4.21: Three-layer feedforward neural network.

The Lavenberg-Marquardt (L-M) algorithm described in section 3.2.1 of chapter 3 is used to train the NN. This powerful backpropagation algorithm which does not need to compute the exact Hessian matrix, is used to train the NN in offline mode based on the loss function f given in the following equation:

$$f = \sum_{i=1}^{m} ei^2 \tag{4.5}$$

Where e_i is the acceleration tracking error to be minimized, computed between the output of the NN and the target; m is the number of data points.
The gradient vector of the loss function is given by the following equation:

$$\nabla f = 2J^T e \tag{4.6}$$

The performance of the training is judged satisfying based on:

a) The convergence criteria: which indicates that the NN is able to identify the unknown function that maps between the input and the output;

b) The generalization criteria: it represents the main feature of the NN which means that the NN is able to predict the desired output based on unknown data. In order to achieve a high generalization performance, the data are divided into three parts: 70% data set for training, 15% data set for validation and 15% data set for testing;
c) The stop criteria: indicates when the training process will stop based on the defined maximum number of epochs, maximum amount of time or the chosen performance criteria is reached. In this case, the performance function is the MSE (Mean Square Error) and the performance goal is fixed to 10^{-5}.

The database for training, testing, and validating the NN is the acceleration real-time signals recorded on the shaking table during the tests using real earthquake records, with the existing PDFF controller. The NN input is the measured signal, and the target is the prescribed earthquake record. Signals are sampled at 0.2 ms which provide around 70,000 training points: 70% of the data is used for training, 15% for validation, and 15% for test.

The stop criteria of number of epochs for checking the increase of error on the validation data set is selected 5000 and the value of performance goal in term of MSE is set to 10^{-5}.

The performance of the NN in terms of MSE and coefficient of correlation between the predicted signal and the reference is represented in Figure 4.22 and Figure 4.23, respectively.

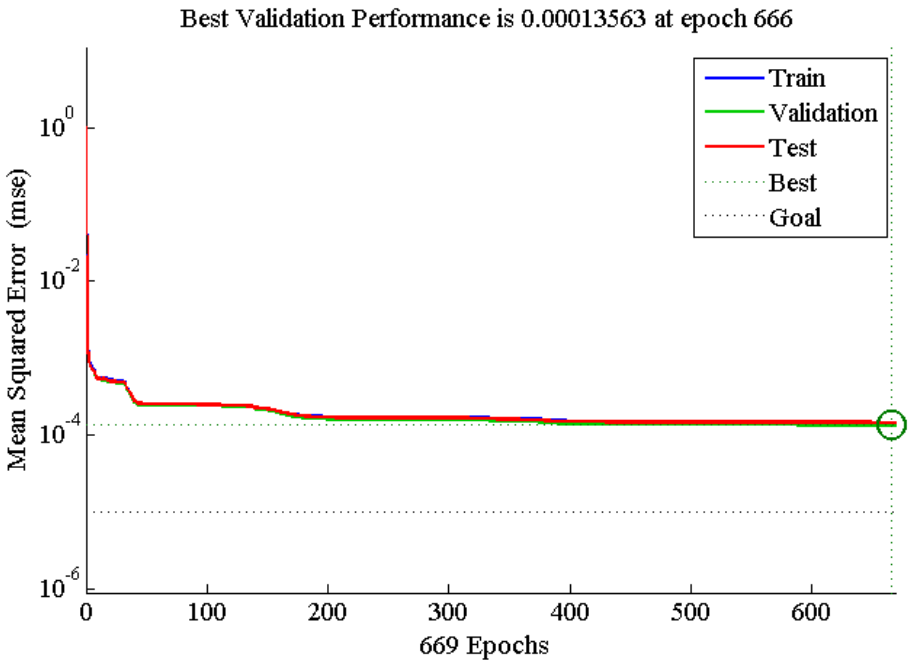

Figure 4.22: NN training performance.

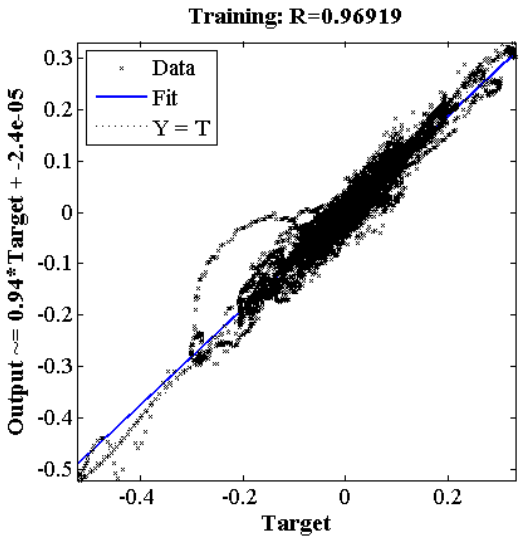

Figure 4.23: Linear regression between the NN output and the target.

The computed mean square error (MSE) between the NN output signal and the target reached the value of 10^{-4} in about 666 epochs. A linear regression is performed between the desired and the predicted acceleration and the fitting line demonstrates that the prediction of the desired signal by the NN is achieved with an accuracy of 97%. A representative comparison of the acceleration predicted by the NN and the desired acceleration is illustrated in Figure 4.24. It is noticeable that the well-trained NN is able to predict a desired acceleration signal with high accuracy.

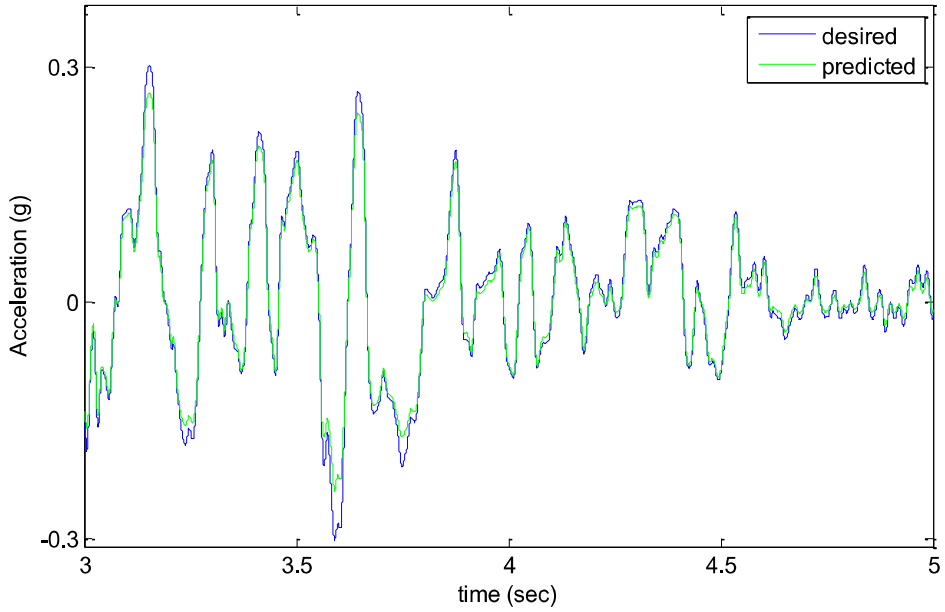

Figure 4.24: Desired and predicted acceleration comparison in a time window of 2s of El-Centro earthquake record.

Once the performance of the NN meets the required performance in terms of convergence, generalization and performance function goal, the NN is implemented in the MATLAB/Simulink based control system of the QUANSER STIII. It performs in an online mode in combination with the original PDFF controller.

4.5. Performance of the PDFF-based NN controller

The implementation of NNs in the control loops is widely employed in various dynamic systems. Based on the literature, different topologies of implementing the NN in the control framework have been attempted. The optimal scheme of the NN implementation in the QUANSER STIII is determined through number of real-time shaking table tests that have led to the best signal matching. The overall implementation of the NN control block is presented in Figure 4.25.

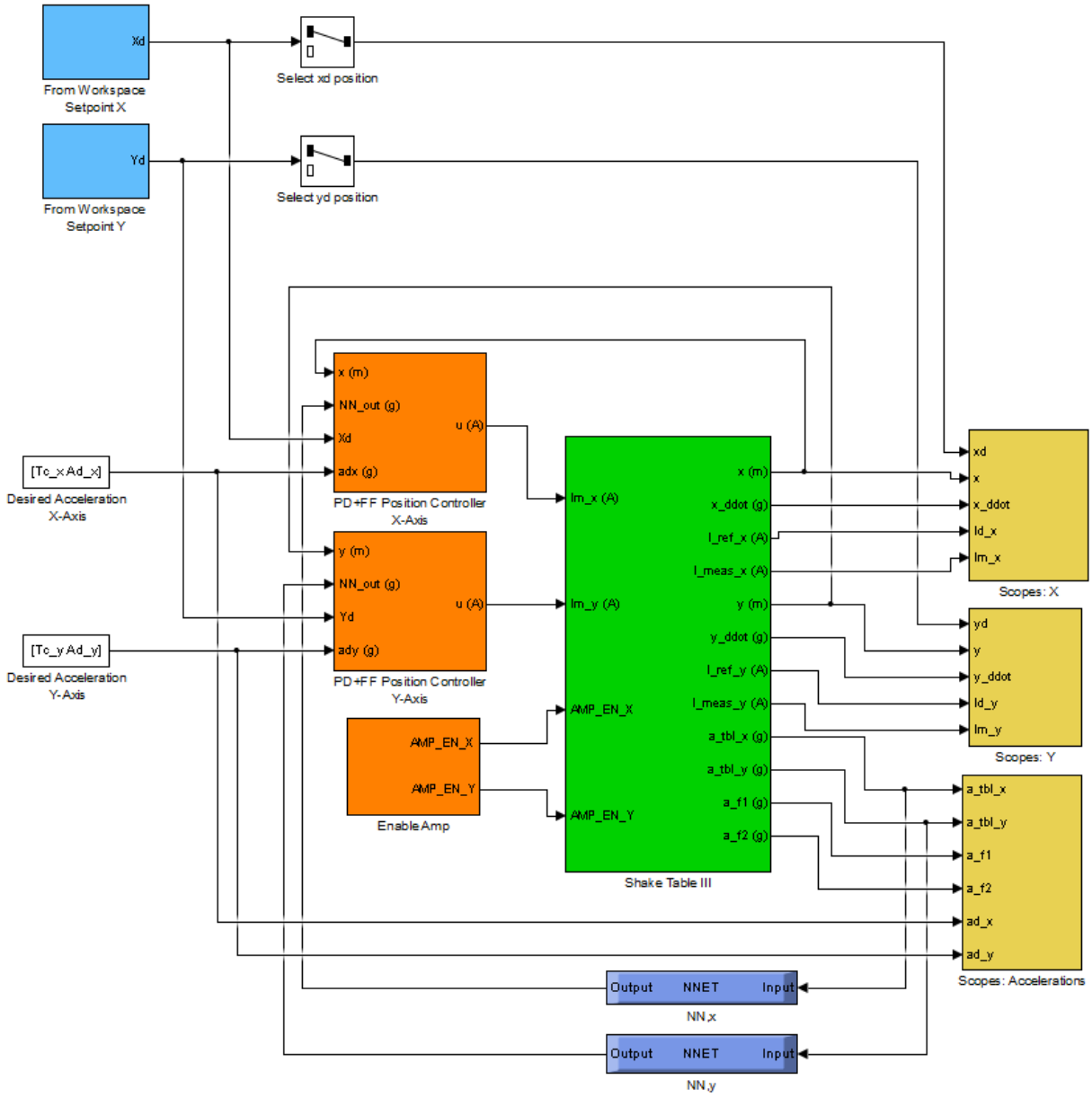

Figure 4.25: Simulink diagram of the QUANSER STIII with online NN-PDFF controller.

This control scheme is a combination of the original PDFF controller and the designed NN control function. The proposed controller is composed of an initially existing PD controller for displacement control, an FF controller for acceleration control to stabilize the shaking table system, and a NN-based control algorithm to enhance the acceleration replication accuracy.

The aim of the designed neural controller is to compensate for the distortions measured in the feedback signals by acting on the command signal to produce reference signals on the top stage with small tracking errors.

For a comparison purpose, the experimental acceleration closed-loop frequency response of the QUANSER STIII with and without NN is depicted in Figure 4.26.

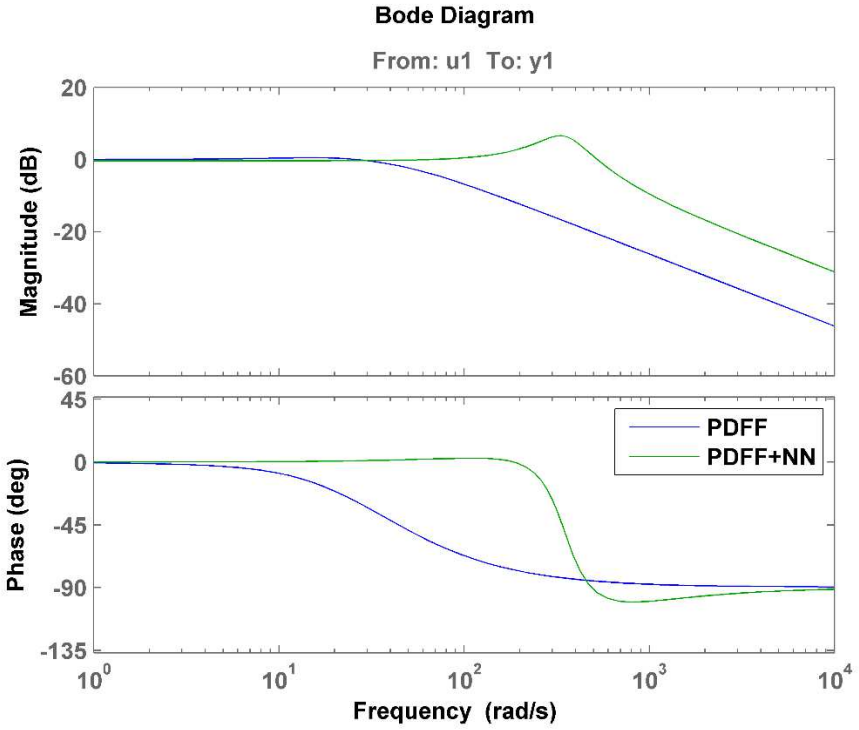

Figure 4.26: Response frequency characteristics of the shaking table: Magnitude and phase characteristics from reference to measured acceleration.

As can be seen from the figure, the implementation of the NN block extended the frequency bandwidth of the acceleration closed-loop system from approximately 5Hz with the PDFF controller to 55Hz with the NN-PDFF controller.

To assess the potential of the NN controller to enhance the acceleration tracking accuracy of the shaking table system for different load conditions, a first shaking table tests are carried out with no payload. In the second stage of this study, a 69Kg steel specimen representing 70% of the payload with a natural frequency of 3.5Hz, is mounted on the platform. Feedback accelerations are filtered using a Kalman filter to reduce noise measurements without causing time delay.

As presented previously, the acceleration RMSE computed between the measured and the desired acceleration, in both time and frequency domains, and the error in the reproduction of the PGA of the ground motion, ε (PGA), are both used as quantitative evaluation index to assess, objectively, the capability of the NN controller to increase the accuracy in the reproduction of the defined acceleration time histories.

It is important to note that the number of frequencies in Fourier Transform used to compute the RME_F is chosen to cover the frequency bandwidth of interest. In this study, the frequency range of 0-100 Hz is adopted.

4.5.1. Tests results: unloaded shaking table testing

A number of comparisons are undertaken to evaluate the fidelity in signal reproduction of the bare shaking table in terms of intended and achieved responses in time and frequency domains as well as attained and desired PGA. Figures 4.27 to 4.29 show a comparison between the reproduced and desired acceleration time histories under El-Centro, Cape-Mendocino and Northridge earthquake records, respectively.

Figure 4.30 to Figure 4.33 show a comparison between the achieved and reference spectral accelerations under the same earthquake records.

The present results confirm that the designed NN control algorithm helped the PDFF controller to track desired accelerations by reducing the distortion between the reference signal and the measured response, in both time and frequency domains.

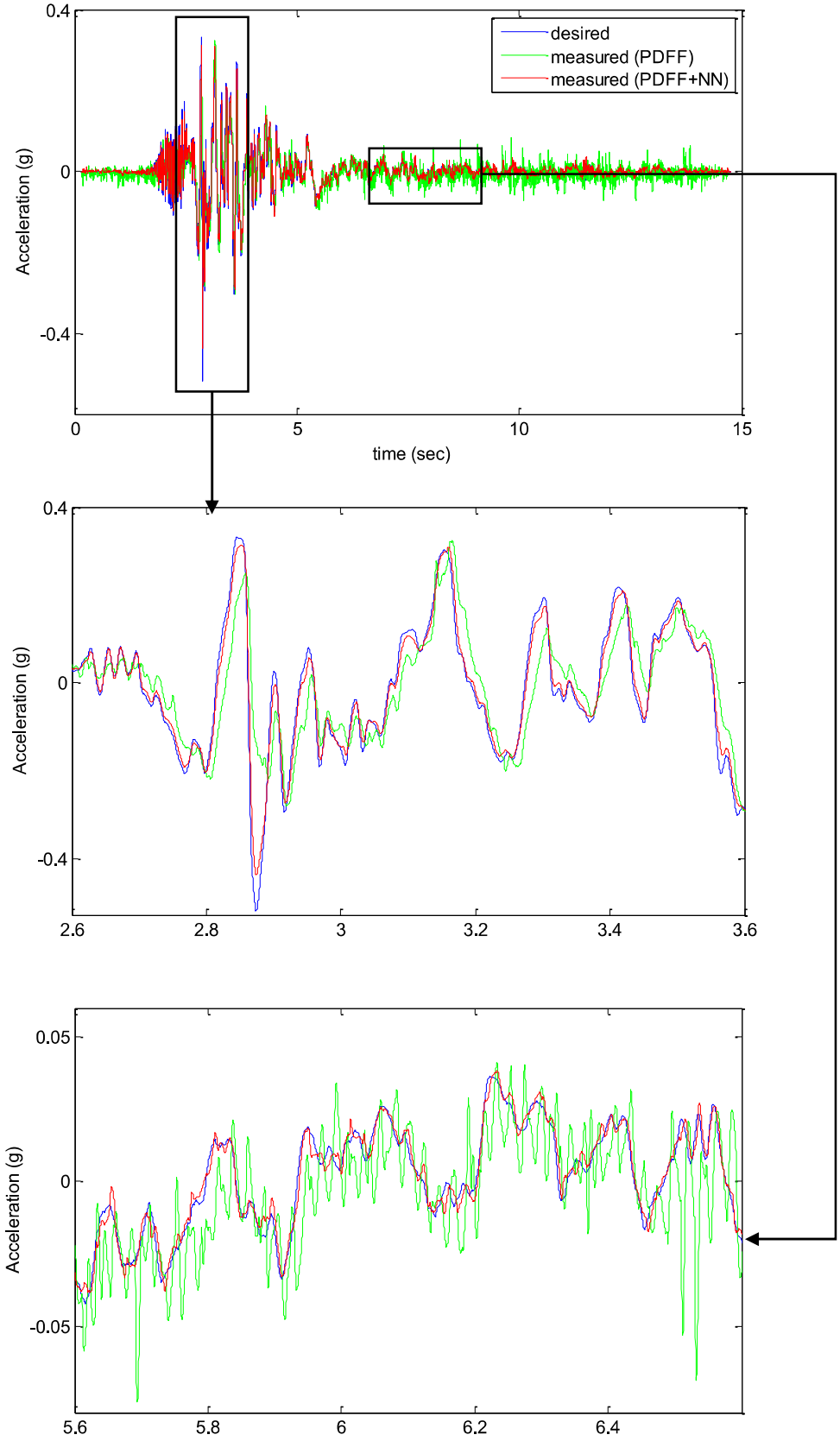

Figure 4.27: Enhanced acceleration response achieved with the PDFF-based NN controller under El-Centro earthquake record (unloaded table).

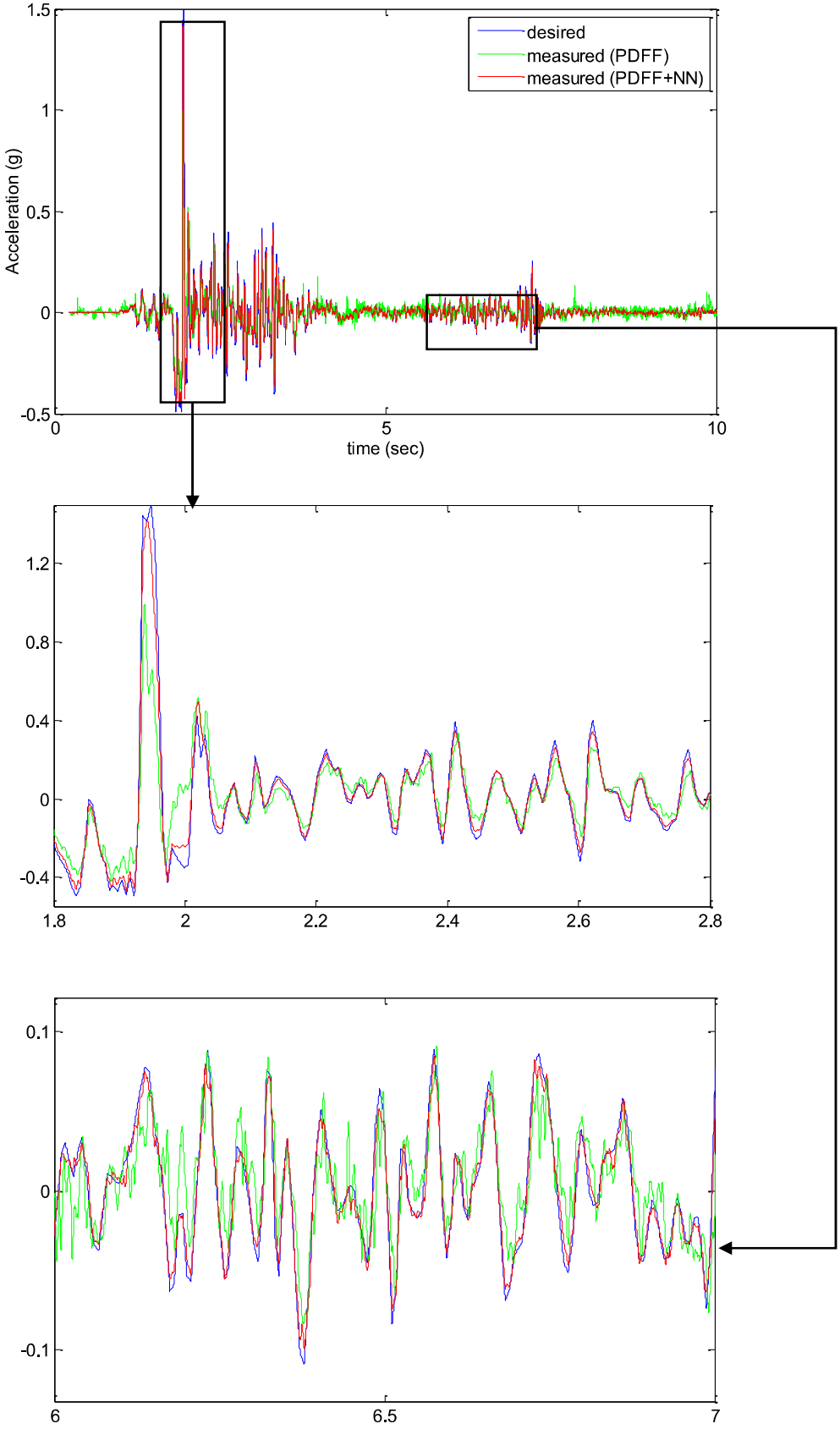

Figure 4.28: Enhanced acceleration response achieved with the PDFF-based NN controller under Cape-Mendocino earthquake record (unloaded table).

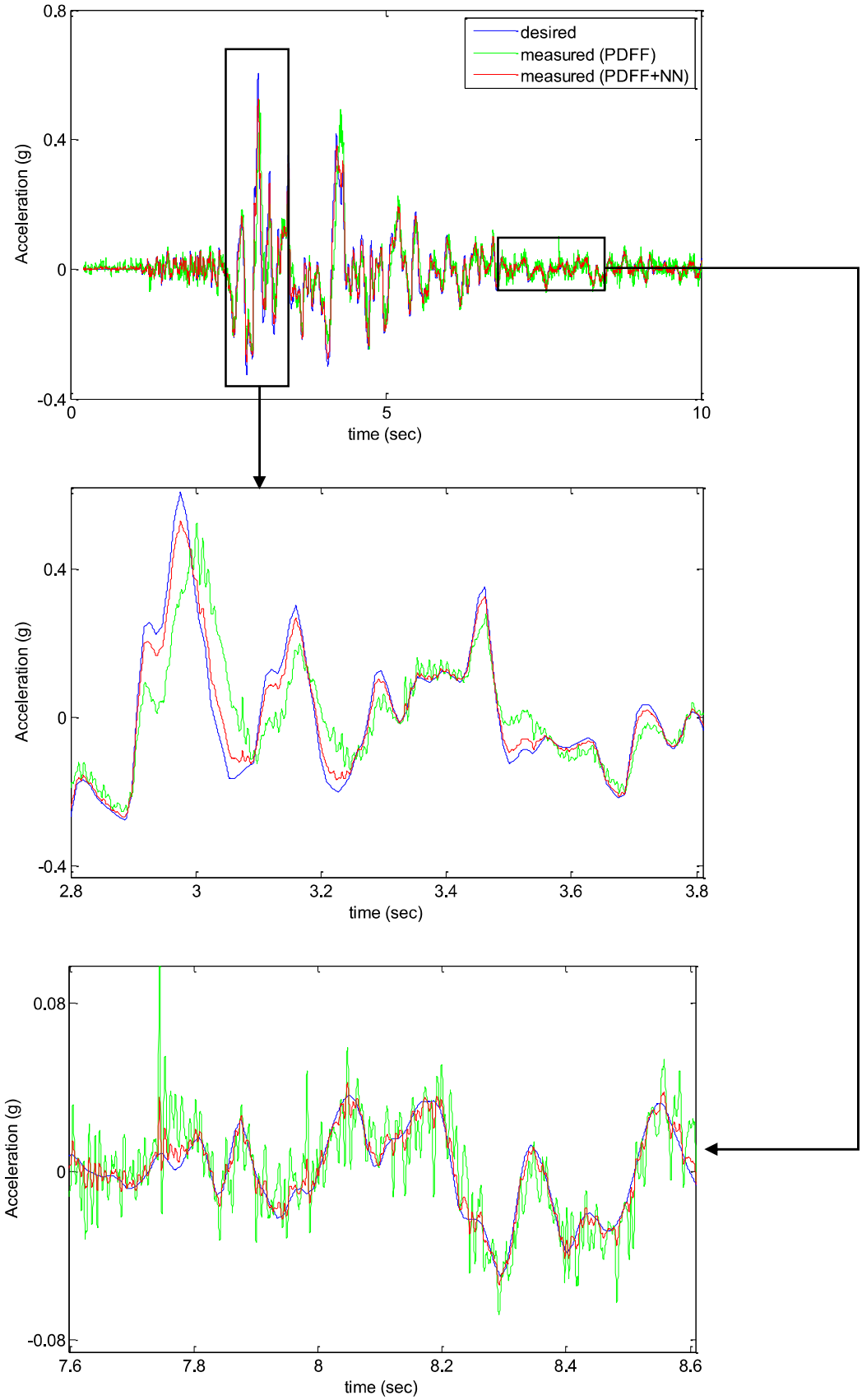

Figure 4.29: Enhanced acceleration response achieved with the PDFF-based NN controller under Northridge earthquake record (unloaded table).

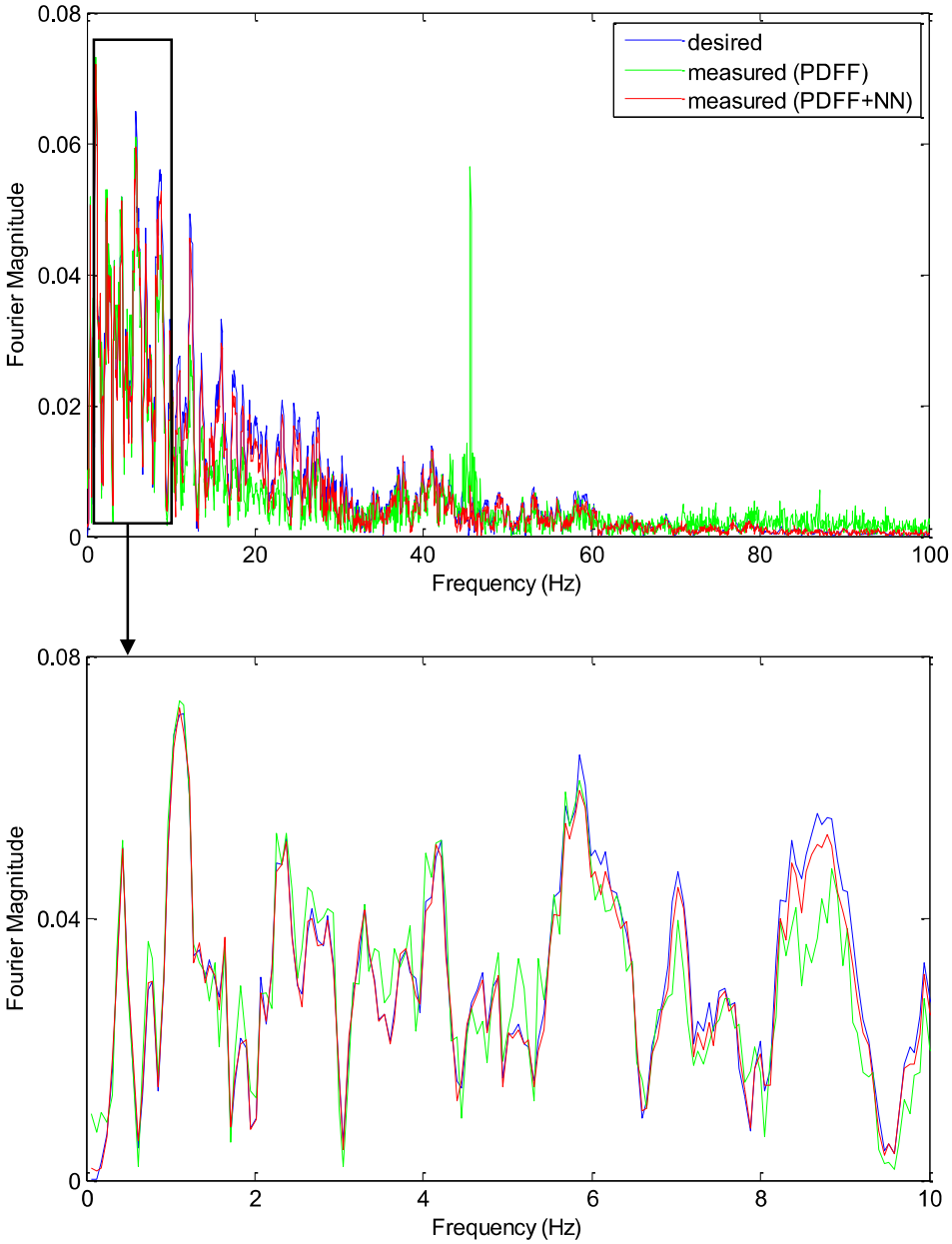

Figure 4.30: FFT comparison between the measured and the desired signal for El-Centro earthquake record (unloaded table).

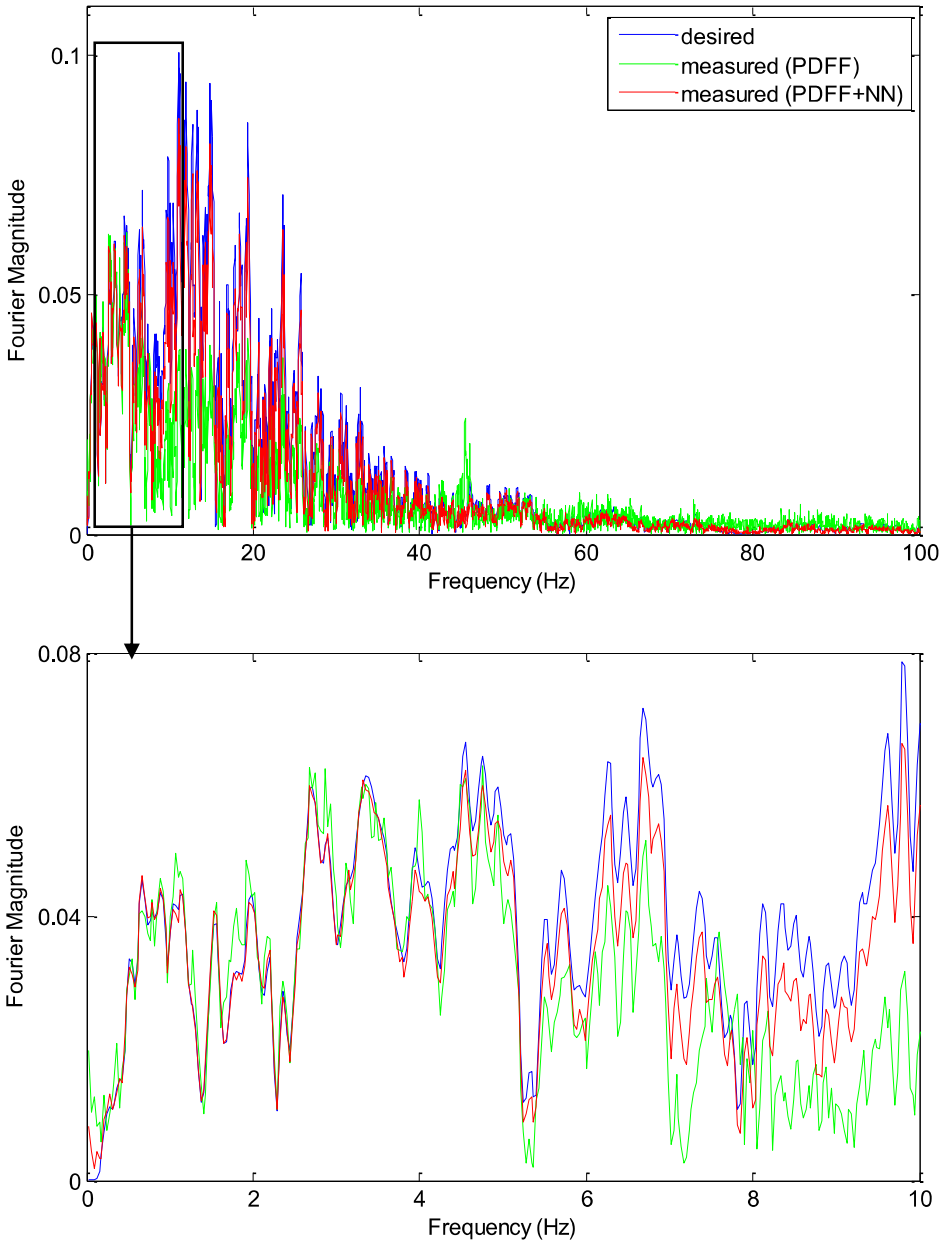

Figure 4.31: FFT comparison between the measured and the desired signal for Cape-Mendocino earthquake record (unloaded table).

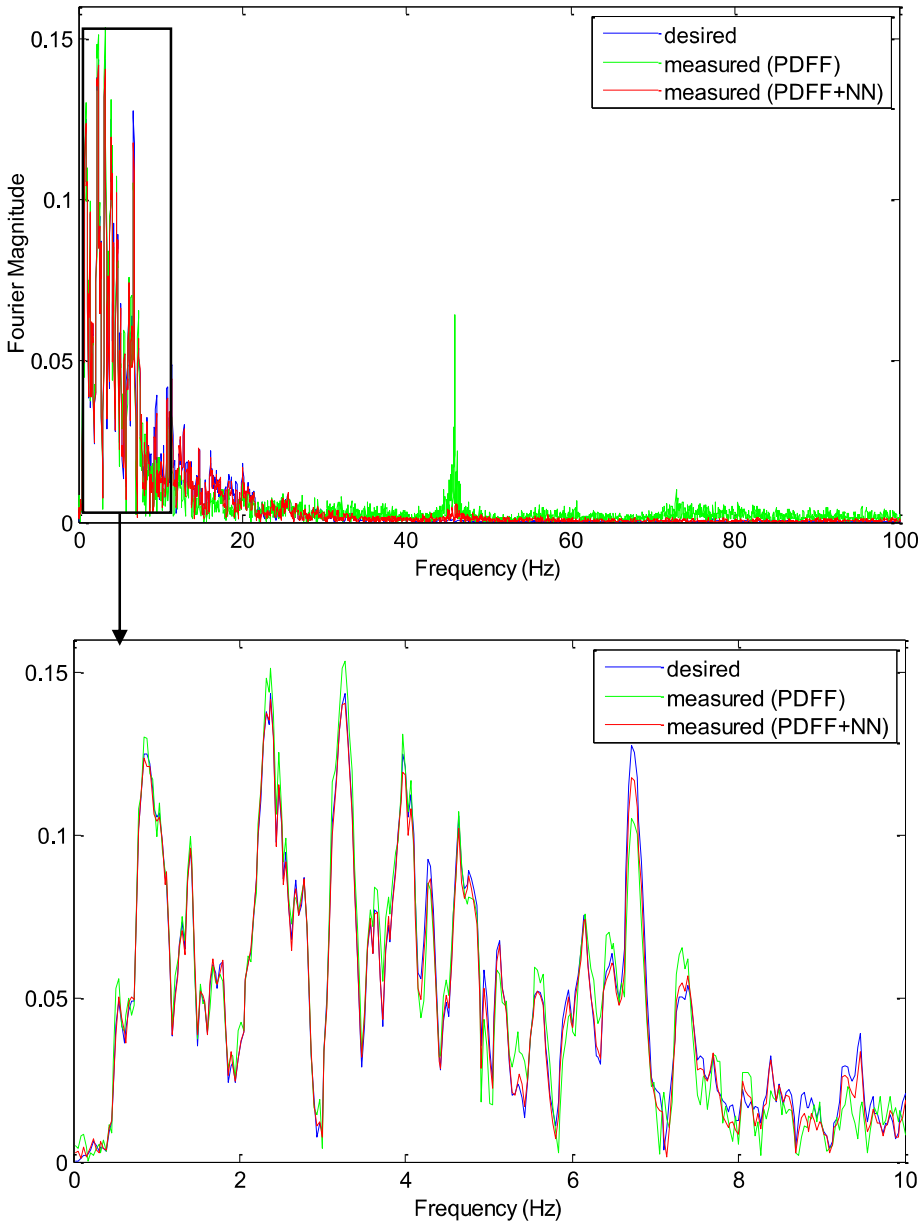

Figure 4.32: FFT comparison between the measured and the desired signal for Northridge earthquake record (unloaded table).

It is clear that with the proposed PDFF-based NN controller, an improved accuracy in the reproduced signals has been achieved. As illustrated by the acceleration feedback that is getting closer to the target signal especially in the vicinity of the peak magnitudes and by a decrease in the time delay.

The frequency response amplification of the system around a critical frequency of 45 Hz has been significantly attenuated by the additional neural control function. This prominent advantage provided by the implementation of NN

control algorithm demonstrates the high capacity of the NN to cope with nonlinear aspects and resonance frequencies of the shaking table system.
Using the equations 4.2 and 4.3, the values of $RMSE_T$ and $RMSE_F$ for the used earthquake records have significantly decreased, after the implementation of the additional NN control algorithm. A summary of the computed RMSE of both acceleration time histories and Fourier magnitudes, for the three earthquake records that were used, is provided in Table 4.6.

Table 4.6: RMSE relative error values for different earthquake records in time and frequency domain analysis (unloaded table).

	$RMSE_T$ (%)		$RMSE_F$ (%)	
	PDFF	Proposed	PDFF	Proposed
El-Centro	63.62	16.33	35.33	09.90
Cape-Mendocino	54.80	09.27	28.20	02.30
Northridge	54.31	12.9	22.78	06.87

To further assess the enhancement provided by the hybrid controller presented in this study, a comparison between the reproduced PGA and the desired PGA has been carried out. Results showed that the PGA is reproduced within 10% error in the presence of the additional neural controller. The values of the errors obtained using both the PDFF and the PDFF-based NN controllers are listed in Table 4.7.

Table 4.7: Error relative in PGA reproduction for different earthquake records (unloaded table).

	Desired PGA (g)	PDFF		Proposed	
		Reproduced PGA (g)	ε(%)	Reproduced PGA (g)	ε(%)
El-Centro	0.3311	0.3227	02.56	0.2962	10.56
Cape-Mendocino	1.4966	0.9922	33.70	1.4147	05.47
Northridge	0.6044	0.6617	09.48	0.5556	08.06

4.5.2. Tests results: loaded shaking table testing

In the first shaking table tests performed on an unloaded table, the designed NN control algorithm proved its efficiency to compensate for the shaking table system nonlinearities and track the desired acceleration signal with accuracy. In order to investigate its robustness for dealing with a table-specimen interaction, a second experimental shaking table tests are carried out for a loaded table. The same described specimen is mounted on the top stage of the shaking table, and the same earthquake records are applied. Similarly, a number of comparisons are performed to assess the performance of the proposed PDFF-based NN controller over the PDFF controller alone. Figure 4.33 to 4.35 and Figure 4.36 to 4.39 show the comparison of the measured time histories and spectral accelerations responses of the table with the target, respectively. The proposed PDFF-based NN controller achieves a better accuracy in reproducing desired accelerations on the table. Also, it suppressed the system resonant frequencies around 45 Hz and enhanced the spectral amplitudes in the frequency range of interest.

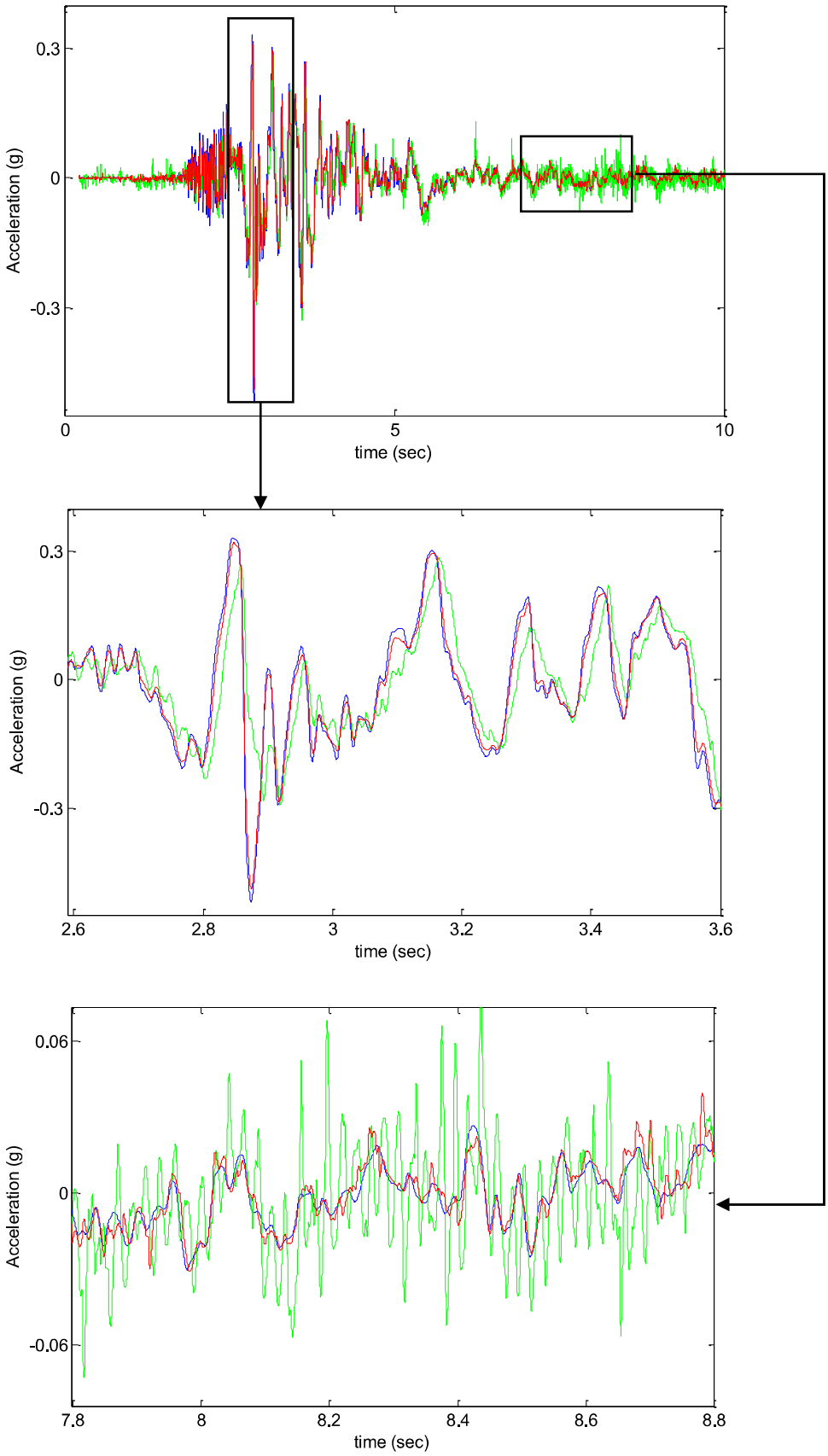

Figure 4.33: Enhanced acceleration response achieved with the PDFF-based NN controller under El-Centro earthquake record (table + payload).

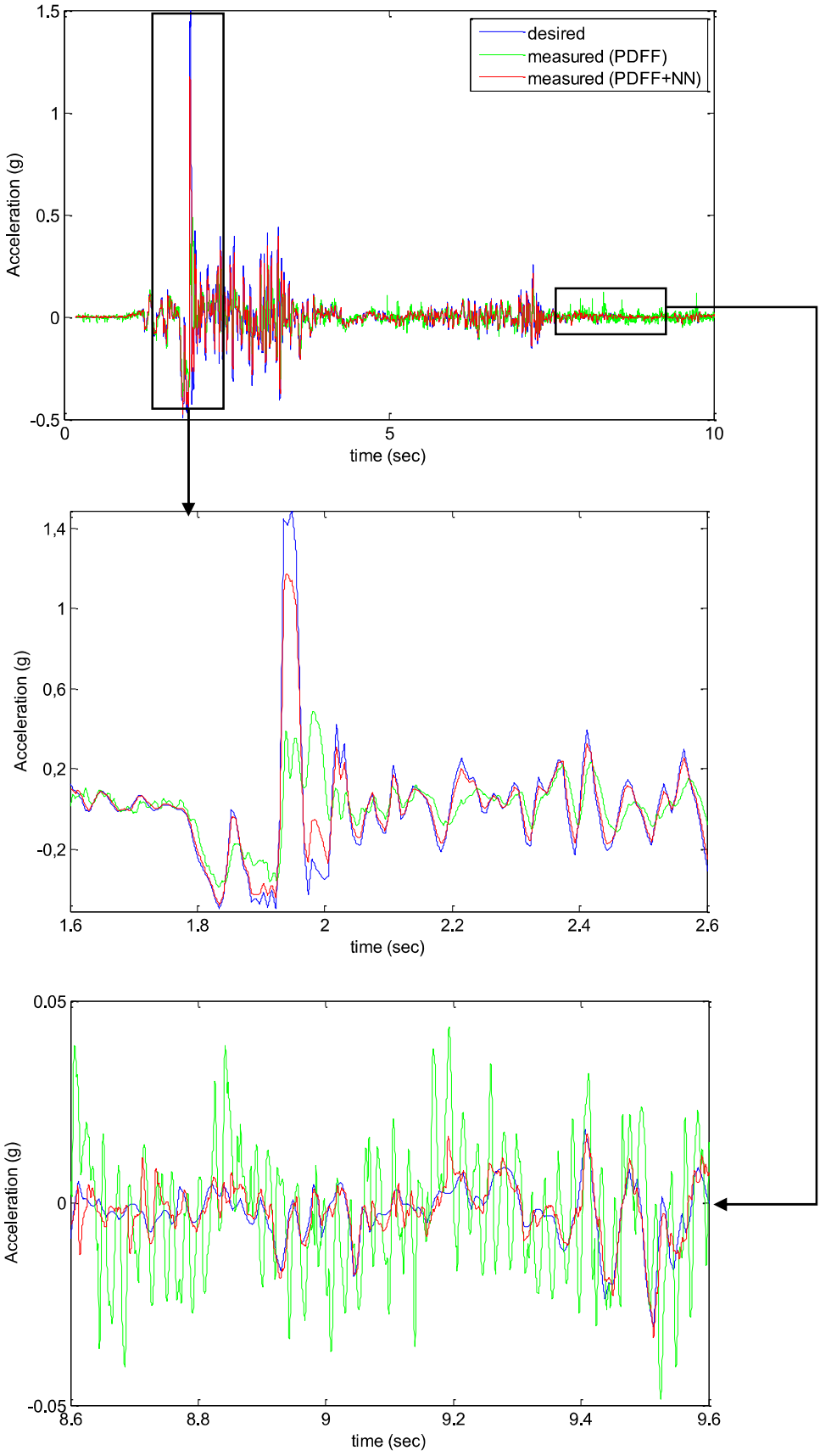

Figure 4.34: Enhanced acceleration response achieved with the PDFF-based NN controller under Cape-Mendocino earthquake record (table + payload).

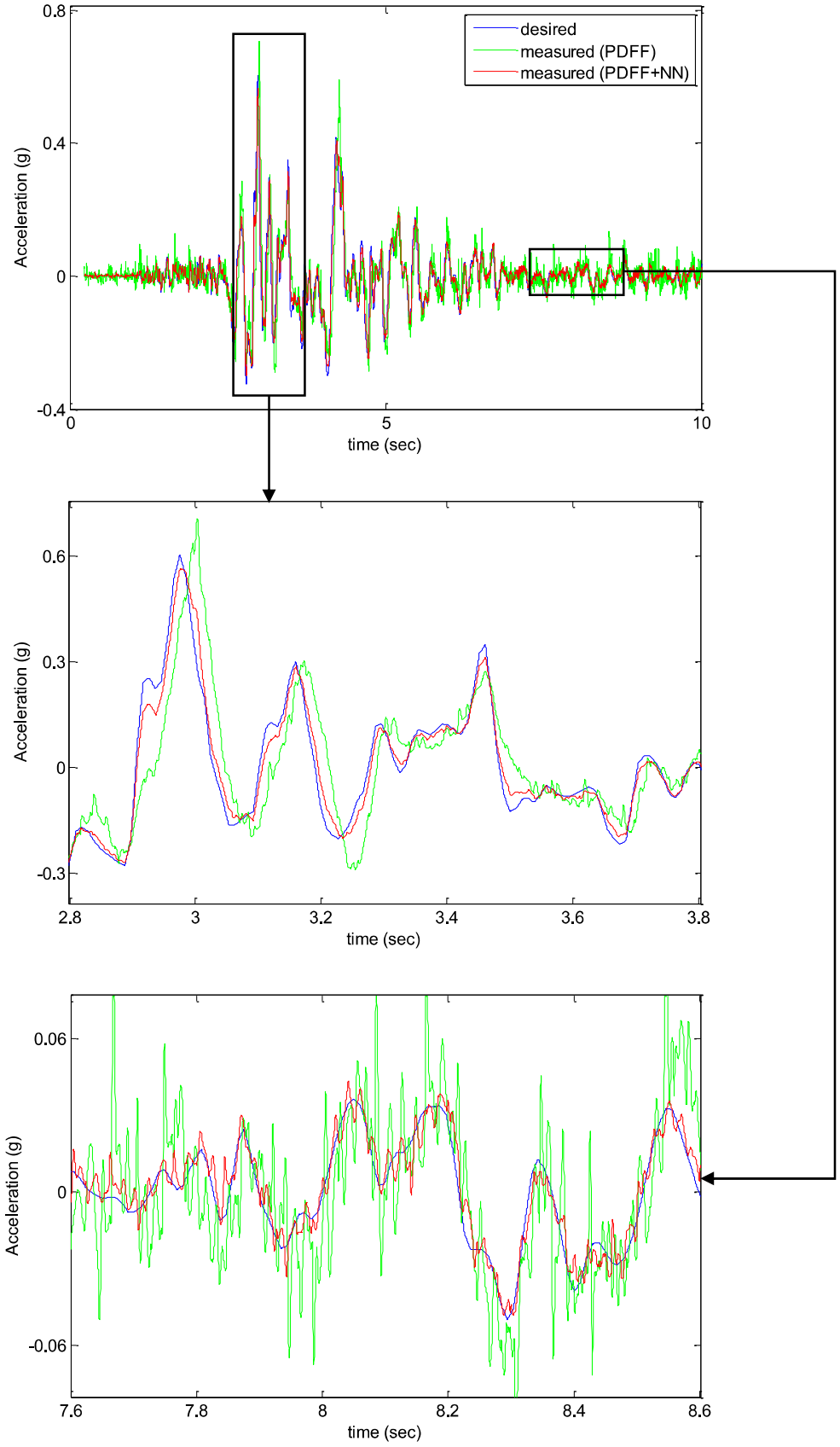

Figure 4.35: Enhanced acceleration response achieved with the PDFF-based NN controller under Northridge earthquake record (table + payload).

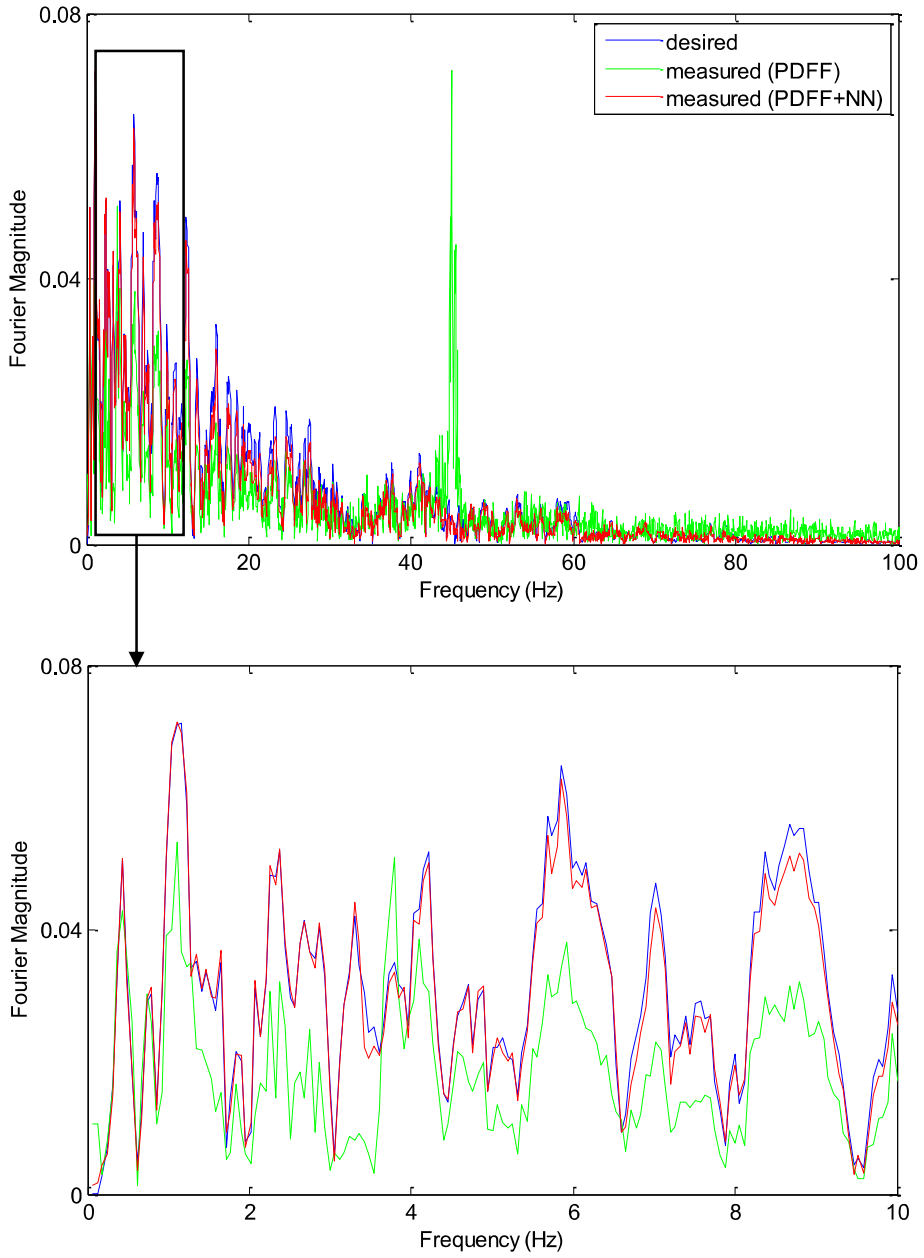

Figure 4.36: FFT comparison between the measured and the desired signal for El-Centro earthquake record (table + payload).

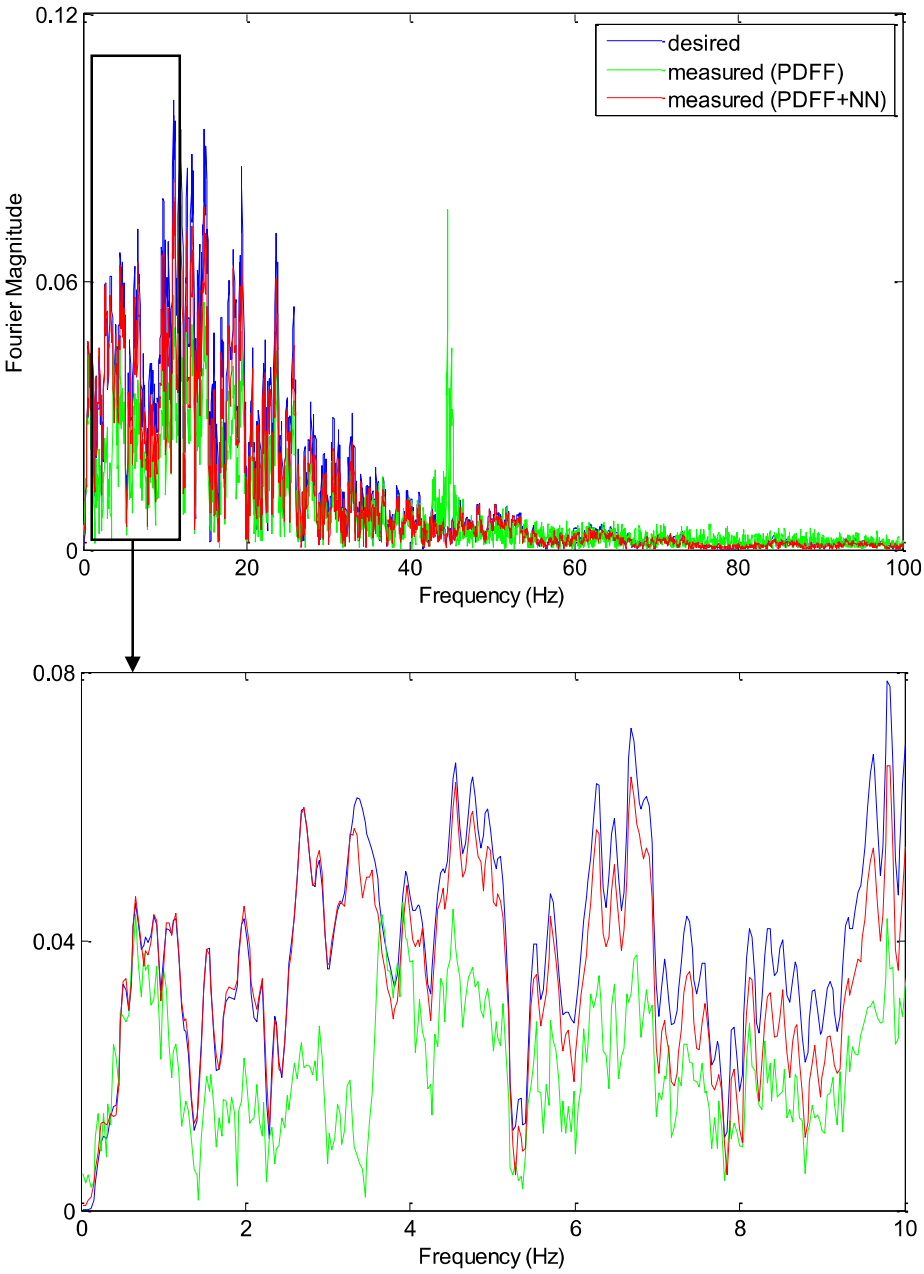

Figure 4.37: FFT comparison between the measured and the desired signal for Cape-Mendocino earthquake record (table + payload).

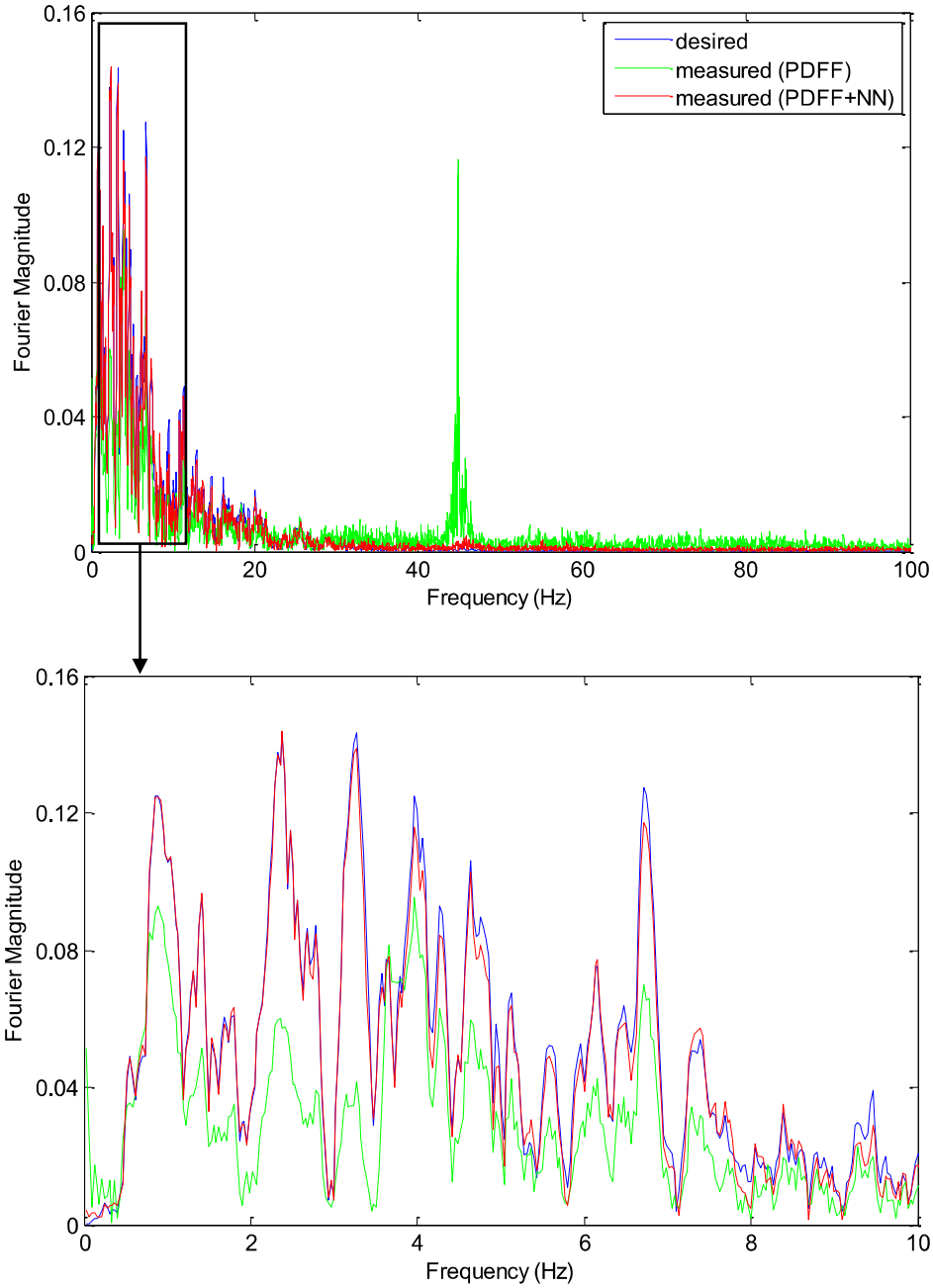

Figure 4.38: FFT comparison between the measured and the desired signal for Northridge earthquake record (table + payload).

Similarly to the first shaking table tests program, the RMSE is used as a principle performance assessment index to quantify this enhancement obtained after implementing the NN control algorithm in the closed loop of the shaking table system. The proposed tracking control strategy has significantly reduced the $RMSE_T$ as well as the $RMSE_F$ for the all the applied earthquake records. The computed $RMSE_T$ of the acceleration time histories and spectral acceleration responses for the three earthquake records are summarized in Table 4.8.

Table 4.8: RMSE relative error values for different earthquake records in time and frequency domain analysis (table + payload).

	$RMSE_T$ (%)		$RMSE_F$ (%)	
	PDFF	Proposed	PDFF	Proposed
El-Centro	68.02	18.07	53.62	11.61
Cape-Mendocino	69.81	17.70	38.20	02.30
Northridge	63.04	16.61	55.86	09.34

The fidelity in the reproduction of the PGA on the table with a specimen has been evaluated using the assessment index given in equation 4.4. The PGA reproduced at the base of the specimen was in the range of 12% error maximum, for the three earthquake records that have been used. The computed errors between the target and the achieved PGA with the PDFF and with the PDFF-based NN controller are listed in Table 4.9.

Table 4.9: Error relative in PGA reproduction for different earthquake records (table + payload).

	Desired PGA (g)	PDFF		Proposed	
		Reproduced PGA (g)	ε(%)	Reproduced PGA (g)	ε(%)
El-Centro	0.3311	0.2843	14.14	0.3002	09.34
Cape-Mendocino	1.4966	0.4890	67.32	1.1747	21.50
Northridge	0.6044	0.7319	22.30	0.5531	08.48

Based on these result analyses, a remarkable enhancement in reducing the acceleration errors between the reference signal and the closed-loop system output was achieved when implementing the NN block. In fact, the NN control algorithm demonstrated the same level of efficiency and robustness to deal with the dynamic interaction between the shaking table and the specimen as well as system's nonlinearities.

4.6. Conclusion

Based on the numerical results that showed the efficiency of the NN algorithm to improve the acceleration tracking performance of simulated shaking tables, experimental real-time tests have been carried out on the QUANSER STIII to assess the robustness and the performance of the designed NN control algorithm on the shaking table. The proposed control methodology combines the three-layer feedforward NN and the original PDFF controller. At a first stage, experimental data were acquired in real time using the existing PDFF controller to constitute a database to train the feedforward NN offline using the Lavenberg–Marquardt algorithm. Afterwards, the well-trained NN is implemented online in the outer acceleration closed-loop of the Simulink-based PDFF control system of QUANSER STIII. Along this control scheme, the acceleration feedback is shaped by the NN control function before being introduced into the acceleration tracking controller which is the FF controller. Several real-time shaking table tests have been conducted using three real earthquake records for different load conditions by using the same NN model. A comparative analysis was carried out for the two testing conditions, and the results clearly proved that the closed-loop system performance for acceleration tracking with the PDFF-based NN controller is significantly enhanced. The NN controller addresses the high amplitude distortions and time delays, producing accelerations closer to the target time histories as well as spectral acceleration amplitudes. The acceleration responses have been produced within a range of 7% to 20% RMSE and the PGA within a range of 8% to 12% errors. The notable reduction in acceleration tracking errors due to the new neural control strategy affirmed the high capabilities of the NN to enhance the existing PDFF acceleration control accuracy and to cope with inherent nonlinearities and resonant frequencies of the system as well as the coupling effect due to the interaction between the shaking table system and the specimen, which is an important source of classic control defiance.

Additionally, the obtained improvement in the acceleration tracking performance of the shaking table using the same NN structure after a unique training process, for different excitation signals and different load conditions attests of the robustness of the proposed control methodology which represents a major advantage.

CONCLUSION AND FUTURE WORK

The performance of a shaking table directly relies on the capability of the control system to replicate earthquake ground motion and other type of signals on its platform. Since dynamical characteristics of the specimens change during the test due to severe nonlinear deformations and structural damages, conventional tuning control systems may not be sufficient to achieve acceptable results. In addition, the shaking table system by its own contains inherent nonlinearities, friction, dynamic coupling effects between the different DOFs, uncertainties and external disturbances which seriously deteriorate the tracking accuracy of the control systems.

In the past decades, numerous advanced control techniques have been developed aiming to improve the robustness, stability and performance of shaking tables' controllers. A significant amount of research works have developed control systems based on feedforward compensation, iterative learning method, model-based compensation and adaptive control techniques. Even if they have proved their capabilities to achieve better tracking performance, they still have several drawbacks. Currently, instead of designing sophisticated and complex nonlinear controllers, hard to be implemented in real world shaking tables, the research community have focused on a new approach by preserving the conventional controllers of industrial shaking tables and working on the improvement of their performance and robustness. Recent development in Artificial Intelligence (AI) have created new possibilities in the field of shaking table control, to achieve a further enhancement in signal reproduction over traditional controllers. Within this frame of reference, this thesis investigates the potential of different schemes of NN-based controllers to increase the acceleration tracking performance of a shaking table. After a numerical validation via several simulations, the proposed neural controller has been implemented in the outer-loop of the QUANSER STIII control system. Experiments have proved the capabilities of the NN to significantly reduce the acceleration distortions in the experimental shaking table responses. The most relevant contribution of this thesis is that the enhancement in shaking table performance is achieved using a novel NN-based control algorithm developed in MATLAB/Simulink and validated experimentally. The acceleration tracking improvement of the shaking table driven by the additional NN controller is obtained using the same structure of the NN and a unique training process performed offline. The same degree of performance is achieved for different input signals and

different load conditions which attests the robustness of the proposed control methodology. The most important conclusions of the work undertaken in this thesis are outlined in the following sections:

1. Concept of the NN control strategy and numerical simulations

Numerical models representing a shaking table system are developed in Chapter 3, aiming to replicate the behaviour of real shaking tables as accurately as possible.

- An early simplified model of a shaking table is developed in form of finite element model to simulate the global behavior of a typical shaking table in unloaded and loaded conditions under dynamic excitations. Then, a global transfer function is estimated based on input/output data collected after dynamic simulations of the model. An optimal tuned controller, which is the conventional PID controller is added. Then, once the designed NN is trained, two control strategies are proposed: a first offline control attempts to produce the appropriate command signal to the shaking table, so as to obtain a response as close to the desired accelerations as possible. The second proposed control strategy, which is an online control, uses the NN as an additional improvement of the signal replication achieved by the PID controller. Comparisons between the measured accelerations with the implementation of the NN control function confirm the performance of the proposed NN algorithm in minimizing the errors in producing more accurate acceleration responses over the PID controller alone.
- A representative model of the QUANSER STIII shaking table, described in Chapter 2, is developed in Simulink. The simulated acceleration is able to track the measured acceleration obtained experimentally with a good accuracy. By using several earthquake records as excitation signals, a database for training, validating and testing the designed NN is constituted. Similarly to the implementation schemes of the NN in the first model, the neural control function runs in an offline and online modes. Numerous earthquake leading simulations are carried out, demonstrating the capabilities of the additional NN control function to achieve a higher accuracy in the reproduced accelerations in both offline and online control scheme.

Based on the results of the numerical procedure of implementing the proposed NN control algorithm, it is shown that the NN controller is able to compensate for the limitations of a traditional controller like the PID and to improve the accuracy of the shaking table responses in terms of amplitudes and time delays. Therefore, experiments through real-time shaking table tests are required to validate the presented control methodology to achieve a better acceleration tracking performance of the shaking table.

2. Experimental validation of the NN control technique

The NN control algorithm is implemented online in the acceleration closed-loop of the real QUANSER STIII control system to experimentally evaluate the robustness of the proposed controller combined with the existing controller. The approach that is proposed in the experimental investigation of this work allows the PD controller to control the stage position and velocity, the FF controller to control the acceleration and stabilize the table and the additional NN control algorithm to improve the accuracy of the acceleration replication.

The experimental results confirmed that the proposed NN control algorithm helped the PDFF controller to track desired accelerations by increasing the quality of the acceleration feedback, for both unloaded and loaded table conditions, in time and frequency domains. The notable reduction in acceleration tracking errors in terms of amplitude distortions and time delays in the measured responses demonstrates the high capacity of the NN to cope with nonlinear aspects and resonance frequencies of the shaking table system.

3. Future works

3.1. Short term

Based on the main achievements of this thesis, the short term future works can be cited as follows:

a. The development the QUANSER STIII serves as a realistic shaking table model, able to be easily implemented in MATLAB/Simulink and controlled with any designed controller; the application of other intelligent control algorithm is worth to be explored;

b. The results obtained herein for a small electric bi-axial shaking table encourage to implement the proposed control algorithm in other type of shaking tables;
c. An interesting research expansion can be investigated by using the real-time acceleration data collected during shaking table tests to carry out an experimental identification of the QUANSER STIII shaking table.

3.2. Long term

The inner-loop control of the QUANSER STIII shaking table, composed of the PDFF controller, cannot be improved with a tuning of the predefined gains, it is worth investigating the substitution of the original controller entirely by a neuro-controller. Since the Reinforcement Learning (RL) has become the most recent advancement in machine learning and control techniques for the last 20 years, it could be an interesting approach to apply this methodology to shaking tables. The RL approach is designed to solve problems in which the agent interacts directly with the environment (the system to be controlled) and learns to choose the appropriate task (command) by trial and error. It presents an intelligent adaptive controller that produces in real-time the adequate command data at each time step, based on the recorded system state which is the measured acceleration. Deep Neural Networks (DNN) can be used to approximate the optimal command signal point to point, driving the table stage along the desired trajectory.

1. Abuowda, K., Dyke, D. and Noroozi, S., “Dynamic Performance Analysis of PID and Fuzzy Logic Controllers Applicable in Electrohydraulic Servo Actuator”, in: 3th APCA International Conference on Automatic Control and Soft Computing (CONTROLO 2018), 4-6 June 2018, Ponta Delgada, São Miguel Island, Azores, Portugal (2018).

2. Ahmed, S., Mahdi, S. M., Mohammedridha, T. and Mashari, M. H., “Sliding Mode Control for Electro-Hydraulic Servo System”, Engineering Journal, V .15, n° 3, (2015), 1-10.

3. Airouche, A., Bechoutoula, H., Aknouche H., Thoen, B.K. and Benouar, D., “Experimental identification of the six DOF C.G.S., Algeria, shaking table system”, Smart Structures and Systems, V. 13, n° 01, (2014), 137-154.

4. Aly A. A., “PID Parameters Optimization Using Genetic Algorithm Technique for Electrohydraulic Servo Control System”, Intelligent Control and Automation, V. 2, n° 02, (2011), 69-76.

5. Andrásik, A., Meszaros, A. and Azevedo, S. F., “On-line tuning of a neural PID controller based on plant hybrid modeling”, Computers & Chemical Engineering, V. 28, n° 8, (2004), 1499-1509.

6. Araghi, L. F., Korayem, M. H., Nikoobin, A. and Setoudeh, F., “Neural Network Controller Based on PID Controller for Two links- Robotic Manipulator”, Proceedings of the World Congress on Engineering and Computer Science 2008 WCECS 2008, October 22 - 24, 2008, San Francisco, USA, (2008).

7. Asan, M. K., Saravanakumar, G., Valamarthi, K., Devaraj, D. and Radhakrishnan, T. K., “Real-Coded Genetic Algorithm for System Identification and Tuning of a Modified Model Reference Adaptive Controller for a Hybrid Tank System”, Applied Mathematical Modelling, V. 37, n° 6, (March 2013), 3829-3847.

8. Bahrami, M. and Tait, K.E., “Model reference direct adaptive control of nonlinear plants using NN”, International Journal of Neural Systems, V. 5, n° 1,(1994), 77-82.

9. Baldovino R.G. and Dadios, E.P, “Design and development of a fuzzy-PLC for an earthquake simulator/shake table", International Conference on Humanoid, Nanotechnology, Information Technology, Communication and Control, Environment and Management (HNICEM), Palawan, (2014), 1-6.

10. Baldovino, R.G., “Design and Development of a Fuzzy-PLC Controller for an Earthquake Simulator / Shake Table”, Thesis for: Master of Science in Electronics and Communications Engineering, (2014).

11. Blondet, M. and Esparza, C., “Analysis of shaking table-structure interaction effects during seismic simulation tests”, Earthquake Engineering and Structural Dynamics, V. 16, n° 4, (1988), 473-490.

12. Bouslama, F. and Ichikawa, A., “Fuzzy control rules and their natural control laws”, Fuzzy Sets and Systems, V. 48, n° 1, (May 1992), 65-86.

13. Burton, R.T., Ukrainetz, P.R., Nikiforuk, P.N. and Schoenau, G.J., “Neural Networks and Hydraulic Control-From Simple to Complex Applications”, Proceedings of the Institution of Mechanical Engineers, Part I: Journal of Systems and Control Engineering, V. 213, n° 5, (1999), 349–358.

14. Calvi, G.M. and Kingsley, G.R., “Problems and certainties in the experimental simulation of the seismic response of MDOF structures”, Engineering structures, V. 18, n° 3, (1996), 213-226.

15. Chase, J. G., Hudson, N. H., Lin, J., Elliot, R. and Sim, A., “Non-linear shake table identification and control for near-field earthquake testing”, Journal of Earthquake Engineering, V. 9, n° 4, (2005), 461–482.

16. Chen, C., “An integrating genetic algorithm and modified Newton method for tracking control and vibration suppression”, Artificial Intelligence Review, V. 53, (2020), 3177–3199.

17. Chen, C. Y., Liao, P. and Cheng, H., “Fuzzy Controller Design for Positioning and Synchronization of Electrohydraulic System”, 2007 2nd IEEE Conference on Industrial Electronics and Applications, Harbin, (2007), 971-976.

18. Chen, P.C., Lin, P. Y. and Chiang, H. W., “Development of a multiple seismic shaking table test system”, Proceedings of the 12th International Conference on Motion and Vibration MOVIC 2014, Japan, (2014).

19. Chen, Y., He, Y. and Zhou, M., “Decentralized PID neural network control for a quadrotor helicopter subjected to wind disturbance”, Journal of Central South University, V. 22, (2015), 168–179.

20. Chertovskikh, P.A., Seredkin, A. V., Gobyzov, O. A., Styuf, A. S., et al., “An adaptive PID controller with an online auto-tuning by a pretrained neural network”, Journal of Physics: Conference Series, V. 1359, n° 2019, (2019), 012090.

21. Cho S. H., Linjama, M., Sairiala, H., Koskinen, K. T. and Vilenius, M., “Sliding mode tracking control of a low-pressure water hydraulic cylinder under nonlinear friction”, Proceedings of the Institution of Mechanical Engineers, Part I: Journal of Systems and Control Engineering, V. 216, n° 5, (2002), 383-392.

22. Cho S.H., “Trajectory Tracking Control of a Pneumatic XY Table Using Neural Network Based PID Control”, International Journal of Precision Engineering and Manufacturing, V. 10, n° 5, (2009), 37-44.

23. Cho, S. H. and Edge, K. A., “Adaptive sliding mode tracking control of hydraulic servosystems with unknown non-linear friction and modelling error”, Proceedings of the Institution of Mechanical Engineers, Part I: Journal of Systems and Control Engineering, V. 214, n° 4, (2000), 247–257.

24. Conte, J.P. and Trombetti, T.L., “Linear dynamic modeling of a uni-axial servo-hydraulic shaking table system”, Earthquake Engineering and Structural Dynamics, V. 29, n° 9, (2000), 1375-1404.

25. Cozma, A. and Pitica, D., “Artificial Neural Network and PID Based Control System for DC Motor Drives”, International Conference on Optimization of Electrical and Electronic Equipment, OPTIM 2008: 11th, (May 2008), 161 –166.

26. Dange, N. A. and Pawer, A., “Position Control of Servo Motor Using Fuzzy Logic Controller”, International Journal of Advanced Research in Electrical, Electronics and Instrumentation Engineering, V. 5, n° 6, (2016), 5541-5552.

27. Dertimanis, V.K., Harris P., Mouzakis, H. P., Ioannis N. et al., “On the acceleration-based adaptive inverse control of shaking table”, Earthquake Engineering and structural dynamics, V. 44, n° 9, (2015), 1329-1350.

28. Detiček, E., Župerl, U., “An Intelligent Electro-Hydraulic Servo Drive Positioning”, Strojniški vestnik - Journal of Mechanical Engineering, V. 57, n° 5, (2011), 394-404.

29. Dozono, Y., Horiuchi, T., Katsumata, H. and Konno, T., “Shaking-Table Control by Real-Time Compensation of the Reaction Force Caused by a Nonlinear Specimen”, Journal of Pressure Vessel Technology, V. 126, n° 1, (2004), 122-127.

30. Dyke, S. J., Spencer, B. F., Quast, P. and Sain, M. K., “The Role of Control-Structure Interaction in Protective System Design”, Journal of Engineering Mechanics, V. 121, n° 2, (1995).

31. Edge, K.A., “The control of fluid power systems-responding to the challenges”, Proceedings of the Institution of Mechanical Engineers, Part I: Journal of Systems and Control Engineering, V. 211, n° 2, (1997), 91- 110.

32. El-Araby, M., El-Kafrawy, A. and Abass, A., “Dynamic performance of a nonlinear non-dimensional 2-stage electrohydraulic servovalve system”, International Journal of Mechanics and Materials in Design, V. 7, n° 2, (2010), 99-110.

33. Elbayomy, K. M., Zongxia, J. and Huaqing, Z., “PID Controller Optimization by GA and Its Performances on the Electro-hydraulic Servo Control System”, Chinese Journal of Aeronautics, V. 21, n° 4, (August 2008), 378-384.

34. Enokida, R. and Kajiwara, K., “Nonlinear Signal Based Control for single axis ST supporting nonlinear structural systems”, Structural Control and Health Monitoring, V. 26, (2019), 1-20.

35. Errachdi, A., Benrejeb, M., “Model reference adaptive control based on NN for nonlinear time-varying systems”, Proceeding of the International conference on systems, control and informatics, November 19-20, 2013, Jakarta, Indonesia, (2013).

36. Esparza C., Núñez R. and González, F., “Model Reference Adaptive Position Controller with Smith Predictor for a Shaking-Table in Two Axes”, in: Batyrshin I., Mendoza M.G. (eds) Advances in Computational Intelligence. MICAI 2012. Lecture Notes in Computer Science, V. 7630, (2013).

37. Fahmy, R. A., Badr, R. I. and Rahman, F. A., “Adaptive PID controller using RLS for SISO stable and unstable systems”, Advances in Power Electronics, V. 2014, Article ID 507142, (2018).

38. Fangfang, L., Li, X. and Juke Wang J., “Effects of Interaction between Dual Shaking Tables and Specimen and Force Feedback Compensation Control”, Shock and vibration, V. 2018, Article ID 6795763, (2018), 12 pages.

39. Fleming, P. J. and Purshouse, C. M., “Genetic algorithms in control systems engineering”, IFAC Proceedings Volumes, V. 26, n° 2, part 2, (July 1993), 605-612.

40. Furuta, H., Okanan, H., Kaneyoshi, M. and Tanaka, H., “Application of Fuzzy logic to structural vibration control”, Uncertainty modeling in vibration and fuzzy analysis of structural systems, (1997), 233-251.

41. Gao, C-h., Yuan, X-b., “Development of the Shaking Table and Array System Technology in China”, Advances in Civil Engineering, V. 2019, (2019), 1-11.

42. Goto, K., Seki, K., Kawafuku, M., et al., “Modeling of shaking table systems and optimization of feedback gain using GA”, Proceedings of the JSME annual meeting 2008.5, (2008), 153-154.

43. Guan, C. and Zhu, S., “Adaptive time-varying sliding mode control for hydraulic servo system”, Proceedings of ICARCV 2004 8th control, automation, robotics and vision Conference, Kunming, China, V. 3, (2004), 1774-1779.

44. Guan, C. and Pan, S., “Adaptive sliding mode control of electro-hydraulic system with nonlinear unknown parameters”, Control Engineering Practice, V. 16, n° 11, (2008), 1275– 1284.

45. Guan, G.F., Xiong, W. and Wang, H.T., “Adaptive random control of a two-axis redundantly actuated electro-hydraulic shaking table”, Journal of Vibration and Control, V. 22, n° 16, (2014a), 3455–3469.

46. Guo, K., Wei, J.H. and Tian, Q.J., “Disturbance observer based position tracking of electrohydraulic actuator”, Journal of Central South University, V. 22, (2015), 2158-2165.

47. Guo, W., Shao, P., Li, H-Y., Long, Y. and Mao, J-f., “Accuracy assessment of shaking table device on strong earthquake output”, Advances in civil engineering, V. 2019, Article ID 9372505, (2019), 23 pages.

48. Has, Z., Rahmat, M.F., Husain, A.R. et al., “Robust Position Tracking Control of an Electro-Hydraulic Actuator in the Presence of Friction and Internal Leakage”, Arabian Journal of Science Engineering, V. 39, (2014), 2965–2978.

49. Hasanpour, H., Ben, M. H. and Askari, M., “Adaptive PID control based on RBF NN for quadrotor”, International Research Journal of Applied and basic Sciences, V. 11, n° 2, (2017), 177-186.

50. Hassan, M.Y. and Kothapalli, G., “Comparison between neural network based PI and PID controllers”, Proceedings of the 7th International Multi-Conference on Systems, Signals and Devices, (2010).

51. Hirata, G., Joaquin Alvarez, J. and Cuesta, R., “Robust tracking control of a shaking table with dry friction”, Nonlinear Dynamics, V. 85, n° 3, (2016), 1535–1547.

52. Hu, H., Liu, J. and Wang, L., “Model reference neural network control strategy for flight simulator”, 2010 IEEE International Conference on Mechatronics and Automation, Xi'an, (2010), 1483-1488.

53. Hyun, J. H. and Lee, C. O., “Optimization of feedback gains for a hydraulic servo system by genetic algorithms”, Proceedings of the Institution of Mechanical Engineers, Part I: Journal of Systems and Control Engineering, V. 212, n° 5, (1998), 395-401.

54. Ishaque, K., Abdullah, S., Md, S. and Salam, Z., “A simplified approach to design FLC for an underwater vehicle”, Ocean Engineering, V. 38, n° 1, (2011), 271-284.

55. Iwasaki, M., Ito, K., Kawafuku, M., H. Hirai, H. et al., “Disturbance observer-based practical control of shaking tables with nonlinear specimen”, Proceedings of the

16th IFAC World Congress (IFAC 2005), Prague, Czech, July 2005, V. 38, (2005), 251–256.

56. Jaen-Cuellar, A. Y., Romero- Troncoso, R.J., Morales- Velazquez, L. et al., “PID-Controller Tuning Optimization with Genetic Algorithms in Servo Systems”, International Journal of Advanced Robotic Systems, V. 10, n° 9, (2013), 1-14.

57. Joshi, G. and Chowdhary, G., “Deep Model Reference Adaptive Control”, 2019 IEEE 58th Conference on Decision and Control (CDC), Nice, France, (2019), 4601-4608.

58. Kakegawa, T., Suzuki, T., Sato, E., Kajiwara, K. and Tagawa, Y., “Linear model derivation and three-variable control (TVC) of the world's largest 3-D full-scale shaking table”, Transactions of the Japan Society of Mechanical Engineers, Part C, V. 69, n° 2, (2003), 343–348 (in Japanese).

59. Kalyoncu, M. and Haydim, M., “Mathematical modelling and fuzzy logic based position control of an electrohydraulic servosystem with internal leakage”, Mechatronics, V. 19, n° 6, (2009), 847–858.

60. Kang, J., Meng, W., Abraham, A. and Liu, H., “An adaptive PID neural network for complex nonlinear system control”, Neurocomputing, V. 135, (July 2014), 79-85.

61. Karam, Z.A., “PI-like Fuzzy Logic Position Controller Design for Electrohydraulic Servo-actuator Based on Particle Swarm Optimization and Artificial Bee Colony Algorithms”, Al-Nahrain Journal for Engineering Sciences (NUCEJ), V. 19, n° 2, (2016), 395 – 406.

62. Karshenas, M., Dunnigan, M. W. and Williams, B. W., “Adaptive inverse control algorithm for shock testing”, IEE Proceedings - Control Theory and Applications, V. 147, n° 3, (2000), 267-276.

63. Khairudin, M. and Kholis, N., “MRC NN controller for arm robot manipulator”, Proceedings of the 1st International Conference on Information Technology, Computer, and Electrical Engineering, Semarang, (2014), 41-45.

64. Kim, Y. J., Ghaboussi, J., “A new method of reduced order feedback control using Genetic Algorithms”, Earthquake Engineering & Structural Dynamics, V. 28, n° 2, (1999), 193 – 212.

65. Kirecci A., Topalbekiroglu, M. and Eker, I., “Experimental evaluation of a MRAC for a hydraulic robot: a case study”, Robotica, V. 21, n° 1, (2003), 71-78.

66. Krawinkler, H. A perspective on experimental research in earthquake engineering, Guest editor’s note.

67. Kumar, V., Gaur, P. and Mittal, A. P., “ANN based self-tuned PID like adaptive controller design for high performance PMSM position control”, Expert Systems with Applications, V. 41, n° 17, (2014), 7995–8002.

68. Larbi, S.H., Bourahla, N., Benchoubane, H. and Choutri, K., “Offline matching of signals on a shaking table using neural networks”, Proceedings of the International Conference on Earthquake Engineering and Seismology, V. 12, (2015).

69. Larbi, S.H., Bourahla, N., Benchoubane, H. and Choutri, K., “Developing a neural network algorithm as an additional online controller to the PID controller”, Proceedings

of the 16th World Conference on Earthquake Engineering, Santiago, Chile, (January 2017).

70. Le Maoult, A., Queval, J-C. and Bairrao, R., “Dynamic interaction between the shaking table and the specimen during seismic tests”, Advances in Performance-Based Earthquake Engineering, V. 13, (2010), 431-440.

71. Le, T.D., Kang, H-J., Suh, Y-S. and Ro, Y-S., “An online self-gain tuning method using neural networks for nonlinear PD computed torque controller of a 2-dof parallel manipulator”, Neurocomputing, V. 116, (2013), 53–61.

72. Li, Y. H., Yang, M. L., Zhang, Z. H., “Study on second-order sliding mode control law for electro-hydraulic servo system”, In: Chinese Journal of Mechanical Engineering 41.3, (2005), 72–75.

73. Li, F., Li, X. and Juke, W., “Effects of Interaction between Dual Shaking Tables and Specimen and Force Feedback Compensation Control”, Shock and Vibration, V. 2018, (2018), 1-12.

74. Li, H. Y., “The Adaptive Niche Genetic Algorithm for Optimum Design of PID Controller”, 2007 International Conference on Machine Learning Cybernetics, Hong Kong, China, (2007), 487-491.

75. Li, L., “Simulation and Control of Servo Hydraulic Actuators for Test Applications”, PhD thesis, Graz University of Technology, Austria, (2015).

76. Lin, F. J. and Shen, P. H., “Robust fuzzy-neural-network control for two-axis motion control system based on TMS320C32 control computer”, IEEE International Conference on Mechatronics, 2005. ICM '05, Taipei, (2005), 606-610.

77. Lin, F. and Shen, P., “Robust Fuzzy Neural Network Sliding-Mode Control for Two-Axis Motion Control System”, IEEE Transactions on Industrial Electronics, V. 53, n° 4, (2006), 1209-1225.

78. Lin, G., Liu, G. (2010). Tuning PID Controller Using Adaptive Genetic Algorithms. Proceedings of the 5th International Conference on Computer Science & Education, Hefei, (2010), 519-523.

79. Lin, J.Y., “Development of advanced control strategies for high performance shake table tests”, Master thesis, University of British Columbia Vancouver, Canada, (2017).

80. Ling, M. and Zhu, C., “Measurement and identification of nonlinear friction force for electro hydraulic servo shaking able”, Journal of vibration, measurement and diagnosis, V. 37, n° 4, (2017), 687-691.

81. Liu, Y. and Handroos, H., “Control of hydraulically driven flexible manipulator using sliding mode”, In: ASME International Mechanical Engineering Congress and Exposition, V. 7, (November 2000), 9–21.

82. Lu, W., Yang, J. and Liu, X., “The PID Controller Based on the Artificial Neural Network and the Differential Evolution Algorithm”, Journal of Computer Science, V. 7, n° 10, (2012), 2368-2375.

83. Maekinen, E. and Virvalo, T., “On the motion control of a water hydraulic servo cylinder drive”, Proceedings of the 7th Scandinavian international conference on fluid power, Linköping, Sweden, (May 30 - June 1, 2001).

84. Maghareh, A., Silva, C. E. and Dykeb S. J., “Parametric model of servo-hydraulic actuator coupled with a nonlinear system: Experimental validation”, Mechanical Systems and Signal Processing, V. 104, (May 2018), 663-672.

85. Manikandan, R. and Murugan, A., “Position control of DC servo drive using fuzzy logic controller”, International Conference on Advances in Electrical Engineering (ICAEE), Vellore, (2014), 1-5.

86. Meena, D. K. and Chahar, S., “ (2017). Speed control of DC servo motor using genetic algorithm”, International Conference on Information, Communication, Instrumentation and Control (ICICIC), Indore, (2017), 1-7.

87. Merritt, H. E., “Hydraulic control systems”, John Wiley & Sons, (January 1991), 368 pages.

88. Moghaddam, H., Farzanian, K. and Taheri, E., “An investigation on dynamic behaviour and characteristics of Sharif University of Technology Shaking table (SST)”, Proceedings of the 2nd European Conference on Earthquake Engineering and Seismology, Istanbul, Turkey, (25-29 August, 2014).

89. Mohamed S. R. B. A., “Neural Network controller design for position control system improvement”, Master thesis, University Tun Hussein Of Malaysia, (2013).

90. Mota, M.A.C.A., “Shake Table Acceleration Tracking Performance Impact on Dynamic Similitude”, PhD thesis, Drexel University, (2011).

91. Nakata N., “Acceleration trajectory tracking control for earthquake simulators”, Engineering and Structures, V. 32, n° 8, (2010), 2229-2236.

92. Ninos, K., Giannakakis, C., Kompogiannis, Stavrakas, I., and Alexandridis, A., “Nonlinear control of a DC-motor based on radial basis function neural networks”, International Symposium on Innovations in Intelligent Systems and Applications (INISTA), (June 2011), 611 – 615.

93. Norgaard. M., Ravn, O., Poulsen, N.K. and Hansen, L.K., “Neural Network for Modeling and Control of Dynamic Systems”, Springer Press, New York, NY, USA, (2002).

94. O’Hagan, J.T. and Ma, Q.T., “Experimental assessment of PID control for a uniaxial shake table”, Proceedings of the 15th World Conference on Earthquake Engineering Lisbon, Portugal, (2012).

95. Ogawa, N., Ohtani, K., Tsuneo Katayama, T. and Shibata, H., “Construction of a three–dimensional, large–scale shaking table and development of core technology”, Philosophical Transactions of the Royal Society A, Mathematical, Physical and Engineering science, V. 359, n° 1786, (2001).

96. Ohtani, K., Ogawa, N., Katayama, T., Shibata, H., “Construction of E-DEFENSE (3-D full-scale earthquake testing facility)”, Proceedings of the 13th WCEE Vancouver, Canada, (2004).

97. Ota, T. and Omatu, S., “Tuning of the PID control gains by GA”, Proceedings of IEEE conference on Emerging Technologies and Factory Automation. ETFA '96, Kauai, HI, USA, (1996), 272-274.

98. Ouyang, X., Morgan, C. and Nwagboso, C., “Neural network adaptive control for servo systems with nonlinear disturbances”, In: Hayhurst D.R. et al. (eds) Proceedings of the 33rd International MATADOR Conference, (2000).

99. Ouyang, Y., Shi, W., Shan, J. and Spencer, B.F., “Backstepping adaptive control for real-time hybrid simulation including servo-hydraulic dynamics”, Mechanical Systems and Signal Processing, V. 130, (2019), 732–754.

100. Ozcelik, O., Luco, J., Conte, J., Trombetti, T. and Restrepo, J., “(2008). Experimental characterization, modeling and identification of the NEES-UCSD shake table mechanical system”, Journal of Earthquake Engineering and Structural Dynamics, V. 37, n° 2, (2008), 243-264.

101. Pan Y., Song P. and Li, K., “PID Control of Miniature Unmanned Helicopter Yaw System Based on RBF Neural Network”, In: Chen R. (eds) Intelligent Computing and Information Science. ICICIS 2011. Communications in Computer and Information Science, V. 135, (2011).

102. Pan, I., Das, S. and Gupta, A., “Tuning of an Optimal Fuzzy PID Controller with Stochastic Algorithms for Networked Control Systems with Random Time Delay”, ISA Transactions, V. 50, n° 1, (2011), 28-36.

103. Pei, Z., Y. Zhang, Y. and Tang, Z., “Model reference adaptive PID control of hydraulic parallel robot based on RBF neural network”, Proceedings of the 2007 IEEE International Conference on Robotics and Biomimetics (ROBIO), Sanya, (2007), 1383-1387.

104. Phillips, B.M., Wierschem, N.E. and Spencer, B.F Jr., “Model-based control of shake tables with multi-metric feedback”, Earthquake Engineering and Structural dynamics, V. 43, n° 5, (2013), 681-699.

105. Plummer A.R., “A detailed dynamic model of a six-axis shaking table”, Journal of Earthquake Engineering, V. 12, n° 4, (2008), 631–662.

106. Plummer, A.R., “Control techniques for structural testing: a review”, Proceedings of the Institution of Mechanical Engineers, Part I, Journal of Systems and Control Engineering, V. 221, n° 2, (2007), 139–169.

107. Plummer, A.R., “A general co-ordinate transformation framework for multi- axis motion control with applications in the testing industry”, Control Engineering Practice, V. 18, (2010), 598–607.

108. Plummer, A.R., “Model-based motion control for multi-axis servo hydraulic shaking tables”, Control Engineering Practice, V. 53, n° 2016, (2016), 109–122.

109. Porter, B. and Jones, A. H., “Genetic tuning of digital PID controllers”, Electronics Letters, V. 28, n° 9, (1992), 843–844.

110. Priva, J., Jeevananham, A. and Rajalashmi, K., “Fuzzy Logic Controller for Position Control of Servo Motor”, International Journal of Innovative Technology and Exploring Engineering (IJITEE), V. 8, n° 3, (2019), 99-102.

111. Psillakis, H., “An adaptive NN controller with second order SMC-based NN weight update law for asymptotic tracking”, in: Alippi C., Polycarpou M., Panayiotou C., Ellinas G. (eds) Artificial Neural Networks – ICANN 2009. Lecture Notes in Computer Science, V. 5769. Springer, Berlin, Heidelberg, (2009).

112. Qu, Z.Y. and Ye, Z.M., “Model Reference adaptive control on hydraulic servo system”, Advanced Materials research, V. 268- 270, (2011), 505-508.

113. Reinhorn, A. M., Ryu, K. P. and Maddaloni, G., “Modeling and seismic evaluation of nonstructural components: testing frame for experimental evaluation of suspended ceiling systems”, Technical Report MCEER-10-0004, Buffalo, NY, (2010).

114. Renner, G. and Ekart, A., “Genetic Algorithms in Computer Aided Design”, Computer-Aided Design, V. 35, n° 8, (2003), 709 – 726

115. Rinawi, A. M. and Clough, R. W., “Shaking table–structure interaction”, EERC Report No. 91/13, Earthquake Engineering Research Center, University of California at Berkeley, CA, (1991).

116. Ryu, K. P. and Reinhorn, A. M., “Real-time control of shake tables for nonlinear hysteresis systems”, Structural Control and Health Monitoring, V. 24, n° 2, (2016).

117. Salim, S.N.S., Rahmat, M.F., Faudzi, A.A.M, Ismail, Z.H. et al., “Robust control strategy for pneumatic drive system via enhanced nonlinear PID Controller”, International Journal of Electrical and Computer Engineering, V. 4, n° 5, (2014), 658-667.

118. Seki, K. and Iwasaki, M., “ (2017). Model-based adaptive feedforward compensation for disturbance caused by overturning moment in 2-dimensional shaking table systems”, Mechanical Engineering Journal, V. 4, n° 3, (2017), 16-00427.

119. Seki, K., Iwasaki, M., Kawafuku, M. and Hirai, H., “Improvement of control performance in shaking-tables by feedback compensation for reaction force”, Proceedings of the 2008 34th Annual Conference of IEEE Industrial Electronics Conference (IECON2008), Orlando, FL, USA, (November 2008), 2551–2556.

120. Seki, K., Iwasaki, M., Kawafuku, M., Hirai, H. and Yasuda, K., “Adaptive feedforward compensation for reaction force with nonlinear specimen in shaking table”, Proceedings of the 2009 IEEE International Conference on mechatronics, Malaga, Spain (2009).

121. Seki, K., Iwasaki, M., Kawafuku, M., Hirai, H. and Yasuda, K., “ (2009). Adaptive compensation for reaction forces with frequency variation in shaking table systems”, Industrial electronics IEEE transactions, V. 56, n° 10, (2009), 3864-3871.

122. Seki, K., M. Iwasaki, M. and Hirai, H., “Reaction force compensation with frequency identifier in shaking table systems”, Proceedings of the 2010 11th IEEE International Workshop on Advanced Motion Control (AMC), Nagaoka, Niigata, Japan, (November 2010), 673–678.

123. Severn R.T., “The Contribution of Shaking Tables to Early Developments in Earthquake Engineering”, in: Garevski M., Ansal A. (eds) Earthquake Engineering in Europe. eotechnical, Geological, and Earthquake Engineering, V. 17, (2010).

124. Severn R.T., “The development of shaking tables–A historical note”, Earthquake Engineering and Structural Dynamics, V. 40, n° 2, (2011), 195-213.

125. Severn, R. T., Stoten, D. P. and Tagawa, Y., “The contribution of shaking tables to earthquake engineering”, Proceedings of the 15th world conference on earthquake engineering, Lisbon, Portugal, (2012).

126. Shahraki F., Fanaei M.A. and Arjomandzadeh A.R., “Adaptive system control with PID neural networks”, Chemical Engineering Transaction, V. 17, (2009), 1395-1400.

127. Shen G., Zhu Z., Li X., Li G. et al., “Experimental evaluation of acceleration waveform replication on electrohydraulic shaking tables: A review”, International Journal of Advanced Robotic Systems, V. 13, n° 5, (2016), 1-25.

128. Shen G., Zhu Z-C., Zhang L., Tang Y., et al., “Adaptive feed-forward compensation for hybrid control with acceleration time waveform replication on electro-hydraulic shaking table”, Control Engineering Practice, V. 21, n° 8, (2013), 1128–1142.

129. Shen, G., Li, X., Zhu, Z., Tang, Y. et al., “Acceleration tracking control combining adaptive control and off-line compensators for six-degree-of-freedom electro-hydraulic shaking tables”, ISA Transactions, V. 70, (2017), 322-337.

130. Shen, G., LV, G.M., Ye, Z.M., Cong, D.C. et al., “Feed-forward inverse control for transient waveform replication on electro-hydraulic shaking table”, Journal of Vibration and Control, V. 18, n° 10, (2011), 1474-1493.

131. Shen, G., Zheng, S.T., Ye, Z.M, Yang, Z.D. et al., “Tracking control of an electro-hydraulic shaking table system using a combined feedforward inverse model and adaptive inverse control for real-time testing”, Proceedings of the Institution of Mechanical Engineers, Part I: Journal of Systems and Control Engineering, V. 225, n° 5, (2011), 647-666.

132. Shen, G., Zhu, Z., Tang, Y., Zhang, L. et al., “Combined control strategy using internal model control and adaptive inverse control for electro-hydraulic shaking table”, Proceedings of the Institution of Mechanical Engineers, Part C: Journal of Mechanical Engineering Science, V. 227, n° 10, (2012), 2348–2360.

133. Shen, G., Zhu, Z.C., Li, X., Tang, Y. et al., “Real-time electro-hydraulic hybrid system for structural testing subjected to vibration and force loading”, Mechatronics, V. 33, (2016), 49–70.

134. Shen, G.m., Lv, Ye., Z.m., Cong, D.c. and Han, J.w., “Implementation of electrohydraulic shaking table controllers with a combined adaptive inverse control and minimal control synthesis algorithm”, IET Control Theory and Applications, V. 5, n° 13, (2011), 1471–1483.

135. Shimizu, N., Shinohara, Y., Yabuki, H., and Sato, E., “Control simulation of shaking table with non-linear structure”, Proceedings of ACMD2004, (2004), 478–485.

136. Shinohara, Y., Shimizu, N. and Sato, E., “Experimental study on shaking-table control using adaptive control”, Proceedings of the American society of mechanical engineering, pressure vessel and piping conference, Seismic Engineering, San Diego (CA),USA, (2004), 209–216.

137. Shu, H. L., “PID neural network for decoupling control of strong coupling multivariable time-delay systems”, In: Control Theory and Applications, V. 15.6, (1998), 920–924.

138. Sidhom, L., M.Di Loreto, M., Brun, X., Bideaux, E. and Thomasset, D., “Nonlinear Adaptive Robust control of electro-hydraulic servo-actuator with some unknown parameters”, Proceedings of the 11th Scandinavian International Conference on Fluid Power, SICFP'09, (June 2-4, 2009), Linköping, Sweden.

139. Singh, A., Saxena, P. and Lalwani, S., “A Study of Various Training Algorithms on Neural Network for Angle based Triangular Problem”, International Journal of Computer Applications (0975 – 8887), V. 71, n° 13, (2013).

140. Slama, S., Errachdi, A. and Benrejeb, M., “Adaptive PID controller based on Neural Networks for MIMO nonlinear systems”, Journal of Theoretical and Applied Information Technology, V. 97, n° 2, (2019).

141. Slama, S., Errachdi, A. and Benrejeb, M., “Neural adaptive PID and neural indirect adaptive control switch controller for nonlinear MIMO systems”, Mathematical Problems in Enginering, V. 2019, Article ID 7340392, (2019).

142. Soleymani, M., Soltani, A.K. and Ghanbari, S.B., “Fuzzy-sliding-mode supervisory control of a seismic shake table with variable payload for robust and precise acceleration tracking”, Journal of Earthquake Engineering, V. 23, n° 4, (2019), 539-559.

143. Srivignesh, N., Sowmaya, P., Ramkumar, K. and Balasubramanian, G., “Design of neural based PID control for nonlinear process”, Procedia Engineering, V. 38, (2012), 3283-3291.

144. Stehman, M., “Advances in shake table control and substructure shake table testing”, PhD thesis, University of Baltimore, Maryland, (2014).

145. Stehman, M. and Nakata, N., “ (2013). Direct acceleration feedback control of shake tables with force stabilization”, Journal of Earthquake Engineering, V. 17, n° 5, (2013), 736-749.

146. Stehman, M. and Nakata, N., “IIR compensation in real-time hybrid simulation using shake tables with complex control-structure-interaction”, Journal of Earthquake Engineering, V. 20, n° 4, (2016).

147. Stoten, D. P., “An overview of the minimal control synthesis algorithm”, In Proceedings of Institution of Mechanical Engineers, International Conference on Aerospace Hydraulics and Systems, London, paper C4474-033, (1993), 29-30.

148. Stoten, D. P. and Benchoubane, H., “Robustness of a minimal controller synthesis algorithm”, International Journal of Control, V. 51, n° 4, (1990), 851–861.

149. Stoten, D.P. and Gomez, E., “Real-time adaptive control of shaking tables using the minimal control synthesis algorithm”, Philosophical Transactions of the Royal Society of London A, V. 359, (2001), 1697–1723.

150. Strano, S. and Terzo, M., “A non-linear robust control of a multi-purpose earthquake simulator”, Proceedings of the World Congress on Engineering 2013 Vol III, WCE 2013, (July 3 - 5, 2013), London, U.K.

151. Sullivan, T.J.n Pinho, R. and Pavese, A., “An introduction to structural testing techniques in Earthquake Engineering”, Pavia: IUSS Press, (2004).

152. Sun, Z. and Tsao, T.C., “Adaptive control with asymptotic tracking performance and its application to an electro-hydraulic servo system”, Journal of Dynamic Systems Measurement and Control, V. 122, n° 1, (2000), 188-195.

153. Tagawa, Y. and Kajiwara, K., “Controller development for the E-Defense shaking table”, Proceedings of the Institution of Mechanical Engineers, Part I: Journal of Systems and Control Engineering, V. 221, n° 2, (2007), 171–181.

154. Taghizadeh, S., “Control of a pneumatic system with adaptive Neural Network compensation”, Master thesis, Queen’s university of Ontario, Canada, (2010).

155. Tan, Y., Dang X. and Cauwenberghe A.V., “Generalised nonlinear PID controller based on neural networks”, Information, Decision and Control. Data and Information Fusion Symposium, Signal Processing and Communications Symposium and Decision and Control Symposium. Proceedings (Cat. No.99EX251), Adelaide, SA, Australia, (1999), 519-524.

156. Tanaka, K., Yamada, Y., Satoh, T., Uchibori, A. and Uchikado, S., “Model reference adaptive control with neural network for electro-pneumatic servo system”, Proceedings of the 1999 IEEE International conference on control application Kohala Coast, HI, USA, V. 2, (1999), 1716-1721.

157. Tang, H. and Tian, P., “Backstepping integral control for hydraulic servo system based on LuGre friction model”, Journal of Vibroengineering, V. 18, n° 8, (2016), 5252-5265.

158. Tang, T., Zhu, Z., Shen, G. and Zhang, W., “Real Time Acceleration Tracking of Electro-Hydraulic Shake Tables Combining Inverse Compensation Technique and Neural-Based Adaptive Controller”, IEEE Access, V. 5, (2017), 23681-23694.

159. Tang, Y., Zhu, Z. C., Shen, G. and Li, X., “ Improved feedforward inverse control with adaptive refinement for acceleration tracking of electro-hydraulic shake table”, Journal of Vibration and Control, V. 22, n° 19, (2016), 3945-3964.

160. Tang, Z. Y., Li, Z. B., Zhou, D. X. et al., “The effects on the earthquake simulation caused by the characteristics of the specimen in the shaking table tests-part 2: the effects on the replaying precision of the recorded seismic waves and the real-time compensation”, Journal of Beijing University of Technology, V. 36, n° 9, (2010), 1199–1205.

161. Trombetti, T.L. and Conte, J.P., “Shaking table dynamics: results from a test-analysis comparison study”, Journal of Earthquake Engineering, V. 6, n° 4, (2002), 513–551.

162. Valilou, S., “Nonlinear model and control of electro-hydraulic servo-systems”, PhD thesis, University of Bergamo, Italy, (2017).

163. Virvalo, T., “Hydraulic motion control robustness against inertia load changes”, Proceedings of the JFPS International Symposium on Fluid Power, V. 2002, n° 5-2, (2002), 561-566.

164. Wang, M.S., Chen, S.C., Chuang, P. H., Wu, S.Y. and Hsu, F. S., “Neural Network control-based drive design of servomotor and its application to automatic guided vehicle”, Mathematical Problems in Enginering, V. 2015, Article ID 612932, (2015).

165. Wang, P. and Kwok, D. P., “Optimal design of PID process controllers based on genetic algorithms”, Control Engineering Practice, V. 2, n° 4, (1994), 641–648.

166. Wang, X., “An active disturbance rejection control solution for electrohydraulic servo systems”, Cleveland State University, (2012).

167. Weihua, J. and Hao, W., “Improvement of position controller based on Fuzzy control”, Proceedings of the International Conference on Electrical and Control Engineering, Wuhan, (2010), 1180-1182.

168. Weiping, Z., Dongzhou, Y. and Zhanshuang, H., “Parameters optimization for small helicopter highly controller based on genetic algorithm”, World Automation Congress 2012, Puerto Vallarta, Mexico, (2012), 1-4.

169. Williams, D.M., Williams, M.S. and Blakeborough, A., “Numerical modeling of a servohydraulic testing system for structures”, Journal of Engineering Mechanics, V. 127, n° 8, (2001), 816–827.

170. Wonohadidjojo, D. M., Kothapalli, G. and Hassan, M., “Position control of electrohydraulic actuator system using FLC optimized by PSO”, International Journal of Automation and Computing, V. 10, n° 3, (2013), 181-193.

171. Wos, P. and Dindorf, R., “Adaptive control of the electro-hydraulic servo-system with external disturbances”, Asian Journal of Control, V. 15, n° 4, (2013), 1065–1080.

172. Wos, P., Dindorf, R., “Nonlinear modeling and parameter identification for electro-hydraulic servo system”, 20th International Carpathian Control Conference (ICCC), Krakow-Wieliczka, Poland, (2019), 1-5.

173. Wu, C. J., “Genetic Tuning of PID Controllers Using a Neural Network Model: A Seesaw Example”, Journal of Intelligent and Robotic Systems, V. 25, (1999), 43–59.

174. Wu, Z., Wang, W. and Bai, Z., “Improved Genetic Algorithm Optimizing PID Parameters for Electro-hydraulic Servo System”, In: Zhao M., Sha J. (eds) Communications and Information Processing. Communications in Computer and Information Science, V. 288, (2012).

175. Xu, X., Zhu, D., Zhang, H., Yan, S. and Ding, H., “Application of novel force control strategies to enhance robotic abrasive belt grinding quality of aero-engine blades”, Chinese Journal of Aeronautics, V. 32, n° 10, (2019), 2368-2382.

176. Yachun, T., Peng, P., Dongbin, Z. and Yi, Z., “A Two-Loop control method for shaking table tests combining Model Reference Adaptive Control and Three-Variable Control”, Frontiers of Built environment, V. 4, n° 54, (2018).

177. Yalcin, E., “Dynamic model of a hydraulic servo system for a manipulator robot”, Master thesis, University of Stockholm, Sweden, (2014).

178. Yang T.Y. and Schellenberg, A., “Using nonlinear control algorithms to improve the quality of shaking table tests”, Proceedings of the 14th World Conference on Earthquake Engineering, (October 12-17, 2008), Beijing, China

179. Yang, T. Y., Kang, L., Lin, L., Yuan, J. and Yuanjie, L., “Development of Nonlinear Control Algorithms for Shaking Table Tests”, Proceedings of the ASME 2013 Dynamic Systems and Control Conference, Palo Alto, California, USA. (October 21–23, 2013).

180. Yao, J., Di, D., Jiang, G. and Gao, S., “Acceleration amplitude-phase regulation for electrohydraulic servo shaking table based on LMS adaptive filtering algorithm”, International Journal of Control, V. 85, n° 10, (2012), 1581-1592.

181. Yao J., Dietz MS., Xiao R., Yu H. et al., “An overview of control schemes for hydraulic shaking tables”, Journal of Vibration and Control, V. 22, n° 12, (2016), 2807-2823.

182. Yao, J., “Model-based nonlinear control of hydraulic servo systems: Challenges, developments and perspectives”, Frontiers of Mechanical Engineering, V. 13, (2018), 179–210.

183. Yao, J., Wan, Z. and Fu, Y., “Acceleration harmonic estimation in a hydraulic shaking table using water cycle algorithm”, Shock and Vibration, V. 2018, Article ID 7278589, (2018), 12 pages.

184. Yao, J., Wan, Z., Zhao, Y., Yu, J. et al., “Resonance suppression for hydraulic servo shaking table based on adaptive Notch filter”, Shock and Vibration, V. 2019, Article ID9407520, (2019), 12 pages.

185. Yao, J., Yang, G. and Jiao, Z., “High dynamic feedback linearization control of hydraulic actuators with backstepping”, Proceedings of the Institution of Mechanical Engineers, Part I: Journal of Systems and Control Engineering, V. 229, n° 8, (2015), 728-737.

186. Yao, Z., Yao, J., Yao, F., Xu, Q., et al., “Model Reference Adaptive Control for hydraulic servo systems with nonlinear NN”, ISA transactions, V. 100, (May 2020), 396-404.

187. Yildirim, S., Erkaya, S., Uzmay, I. and Kalkat, M., “A Neural based position controller for an electrohydraulic servo system”, Proceedings of the 11th WSEAS international conference on robotics, control and manufacturing technology, and 11th WSEAS international conference on Multimedia systems & signal processing, (march 2011), 31-38.

188. Yousefi, H., Handroos, H. and Mattila, J. K., “Application of fuzzy gain-scheduling in position control of a servo hydraulic system with a flexible load”, International Journal of Fluid Power, V. 8, n° 2, (2007), 25-35.

189. Zhang, L., Cong, D., Yang, Z., Zhang, Y. et al., “Robust tracking and synchronization of double shaking tables based on adaptive sliding mode control with novel reaching law”, IEEE Access, Vol. 4, (2016), 8686-8702.

190. Zhang, L., Yang, Z., Qu, Z. and Han, J., “Modeling and vibration decoupling control of multi-axial shaking table”, Proceedings of International Industrial Informatics and Computer Engineering Conference, (July 22-24, 2015), United Kingdom.

191. Zhao, J., Catharine, C.S. and Posbergh, T., “Nonlinear system modeling and velocity feedback compensation for effective force testing”, Journal of Engineering Mechanics, V. 131, n° 3, (2005), 244–253.

192. Ziaei, K. and Sepehri, N., “Design of a Nonlinear Adaptive Controller for an Electrohydraulic Actuator”, Journal of Dynamic Systems, Measurement and, Control. V. 123, n° 3, (2001), 449-456.

193. Zribi, A., Chtourou, M. and Djemel, M., “A New PID Neural Network Controller Design for Nonlinear Processes”, Journal of Circuits, Systems and Computers, V. 27, n° 04, 1850065 (2018).

194. Zulfatman, H. and Rahmat, M. F., “Application of self-tuning fuzzy PID controller on industrial hydraulic actuator using system identification approach”, International Journal on Smart Sensing and Intelligent Systems, V. 2, n° 2, (2009), 246–261.

195. Zuo, X., Liu, J.W., Wang, X. and Liang, H.Q., “Adaptive PID and Model Reference Adaptive Control switch controller for nonlinear hydraulic actuator”, Mathematical Problems in Engineering, V. 2017, Article ID 6970146, (2017).